IN VITRO – IN VIVO INVESTIGATION OF THE HEPATIC EXTRACTION OF RSD1070, A NOVEL ANTIARRHYTHMIC COMPOUND

by

VINCENT TONG

B.Sc. (Biology), Simon Fraser University, 1997

A THESIS SUBMITTED IN PARTIAL FULFILLMENT OF

THE REQUIREMENTS FOR THE DEGREE OF

MASTER OF SCIENCE

in

THE FACULTY OF GRADUATE STUDIES

Faculty of Pharmaceutical Sciences

Division of Pharmaceutical Chemistry

We accept this thesis as conforming
to the required standard

THE UNIVERSITY OF BRITISH COLUMBIA

APRIL 2000

In presenting this thesis in partial fulfilment of the requirements for an advanced degree at the University of British Columbia, I agree that the Library shall make it freely available for reference and study. I further agree that permission for extensive copying of this thesis for scholarly purposes may be granted by the head of my department or by his or her representatives. It is understood that copying or publication of this thesis for financial gain shall not be allowed without my written permission.

Department of PHARMACEUTICAL SCIENCES

The University of British Columbia
Vancouver, Canada

Date APRIL 25/00

DE-6 (2/88)

ABSTRACT

Purpose. The hepatic extraction of a novel antiarrhythmic, RSD1070, was investigated to test the hypothesis that its poor bioavailability observed in rats is due to high hepatic metabolism. **Methods.** The pharmacokinetics of RSD1070 was examined in rats (n=8) and its metabolism was investigated using parent compound disappearance studies in pooled rat hepatic microsome incubations. The free fraction in plasma and microsomal matrices was determined by equilibrium dialysis. Hepatic extraction was predicted from the scaling-up of the microsomal kinetic data using the well-stirred liver model. **Results.** RSD1070 pharmacokinetics demonstrated a three-compartment model following single iv bolus administration of a dose of 12 mg/kg. RSD1070 exhibited a rapid elimination $t_{1/2}$ (25 ± 8 min) and a CL_{tot} of 71 ± 9 mL/min/kg. Renal clearance based on 24-hour urinary recovery was determined to be insignificant (<< 1% of CL_{tot}). A Michaelis-Menten model described the consumption of RSD1070 with a K_m of 0.45 μg/mL and V_{max} of 2.81 μg/min/mg microsomal protein. The *in vitro* half-life approach examined the first-order consumption rate of RSD1070 (1 μM) in microsomal incubation. Taking the V_{max}/K_m ratio (CL_{int}) and the *in vitro* $t_{1/2}$ as the basis for scaling, the data from the microsomal kinetic studies (75 mL/min/kg) closely approximated the apparent CL_{tot}. Required for the scale-up of *in vitro* CL_{int}, plasma free fraction (1.5 %) and microsomal free fraction (15 %) were determined and incorporated into the well-stirred liver model. **Conclusion.** RSD1070 is a high hepatic extraction compound (E = 0.94) with a predicted *in vitro* CL_h value that accounted for the CL_{tot} observed in rats.

TABLE OF CONTENTS

LIST OF TABLES

LIST OF FIGURES

LIST OF ABBREVIATIONS

μ	Micron
β	Beta, an exponential rate constant (apparent rate of elimination)
μg	Microgram
μL	Microliter
μM	Micromolar
$\approx$	Approximately
AP	Cardiac action potential
ATP	Adenosine triphosphate
AUC	Area under the plasma concentration *vs.* time curve
AUC^{iv}	Area under the plasma concentration time curve following intravenous dosing
AUC^{hp}	Area under the plasma concentration time curve following drug administration via the hepatic portal vein
AUC^{po}	Area under the plasma concentration time curve following oral adminsitration
AV node	Atrioventricular node
Ca^{2+}	Calcium ions
°C	Degrees celsius
CL	Clearance
CL_{int}	Intrinsic clearance
CL_h	Hepatic clearance
CL_r	Renal clearance
CL_{tot}	Total body clearance based on total drug concentrations
CV	Coefficient of variation
D^{iv}	Intravenous administration of a dose
D^{hp}	Hepatic portal vein administration of a dose
D^{po}	Oral adminsitration of a dose
Da	Daltons
E	Hepatic extraction ratio

ECG	Electrocardiogram
ED_{90}	Effective dose, dose required to produce a 90% of a maximal response
EDTA	Ethylenediaminetetraacetic acid
ESP^+	Positive electrospray ionization
et al.	*et alia.*
eV	Electron volts
F	Bioavailability
F_a	Bioavailability after first pass through the gastrointestinal system
F_h	Bioavailability after first pass through the liver
f_u	Free, unbound fraction of drug in plasma
$f_{u\,(mx)}$	Free, unbound fraction of drug in microsomal incubation
G	Gauge, measure of diameter of needle
g	Gram
hr	Hour
HPLC	High performance liquid chromatograph
IC_{50}	Inhibitory concentration, concentration required to result in 50% inhibition of maximal response.
IS	Internal standard
iv	Intravenous
ip	Intraperitoneal
K^+	Potassium ions
KCl	Potassium chloride
kg	Kilogram
K_m	A Michaelis-Menten parameter for enzymatic reactions; substrate concentration at which the reaction velocity is at half-maximal
$K_{m\,(app)}$	Apparent K_m based on free unbound concentrations
kV	Kilovolts
LC	Liquid chromatograph
LOQ	Limit of quantitation of the assay
M	Molar
MW	Molecular weight

m/z	Mass to charge ratio
MeOH	Methanol
mg	Milligram
min	Minute
mm	Millimeter
mM	Millimolar
MRM	Multiple reaction monitoring
MS	Mass spectrometry
MS/MS	Tandem mass spectrometry
msec	Millisecond
Na^+	Sodium ions
NADPH	Reduced β-nicotinamide-adenine dinucleotide tetrasodium salt
NaOH	Sodium hydroxide
ng	Nanogram
pKa	Ionization constant
PAR	Peak area ratio of analyte to IS
PSI	Pounds per square inch
PVC	Premature ventricular contractions
Q	Hepatic blood flow
r^2	Coefficient of determination
rpm	revolutions per minute
SA node	Sinoatrial node
sc	Subcutaneous
SD	Standard deviation
SIM	Single ion monitoring
t	Time
$t_{1/2}$	Terminal elimination half-life in a two-compartment model based on total drug concentrations
V_d	Volume of distribution
V_{area}	Volume of distribution of the terminal elimination phase
V_{max}	Maximal velocity of an enzymatic reaction; a Michaelis-Menten parameter

ACKNOWLEDGEMENTS

I would like to express my gratitude to my supervisor, Dean Frank Abbott, for his excellent support, guidance, and for the opportunity to do work in his laboratory. I am also grateful to the other members of my committee, Dr. G. Bellward (Chair), Dr. S. Bandiera, Dr. T. Chang, Dr. J. McNeill, and Dr. M. Walker. A special thanks to Dr. S. Bandiera for the use of his laboratory and for his assistance in microsome preparation. Sincere thanks to Dr. M. Walker for the inspiration to pursue studies in Pharmaceutical Sciences.

I would also like to thank the kind people from Nortran Pharmaceuticals Ltd. who have given me the opportunity to conduct research with one of their compounds. Within this organization, a special thanks to Dr. Greg Beatch (VP of research), Dr. Lillian Clohs and Mark Buss for their helpful suggestions regarding anlaytical work, Mr. Tao Sheng for the synthesis of RSD1070 and metabolite standards, and to Ms. Salome Mbofana for her assistance in animal surgery.

Thanks are also extended to Mr. Roland Burton for his assistance and all his teachings with the use of the LC/MS. I would like to especially thank my friend and colleague, Mr. Harvey Wong, for all of his support and constructive advice throughout my entire project. As with any project, thanks to my lab inmates Dr. Sashi Gopaul, Ms. Karen Lo, Mr. Robbin Burns, Mr. Eddy Kwan, Mr. Scott Loucks, Mr. Ted Lakowski, Mr. Caly Chien, and Mr. Sam Au-Yeung for making graduate studies a much more enjoyable situation.

Funding from Dr. Michael Walker is acknowledged. This work was supported by the Faculty of Pharmaceutical Sciences, University of British Columbia.

DEDICATION

To my family and friends for their constant support throughout my studies

CHAPTER 1
INTRODUCTION

RSD1070, (±)-trans-[2-Morpholinyl-1-(1-naphthaleneethyloxy] cyclohexane mono-hydrochloride (**Figure 1**), was synthesized and found to have antiarrhythmic activity (Nortran Pharmaceuticals Ltd., unpublished data). At present RSD1070 is in pre-clinical stages of development and is considered as a clinical candidate, however; preliminary studies conducted by Nortran Pharmaceuticals Ltd. indicated poor oral bioavailability when administered to rats. Bioavailability is defined as the fraction of unchanged drug reaching the systemic circulation following administration by any route. Oral bioavailability was determined by comparing the ratio of AUCs following iv and gastric lavage administration of antiarrhythmic doses of 12 and 112 mg/kg RSD1070, respectively (Dr. Richard A. Wall, personal communications).

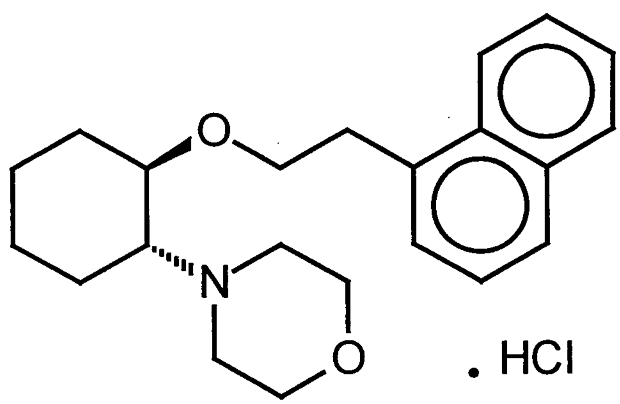

Figure 1. Chemical structure of RSD1070.

The focus of this thesis is the investigation of hepatic clearance and extraction determined by *in vivo* methodology in whole animal studies and predicted by *in vitro* methodology from hepatic microsomal metabolism studies. In order to provide a framework within which the research can be appropriately analyzed, this introduction seeks to provide some background concerning this drug. Firstly, the disease state of arrhythmia will be reviewed with emphasis on its mechanism with regards to cardiac electrophysiology, drugs currently used in the treatment of arrhythmia, and the need for novel antiarrhythmic compounds. Secondly, the status of RSD1070 will be reviewed with regard to the limited information on its pharmacological properties and the need to investigate its metabolism and pharmacokinetics. Thirdly, the use of hepatic microsomes as an *in vitro* method to investigate the metabolism and kinetics of RSD1070 will be discussed with regard to (A) the approach used to calculate intrinsic clearance, (B) the use of scaling factors, and (C) the use of a liver clearance model for the prediction of hepatic clearance and hepatic extraction.

1.1 ARRHYTHMIA

Cardiac arrhythmias are deviations from normal heartbeat. They include abnormalities in impulse generation and/or impulse conduction that alter the heart rate, rhythm, or site of impulse origin (Mutnick, 1998). As a consequence, the normal coordinated sequence of atrial and ventricular contractions is disrupted resulting in clinical effects ranging from the asymptomatic to life threatening. Sudden death due to arrhythmia is the most common cause of death in economically developed countries accounting for approximately 350,000 deaths per year in the US (Rees *et al.*, 1997). One common cause of ventricular arrhythmias is myocardial ischemia which results from coronary artery obstruction in disease states such as atherosclerosis. As a result insufficient blood reaches the myocardium to meet the tissues' oxygen demand, and the arrhythmia originating at this ischemic site may lead to potential cardiac output failure.

1.1.1 Cardiac Electrophysiology

Normal cardiac contraction is a coordinated function involving (1) electrical impulse generation from the sinoatrial node, (2) fast and uniform signal transmission throughout the atria and to the ventricles via the atrioventricular node, and (3) the maintenance of a normal cardiac action potential duration and refractory period (Mutnick, 1998). The ventricular myocardial action potential (AP), which reflects cardiac electrical activity, is essential for cardiac contraction and consists of five phases (**Figure 2**). Normally resting cells are characterized with a transmembrane potential of ≈ -90 mV with the inside of the cell being more electronegative than the outside. Phase 0 is the rapid depolarization phase ("upstroke" of AP), a fast inward current of Na^+ ions across the membrane as a result of Na^+ channel opening. Phase 1 is the early rapid repolarization phase ("notch" of AP) and is due to the opening of K^+ channels that results in the transient outward K^+ current that repolarize the membrane. Phase 2 (plateau) is a result of the slow, inward, depolarizing Ca^{2+} current that is balanced primarily by the outward K^+ current via "delayed rectifier" K^+ channels. However, the delayed rectifier K^+ current increases with time while the Ca^{2+} current inactivates or decreases with time. The result is the Phase 3 rapid repolarization of the cardiac cell. The Phase 4 (slow depolarization) is the result of the ATP-requiring Na^+/K^+ exchange (pump) mechanism shuttling 3 Na^+ ions to the exterior for every 2 K^+ ions to the interior of the cell and intracellular calcium being removed by the ATP-dependent Ca^{2+} pump. The result is a net outward (repolarizing) current and the homeostatic maintenance of K^+, Na^+, and Ca^{2+} ion distribution across the myocyte membrane.

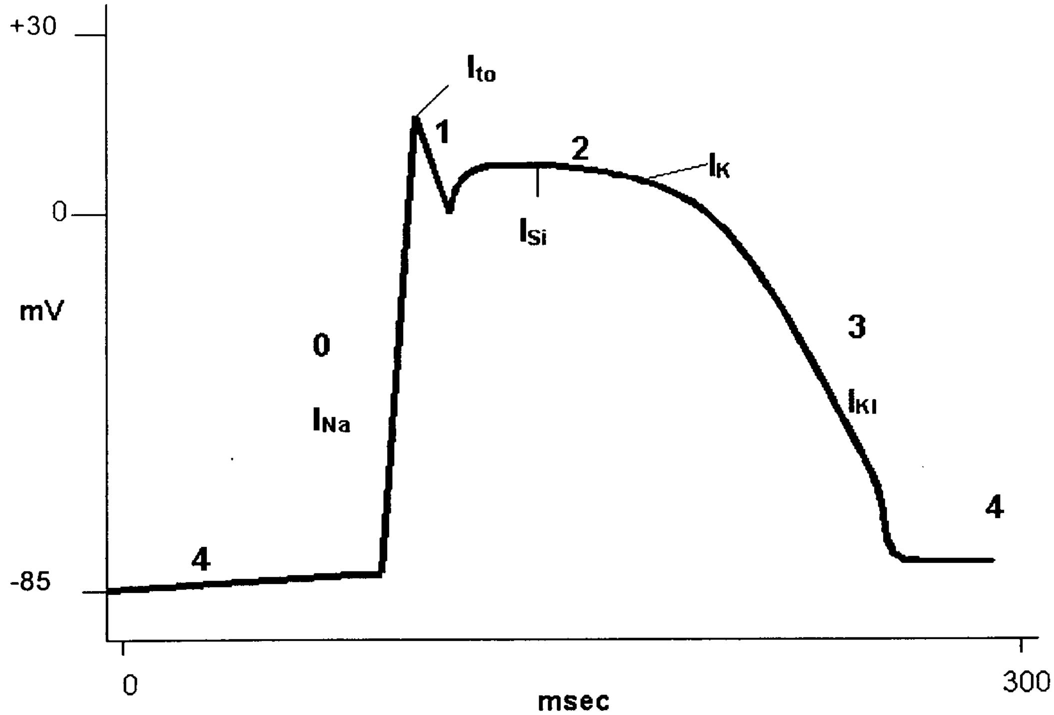

Figure 2. **Configuration of a typical ventricular cardiac action potential showing the activation of the most important ionic currents at each Phase: (0) I_{Na}, fast inward Na^+ current; (1) I_{to}, transient outward K^+ current, (2) I_{Si}, slow inward Ca^{2+} current and I_K, delayed rectifier K^+ current, (3) I_{KI}, inward rectifier K^+ current, and (4) Na^+/K^+-ATPase exchange (Reproduced from Rees *et al.*, 1997).**

The average signal of the depolarizations and repolarizations occuring in all cardiac myocytes can be recorded as a series of electrocardiograph (ECG) waveforms (**Figure 3**) and arrhythmias are defined based on their ECG configuration. A normal ECG waveform consists of 5 segments. The P wave reflects atrial depolarization originating from the sinoatrial node and the QRS complex reflects ventricular depolarization. The time between the P wave and the QRS complex (PR interval) represents the atrioventricular nodal conduction time. The QT segment, which coincides with the Phase 2 plateau of the AP, is the time between the QRS complex and the T-wave and is a measure of ventricular action potential duration. The T wave represents ventricular repolarization corresponding to Phase 3 of the AP.

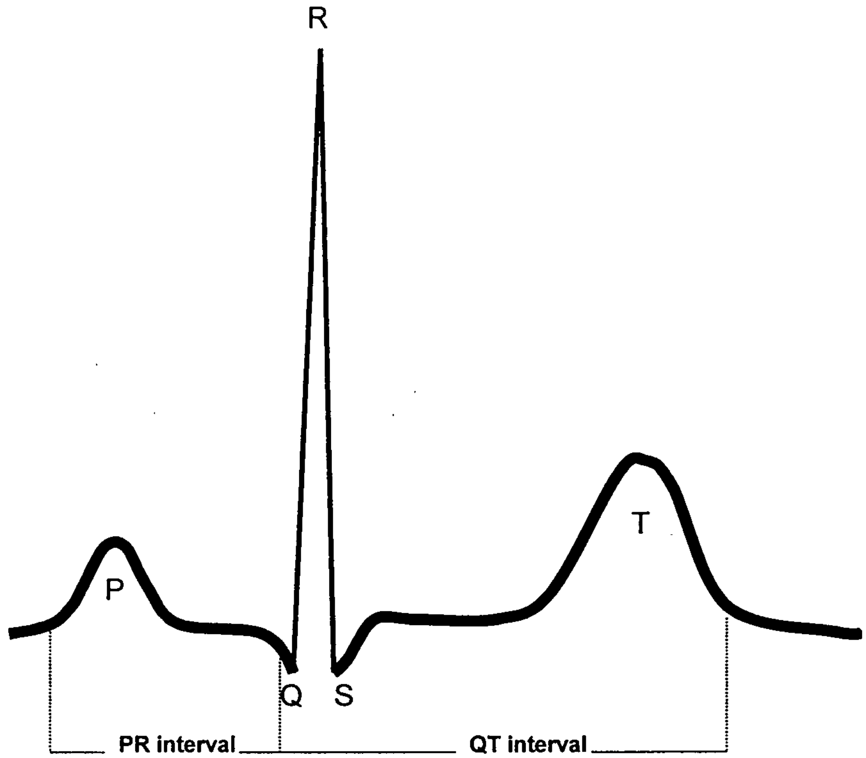

Figure 3. Normal Electrocardiogram (ECG). The P wave represents depolarization of the atria, the QRS complex reflects depolarization of the ventricles, and the T wave, repolarization of the ventricles. PR interval reflects AV nodal conduction time and the QT interval is a measure of ventricular action potential duration.

1.1.2 Mechanisms of Arrhythmia

The two main mechanisms for arrhythmias are abnormal impulse generation and abnormal impulse conduction, or a combination of both, defined according to the ECG (Hondeghem and Mason, 1987). Depressed impulse initiation may result in slow heart rates (bradyarrhythmias) while increased impulse initiation may result in premature ventricular contractions (PVCs) as defined by discreet premature QRS complexes. Ventricular tachycardia is defined by a run of 4 or more consecutive PVCs and lethal ventricular fibrillation is demonstrated as irregular deflections on the ECG.

Arrhythmias that arise from abnormal impulse conduction may be caused by conduction block such that the impulses generated from the SA node propagating to the AV node are slowed (as seen as prolonged PR interval), partially blocked (as seen as absent QRS complex following P wave), or completely blocked (Rees *et al.*, 1997). Reentry is a probable cause of ventricular tachycardia and ventricular fibrillation that originates in the area of unidirectional block of the impulse that can allow reverse (retrograde) conduction (Rees *et al.*, 1997). As a result, the impulse is re-routed into cardiac tissue that has been excited and depolarizes (re-excites) the same tissue more than once to produce multiple impulses.

1.1.3 Drugs Used in the Treatment of Arrhythmias

The ultimate goal of antiarrhythmic therapy is to ensure adequate cardiac output by restoring sinus rhythm, controlling ventricular rate, and preventing the occurrence of arrhythmias. Antiarrhythmic drugs can be categorized according to the Vaughan Williams classification system based on their mechanism of action and on their ability to alter the electrophysiology of the heart (Vaughan Williams, 1989).

Class I antiarrhythmics

Class I antiarrhythmics generally block Na^+ channels. As a result of sodium current blockade the threshold for excitability (automaticity) is decreased and the refractoriness of the action potential is prolonged due to the shift of the voltage dependence of recovery from block (Roden, 1997). The class I antiarrhythmics are further subdivided into 3 groups depending on the rate of recovery from Na^+ channel block:

Class Ia – Exert their effects by blocking Na^+ and K^+ currents. The Na^+ channel is blocked in the open-state and results in an increased threshold for excitability and decreased automaticity with an intermediate recovery time (Roden, 1997). The K^+ channel blockade results in prolonged action potentials. The combination blockade increases the effective refractory period. Representative class 1a compounds are quinidine and disopyramide.

Class Ib – Blocks both open and inactivated Na^+ channel which decreases automaticity and increases the threshold of excitability and results in an increase in the effective refractory period. Class Ib are characterized by a very rapid recovery from block (Hondeghem and Katzung, 1984). Representative compounds are lidocaine and mexilitine.

Class Ic – Channel blockers that block Na^+ current and delayed rectifier and are characterized with very slow recovery from block (Roden and Woosley, 1986). Representative compounds are flecainide and encainide.

Class II antiarrhythmics

Class II antiarrhythmics are β-adrenergic blockers that predominantly antagonize cardiac β1 receptors and act by reducing sympathetic activity in the heart (Roden, 1997). Therefore, β-adrenergic antagonists exert antiarrhythmic action by reducing heart rate, decreasing intracellular Ca^{2+} overload, and reducing sinus node automaticity. β-adrenergic blockers, such as propranolol, timolol, and metoprolol have been shown to reduce mortality in trials of chronic therapy after myocardial infarction (Singh, 1990).

Class III antiarrhythmics

Class III antiarrhythmics are generally K^+ channel blockers that may also non-selectively interact with other ion channels. Potassium channel blockers have the ability to decrease automaticity and increase the effective refractory period by prolonging the AP duration (seen as an increase in QT interval), which should be effective against re-entry arrhythmias (Singh, 1993). However, class III antiarrhythmics such as amiodarone, bretylium, and sotalol have been associated with proarrhythmia due to excessive QT prolongation.

Class IV antiarrhythmics

Class IV antiarrhythmics are Ca^{2+} channel blockers that reduce the slow inward Ca^{2+} current in the sinoatrial and atrioventricular nodes, where Ca^{2+} channels predominate (Roden, 1997). The decrease in AV nodal conduction is seen as an increase in the PR interval of the AP. Representative class IV antiarrhythmics include verapamil and diltiazem.

1.1.4 The Need for New Antiarrhythmic Drugs

The majority of antiarrhythmic drugs that exert their action by ion channel blockade are toxic and will have undesirable consequences on cardiac electrophysiology with increasing concentrations. Such drugs that modify cardiac electrophysiology often demonstrate narrow margins between therapeutic doses and doses that induce arrhythmias with potentially life-threatening consequences (Roden, 1994). Early ion channel blockers, especially Class III K^+ channel blockers, such as amiodarone, were nonselective for their receptor targets and have been associated with inducing arrhythmias (Roden, 1994). Sodium channel blockade may also have adverse effects as demonstrated with two Class I antiarrhythmic agents, flecainide and encainide, in the Cardiac Arrhythmia Suppression Trial (CAST) in 1989 (Cast Investigators, 1989). The clinical trial demonstrated that antiarrhythmics which lacked selectivity could increase the occurrence of arrhythmias. Thus there is a need for more effective and less toxic antiarrhythmic compounds that demonstrate selectivity for damaged heart tissue as opposed to healthy tissue.

1.2 RSD1070

RSD1070, a novel antiarrhythmic agent, is a representative ether analogue of a new class of compounds synthesized by Nortran Pharmaceuticals Ltd. (Vancouver, BC, CANADA). The hydrochloride salt of RSD1070 is a white crystal in appearance and has a molecular weight of 375.9 Da with a melting point temperature of 198-200 °C. It is a basic compound (pKa ≈ 7.8) characterized by an ionizable nitrogen group. The mechanism of action of this compound has not been established at this stage; however, preliminary *in vitro* binding studies on a large group of receptors indicated preferential binding to Na^+ channels, a characteristic of a Class I antiarrhythmic compound (IC_{50} of 1.6 μg/mL or 4.8 μM). RSD1070 is currently in pre-clinical stages of development and is considered as a clinical candidate based on promising results demonstrated in arrhythmia models. Such models include whole animal conscious (oral and infusion administration) and unconscious (infusion) preparations involving arrhythmias physically-induced by coronary artery ligation and electrically-induced arrhythmias. Of particular interest, RSD1070 demonstrated ischaemia-selective activity in the modified Langendorff isolated heart perfusion apparatus. Global myocardial ischaemia was simulated by perfusing hearts with a "ischaemic" buffer solution of relatively greater acidity (pH 6.4) and potassium concentration (10 mM). Greater antiarrhythmic potency was demonstrated in the "ischaemic" buffer compared to "normal" buffer, thus suggesting greater potency in diseased tissue as opposed to normal tissue (Dr. S. Abraham, personal communications). However poor oral bioavailability (≈ 4-5 %) was demonstrated based on calculated plasma AUCs following oral (112 mg/kg) and iv (12 mg/kg) administration to rats during preliminary investigations (Nortan Pharmaceuticals Ltd., unpublished data). To this date, the metabolism of RSD1070 has not been profiled and the involvement of active metabolites contributing to its antiarrhythmic activity has been suspected.

1.3 *IN VITRO* METHODOLOGIES

The application of *in vitro* predictive studies using human tissues with novel pharmaceutical compounds in pre-clinical stages can be of clinical importance. The ability to obtain *in vivo* estimates of pharmacokinetic parameters prior to administration to man may play an important role in the selection of drug candidates for clinical trials. In general, there is a high rate of attrition of drug candidates that enter clinical development and it has been reported that approximately 40% of drug candidates were discontinued due to unacceptable pharmacokinetic properties, for example, poor bioavailability (Prentis *et al.,* 1988). Thus, novel pharmaceuticals may be excluded prior to clinical studies if they are expected to exhibit unsatisfactory human pharmacokinetic properties. Hepatic microsomes are a commonly used tool for investigative metabolism and kinetic studies.

1.3.1 Hepatic Microsomes

Hepatic microsomes are prepared from liver homogenate and result from the fragmentation of the endoplastic reticulum into many smaller (≈ 100 nm diameter) enclosed microvesicles (Dallner, 1974). Microsomes are "artificial", subcellular functional units of endoplasmic reticulum containing membrane-bound enzymes that are commonly used tools for the *in vitro* study of drug biotransformation. In general, microsomes catalyze a variety of reactions (known as Phase I biotransformation) that convert lipophilic endogenous and exogenous compounds to relatively more hydrophilic metabolites that are usually more readily excretable.

1.3.2 Cytochrome P- 450

The predominant hepatic microsomal enzyme system involved in Phase I reactions is the cytochrome P-450 system, also referred to as the mixed-function oxygenase system. The presence of a pigment capable of binding carbon monoxide in liver microsomes has been known since the late 1950's (Klingenberg, 1958; Garfinkel, 1958). Omura and Sato (1964) first demonstrated that reduced and catalytically functional cytochrome P-450 forms a ligand with carbon monixide to produce a maximal absorbance of light at 450 nm. The cytochrome P-450 system has been resolved into three components: cytochrome P-450 (a heme-containing enzyme), NADPH-cytochrome P-450 reductase (Lu and Coon, 1968), and phosphatidylcholine lipid (Lu *et al.*, 1969; Strobel *et al.*, 1970). Cytochrome P-450 serves as the substrate- and oxygen- binding site of the enzyme system, whereas the reductase serves as the electron carrier shuttling electrons from NADPH to cytochrome P-450. The two enzymes are embedded in the phospholipid matrix of the endoplastic reticulum, which provides the surface area for the transfer of electrons from NADPH-cytochrome P-450 reductase to cytochrome P-450. Cytochrome P-450 is a fairly ubiquitous enzyme found extra-hepatically in lung (Guengerich, 1977), small intestine (Stohs *et al.,* 1976), kidney (Ellin *et al*, 1971), colon (Fang and Strobel, 1978), skin and brain (Hodgson *et al.,* 1993), with the highest concentration found in the liver (Okey, 1990).

Cytochrome P-450 reactions primarily add or expose functional groups (e.g. –OH, -SH, $-NH_2$, -COOH), which permit lipid-soluble xenobiotic or endobiotic compounds to become more water soluble. Thus the relatively more lipophilic compound is biotransformed into polar, water-soluble metabolites for excretion, or into compounds that are more susceptible for Phase II conjugation reactions with endogenous moieties (e.g. glucuronic acid, sulfate) prior to elimination in either urine or bile (Sipes and Gandolfi, 1991). The biotransformed metabolites may exhibit no activity, less activity, or greater pharmacological activity or toxicity than the parent compound. More specifically, cytochrome P-450s catalyze a variety of oxidative reactions: hydroxylation of alkanes and aromatics, epoxidation of alkenes, dealkylation of secondary and tertiary amines and ether compounds, deamination of amines, conversion of amines to N-oxides, hydroxyl amines, and nitroso derivatives, and sulfoxidation of thio ethers (Gillette, 1971).

1.3.3 Cytochrome P-450 Catalytic Cycle

The mechanism of reactions catalyzed by cytochrome P-450 is well discussed and often reviewed (**Figure 4**). In essence, cytochrome P-450 catalyzes the incorporation of an oxygen atom from molecular O_2 into a broad range of substrates (RH), coupled with the reduction of the other oxygen atom by two electrons to water (Ortiz de Montellano, 1986). The catalytic site of cytochrome P-450 (**Figure 5**) consists of an iron protoporphyrin IX (heme) with cysteinate as the 5th ligand coordinated to the apoprotein for structural purposes. The 6th coordination site is bound to molecular oxygen and is in close proximity to the hydrophobic substrate-binding site (Groves and Han, 1995). The initial step of cytochrome P-450 catalyzed reactions involve binding of substrate (RH) with the oxidized cytochrome P-450 (Fe^{3+}) to form a substrate-cytochrome P-450 complex. The complex accepts an electron from NADPH via NADPH-cytochrome P-450 reductase, which reduces the iron in the heme moiety to the ferrous state (Fe^{2+}). Molecular oxygen is bound to the complex, which then accepts another electron from NADPH to form the unstable and highly reactive peroxoiron (III) complex. The "activated" O-O bond is protonated and cleaved, resulting in one oxygen atom incorporated into the substrate, while the other is reduced to water. Finally, the oxygenated substrate dissociates, regenerating the oxidized form of cytochrome P-450.

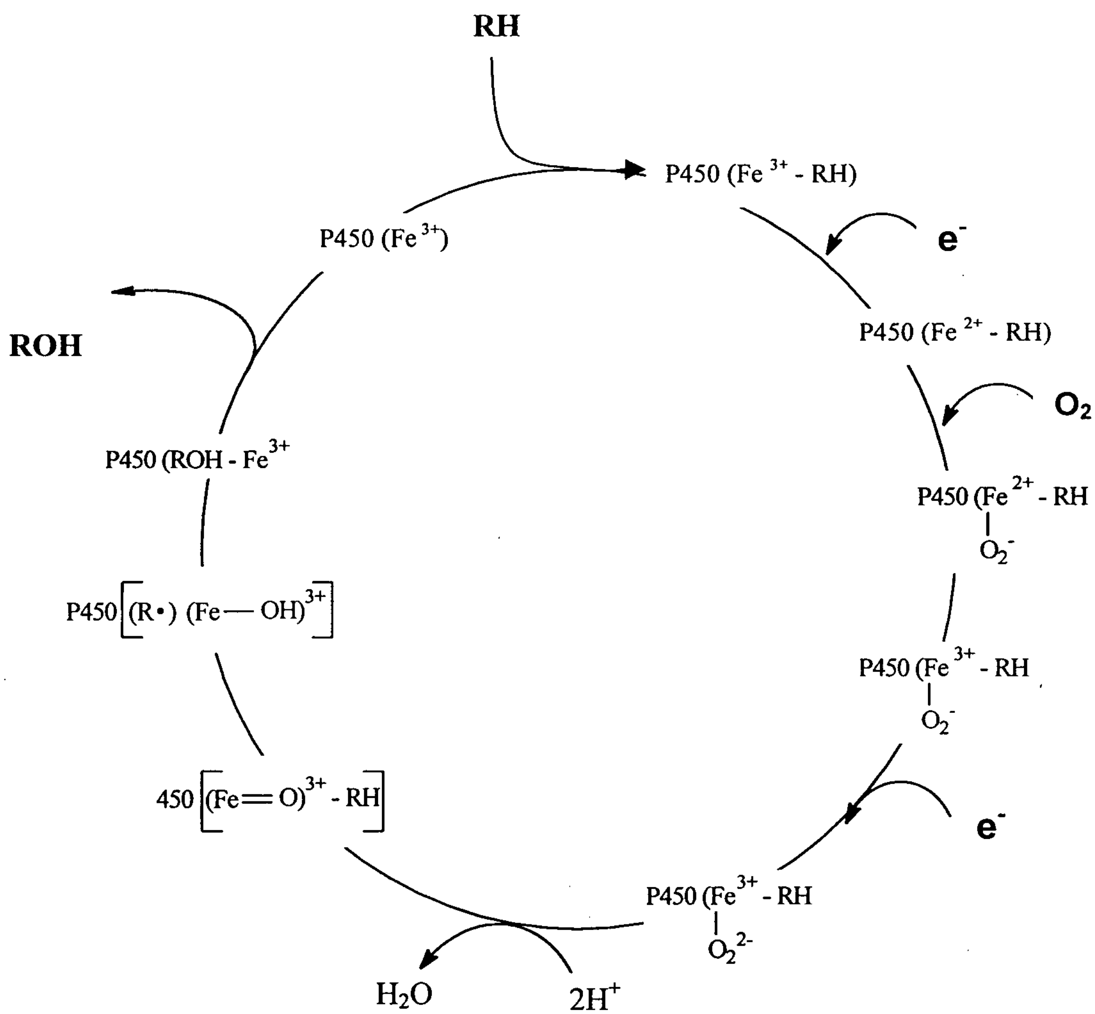

Figure 4. **Schematic of the catalytic cycle of cytochrome P-450. The substrate is RH, and the valence state of the heme iron in cytochrome P-450 is indicated (reproduced from Williams, 1989).**

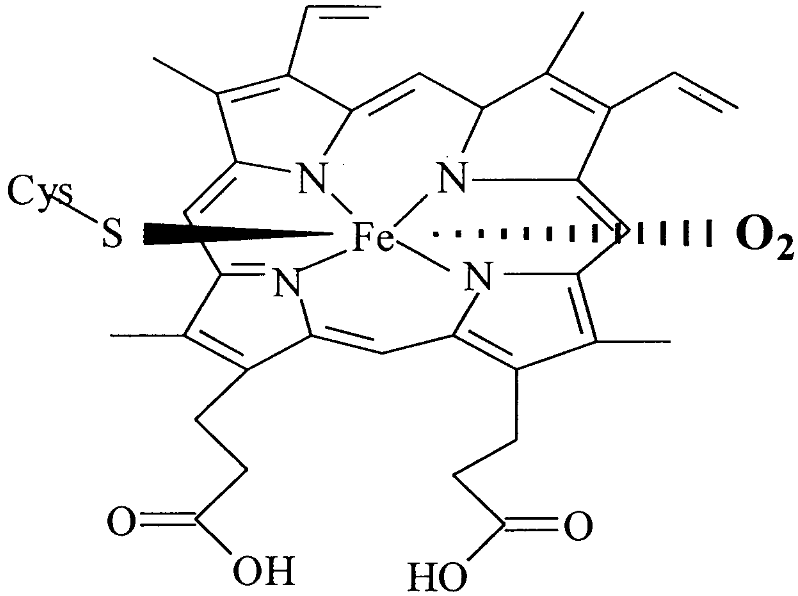

Figure 5. Simplified Structure of Cytochrome P-450. The network consisting of protophyrin heme (Fe) group attached to four nitrogen ligands allows the transfer of electrons from NADPH towards the heme. The 5th ligand is coordinated to a thio group of cysteine for structural purposes and the 6th ligand is coordinated to molecular oxygen in close vicinity to the substrate binding site.

1.4 *IN VITRO* PREDICTION OF *IN VIVO* HEPATIC CLEARANCE

Traditional drug metabolism studies have been interpreted in a qualitative manner with the majority of *in vitro* studies concerned with metabolite identification, establishing the responsible enzyme(s) involved, and investigating the mechanism of reaction (Houston and Carlile, 1997). Through recent advances in *in vitro* methodologies, together with the sensitivity of modern analytical chemistry, there has been drastic increase in quantitative metabolism studies in the last decade (Houston, 1994). Recent *in vitro* methodologies involve the use of liver microsomes, hepatocytes, and precision-cut liver slices as tools for drug metabolism for the prediction of hepatic clearance observed in animal models (reviewed by Houston and Carlile, 1997), and in humans (reviewed by Iwatsubo *et al.,* 1997). Investigations have centered mainly on the liver as this tissue represents the major site of metabolism for most compounds.

The concept of *in vitro* – *in vivo* correlation was first examined in a seminal study by Rane *et al.* (1977), and it was demonstrated, with the use of hepatic (S9) fractions, that the extent of hepatic extraction of several compounds could be estimated from Michaelis-Menten kinetic parameters (V_{max} and K_m). The activity of the drug metabolizing enzymes were expressed as intrinsic clearance (CL_{int}) calculated from the ratio of V_{max} to K_m specific for the oxidative biotransformation of the drugs under first order conditions. CL_{int} is defined as a pure measure of enzyme activity towards a drug and is independent of physiological factors such as hepatic blood flow or plasma protein binding (Wilkinson and Shand, 1975). The parameter CL_{int} serves as the foundation for the *in vitro* - *in vivo* correlation and can be considered as a proportionality constant to describe the relationship between metabolism rate (v_o) and free (unbound) concentration (see Eq.13).

Houston (1994) utilized a strategy that allowed the extrapolation of *in vitro* metabolism data in predicting *in vivo* metabolic clearance estimates using liver microsomes and hepatocytes. The first-stage involves measuring *in vitro* CL_{int} from the ratio of V_{max} to K_m parameters (termed "enzyme kinetic approach" hereafter) from the initial rate of either metabolite formation or parent compound disappearance. The next stage utilizes scaling factors to "scale-up" the *in vitro* CL_{int}, expressed per mg of microsomal protein or 10^6 hepatocytes, to an *in vivo* CL_{int} (mL/min/kg) that reflects the total microsomal protein or hepatocyte content in a liver. The final stage requires the use of a liver clearance model (e.g. well-stirred liver model) to incorporate the *in vivo* CL_{int}, as well as physiological factors such as hepatic blood flow and plasma protein binding into the predicted hepatic clearance (CL_h). Hepatic clearance describes the efficiency of the liver to irreversibly remove a drug from the perfusing blood in terms of the volume of blood from which drug is completely removed in unit time (Wilkinson and Shand, 1975).

The most common liver model used is the well-stirred (venous equilibrium) model, which was first applied by Rowland *et al.,* (1973) to describe kinetics of a drug eliminated by first-order processes in an isolated perfused liver system. Later, the venous equilibrium liver model was refined and extended to describe CL_h and extraction ratio (E) in terms of hepatic blood flow (Q), CL_{int}, and the fraction of unbound drug in plasma (f_u) under apparent first-order conditions (Wilkinson and Shand, 1975) according to the relationship

$$CL_h = QE = Q\left[\frac{f_u\, CL_{\text{int}}}{Q + f_u\, CL_{\text{int}}}\right] \qquad \text{(Eq.1)}$$

In this model, the liver is conceived to be a single well-stirred compartment and the concentration of unbound drug in the emergent blood is in equilibrium with the unbound drug within the liver (Rowland *et al.,* 1973). This physiological approach has been widely used for its simplicity in describing hepatic clearance in terms of the free fraction of drug, the intrinsic clearance of the overall elimination process and hepatic blood flow (Wilkinson and Shand, 1975; Pang and Rowland, 1977). Furthermore, the model allows the prediction of hepatic clearance and the classification of drug metabolism based on the hepatic extraction ratio- the fraction of drug removed by the liver.

An alternative method to the enzyme kinetic approach is the *in vitro* half-life approach, first applied by Obach *et al.*, (1997) for the ability to accurately and successfully predict human clearance. In this method, CL_{int} is determined by measuring the first-order rate for consumption of the substrate under linear conditions (at low substrate concentrations such that $[S] << K_m$), and the values scaled up to project human *in vivo* clearance. The fundamental basis of the *in vitro* half-life method lies in the derivation of the integrated Michaelis-Menten equation and is outlined in Appendix 1.

Obach (1996) investigated the importance of non-specific binding of several test compounds to microsomal matrices and its impact on CL_{int} for *in vitro – in vivo* correlation. It was observed that clearance values predicted from human and animal liver microsome studies were highly underestimated for compounds (primarily lipophilic amines) that exhibited high values of plasma protein binding (low f_u). Since CL_{int} is often calculated as the ratio of the apparent Michaelis-Menten constants (V_{max} to K_m), the determination of a "true" K_m is required based on the theory that only unbound substrate concentration in the incubation matrix is available to interact with the enzyme in a manner to permit catalysis (Obach, 1996). In *in vitro* metabolism systems such as microsomes, the assumption that the drug present in the incubation is unbound and available to interact with the enzyme is not always valid for many compounds. Non-specific binding of compounds to the microsome matrix may occur in the lipid component and/or the protein component of the microsome. Obach corrected the apparent K_m ($K_{m\ (app)}$) obtained from plots of reaction velocity versus initial substrate concentrations with values for free fraction in microsomal incubates ($f_{u\ (mx)}$) obtained by equilibrium dialysis according to the modification of the well-stirred liver model:

$$CL_h = \frac{Q \cdot f_u \cdot \dfrac{V_{\max}}{K_{m\,(app)} \cdot f_{u\,(mx)}}}{Q + f_u \cdot \dfrac{V_{\max}}{K_{m\,(app)} \cdot f_{u\,(mx)}}} \qquad \text{(Eq.2)}$$

where CL_h is hepatic clearance, Q is the hepatic blood flow, f_u and $f_{u(mx)}$ are the free fraction of drug in plasma and microsomal matrices respectively, Vmax is the maximum reaction rate, and $K_{m\,(app)}$ is the apparent Michaelis constant.

In a recent study, the *in vitro* half-life approach was used to extensively examine the significance of microsomal protein binding of a wide panel of drugs in the prediction of human clearance from CL_{int} obtained from microsome metabolism data (Obach, 1999). Good correlation between *in vivo* clearance values and clearance values estimated from *in vitro* CL_{int} were made utilizing the *in vitro* half life-approach with inclusion of both blood and microsome binding parameters.

1.5 RATIONALE AND OBJECTIVES

The *purpose* of this project was to utilize *in vitro* and *in vivo* methodologies to further investigate the metabolism and pharmacokinetics of RSD1070 and provide a possible explanation for the poor oral bioavailability. Although the ultimate goal is to advance RSD1070 into clinical stages of development for testing in man, and despite the availability of human liver microsomes and cryoperserved human hepatocytes, the rat was chosen as the animal for investigation. Since RSD1070 was unable to be tested in man, the rat model allowed for a complete investigation of both whole animal studies and *in vitro* studies, thus allowing for *in vitro* – *in vivo* correlation to be examined. The *hypothesis* is that the poor oral bioavailability of RSD1070 in rats is due to high hepatic extraction. The above hypothesis was tested according to the following objectives:

Objective #1 – To develop and validate a quantitative LC/MS/MS assay for the detection of RSD1070 and the metabolite(s) of interest in various biological matrices.

Objective #2 – To identify RSD1070 metabolites from hepatic microsomal incubates.

Objective #3 – To estimate the contribution of hepatic clearance and hepatic extraction ratio to explain the poor oral bioavailability of RSD1070 from kinetic parameters by conducting pharmacokinetic studies in rat

Objective #4 – To conduct protein binding studies for the estimate of free fraction of RSD1070 in blank plasma and in microsomal incubates.

Objective #5 – To use two approaches (the enzyme kinetic method and the *in vitro* half-life method) to calculate *in vitro* CL_{int} of RSD1070 using hepatic microsomal metabolism studies.

Objective #6 – To assess the use of microsomal studies to predict the observed hepatic clearance and hepatic extraction ratio in rat.

CHAPTER 2

MATERIALS, INSTRUMENTATION AND ASSAY METHODOLOGIES

2.1 MATERIALS

2.1.1 Chemicals

BDH Chemicals Inc. (Toronto, ONT, CANADA)

Ethylenediaminetetraacetic acid (EDTA), formic acid (98%), Phenol Reagent (Folin & Ciocalteu), magnesium chloride hexahydrate, sodium carbonate, di-sodium hydrogen orthophosphate, sodium hydroxide, and hydrochloric acid.

Boehringer Mannheim (GMBH, Germany)

β-nicotinamide-adenine dinucleotide phosphate tetrasodium salt (NADPH).

Caledon Laboratories Ltd. (Georgetown, ONT, CANADA)

Methanol (HPLC grade) and potassium chloride.

Fischer Scientific (Vancouver, BC, CANADA)

Methyl-*tertiary* butyl ether (HPLC grade).

J.T. Baker (Phillipsburg, NJ, USA)

Sodium dithionite.

Mallincrokdt Inc. (Paris, KY, USA)

Sodium phosphate monobasic.

Sigma Chemical Co. (St. Louis, MO, USA)

Trichloroacetic acid, sucrose, glycerol, tris[hydroxymethyl]aminomethane (Trizma® Base), bovine serum albumin (fraction V), anhydrous potassium phosphate (monobasic and dibasic), and sodium potassium/tartarate.

2.1.2 Other Materials

De-ionized high purity water (referred to as 'distilled or deionized water' in text) was produced on-site by reverse osmosis and subsequent filtration using a Milli-Q® water system (Millipore, Bedford, MA, USA).

Sample preparation equipment consisting of micro-centrifuge tubes, borosilicate glass screw top culture tubes, teflon-lined screw caps, borosilicate glass autosample vials and inserts were purchased from VWR Scientific (Edmonton, AB, CANADA). Teflon lined autosample crimp tops were purchased from Hewlett-Packard (Avondale, PA, USA).

Somnotol®, sodium pentobarbital was purchased from MTC Pharmaceuticals and was utilized during animal surgery (Cambridge, ONT, CANADA).

Arterial blood sampling 1cc plastic syringes containing 50 units of lyophilized sodium heparin and heparin Vacutainer® blood collection tubes utilized for sample collection for pharmacokinetic studies were obtained from Fischer Scientific (Vancouver, BC, CANADA).

Hypodermic BD 23 G1, 20 G1.5, 22 G2, 16 G0.5 needles and tuberculin 1cc syringes utilized for drug administration and plasma sample collection were purchased from Canlab (Mississauga, ONT, CANADA).

Polyethylene tubing PE-20 was obtained from Clay Adams (Parsippany, NJ, USA).

2.1.3 RSD1070, N-dealkylated RSD1070 metabolite, and Internal Standard.

RSD1070, (±)-trans-[2-Morpholinyl-1-(1-naphthaleneethyloxy)] cyclohexane mono-hydrochoride, and the N-dealkylated RSD1070 metabolite were synthesized by Nortran Pharmaceuticals Inc., (Vancouver, BC, CANADA). One *m*g/mL stock solution of each was prepared in distilled water and frozen at –20 °C. Further stock solutions were prepared from the 1 mg/mL stock to yield 10 µg/mL stock and 100 ng/mL working solutions. These solutions were also frozen at –20 °C. The internal standard, RSD921, was synthesized by Nortran Pharmaceuticals Ltd, (Vancouver, BC, CANADA). One mg/mL stock solution and 0.5 µg/mL working solution of IS were prepared and frozen at –20 °C. All above working solutions were stored at –20 °C in 15-mL aliquots in glass scintillation vials. Fresh aliquots of RSD1070 and IS working solutions were thawed and used once for each assay.

2.1.4 Animals

Male Sprague-Dawley rats weighing 200-300 g were obtained from the Animal Care Facility at the University of British Columbia (Vancouver, BC, CANADA). The animals were housed in Plexiglass® cages on corn-cob bedding with free access to food and water *ad libitum* and were maintained on a 12 hr light/12 hr dark cycle. Room temperature was maintained at 22 °C and with constant humidity.

2.2 ASSAY PROCEDURES

2.2.1 Sample Extraction

All samples, standards, and quality control samples were assayed as illustrated in **Figure 6**. Appropriate volumes of biological fluids (10-1000 μL) were diluted with their respective blank matrix for analysis. Sample dilution was required to quantitate analyte concentrations within the linearity of the assay. The samples were transferred to borosilicate glass screw top culture tubes. Distilled water was added for a final volume of 1 mL for all plasma samples. Internal standard (100 μL) and 2M NaOH (100 μL) were added and tubes were mixed on a vortexer. Methyl *tert*-butyl ether (5 mL) was added to each tube by bottle pump. The tubes were capped and mixed briefly on a vortexer prior to and after placement in a Labquake® mixer (LabIndustries, Berkeley, CA, USA) for 30 min. In order to separate the organic and aqueous layers, all tubes were centrifuged (3000 rpm x 10 min). The organic layer was removed and transferred to clean borosilicate glass screw top culture tubes by glass Pasteur pipette. The organic layer was dried under a gentle stream of nitrogen for 20 min at 30 °C with a N_2 pressure of 0.5 PSI using a Zymark Turbo Vap® LV Evaporator (Zymark Corporation, Hopkinton, MA, USA).

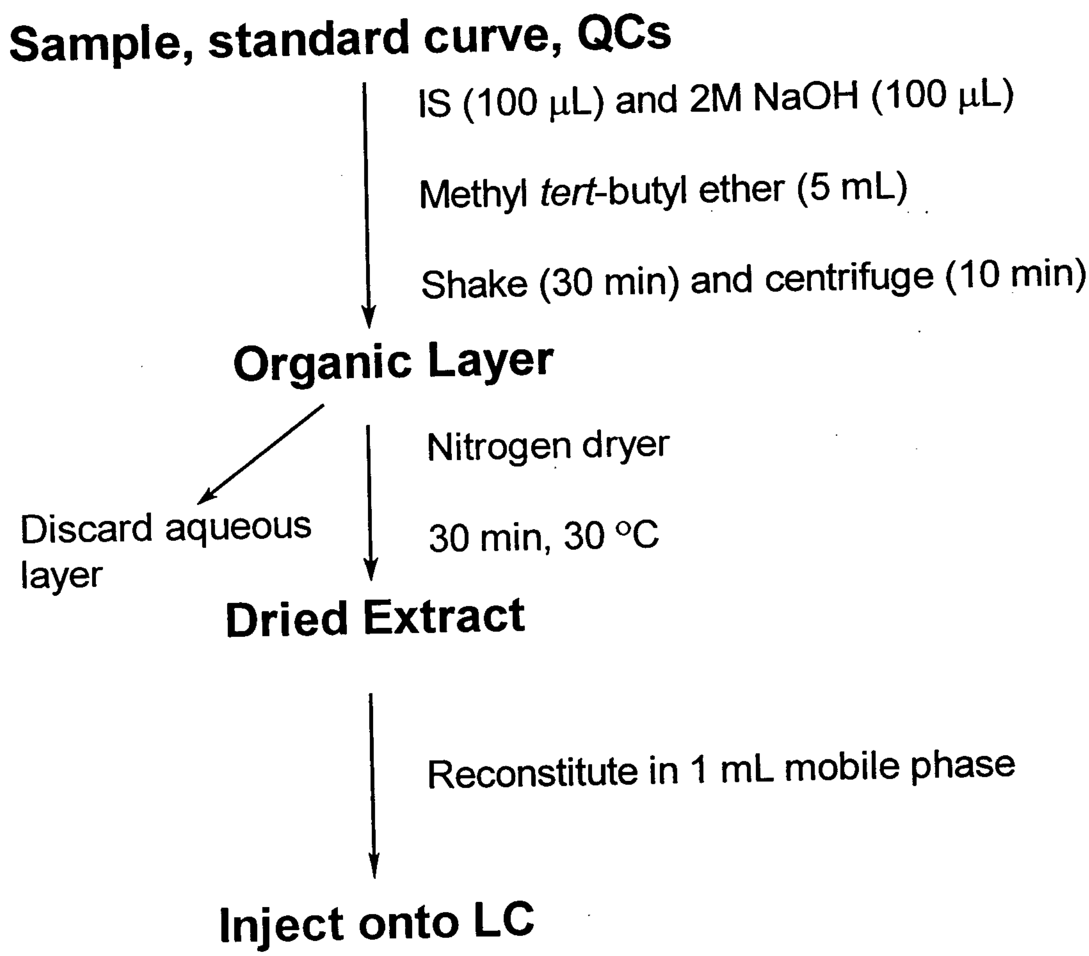

Figure 6. Liquid-liquid extraction procedure for the quantification of RSD1070 and its metabolite in plasma, urine, and microsomal incubates for LC/MS/MS.

2.2.2 Calibration Curves and Quality Control Samples

Samples prepared for calibration curves and quality control (QC) samples were treated in the same manner as test samples. Working stock solutions of 100 ng/mL mixture of RSD1070 and N-dealkyl RSD1070 prepared in distilled water were used for all calibration curve standards. Calibration standards (at concentrations of 2.5, 5, 10, 25, 50, and 100 ng/mL for both RSD1070 and its metabolite) were prepared by adding appropriate amounts of the working stock solution to 150 μL of blank plasma, urine, or boiled microsomal protein. The QC samples of low (3 ng/mL), mid (15 ng/mL) and high (75 ng/mL) concentrations were prepared separately, frozen, and thawed for daily use. Control (blank) standards contained either 150 μL of plasma, urine, or boiled microsomes made up to 1 mL with distilled water. Weighted linear regression ($1/y^2$) was performed between the peak area ratio of each analyte to that of the IS *vs.* the corresponding spiked concentration to reduce bias at the lower concentrations.

2.2.3 Method Validation

Method validation was performed by evaluating inter-assay and intra-assay accuracy (% bias) and precision (% coefficient variation, CV) of the low, mid, and high QC concentrations. This was accomplished by analyzing 6 sets of calibration curves and QC samples on 6 separate days (inter-assay) and on the same day (intra-assay). Quantitation of QC samples was performed by analyzing the calibration curve standards and back calculating the concentration of each QC sample from the obtained slope, intercept and the peak area ratios.

The accuracy of the assay was assessed as the % bias of the nominal concentration observed for the spiked QCs and was calculated as:

$$\% \, bias \;=\; \frac{Back\ calculated\ concentration \;-\; \text{Nominal}\ concentration}{\text{Nominal}\ concentration} \times 100\,\% \qquad \text{(Eq.3)}$$

A bias of < ± 15% at each concentration was considered to be acceptable accuracy.

The precision of the assay (% CV) was determined from the variance observed for the mean of replicate QCs of low, mid and high concentration and was calculated as:

$$\% \, CV \;=\; \frac{Mean\ concentration}{SD} \times 100\% \qquad \text{(Eq.4)}$$

Precision of < 15% CV at the mid and high QC concentrations and < 20% at the low QC concentration was considered to be acceptable variability.

2.2.3 Extraction Efficiency

Relative percent recovery of RSD1070 in plasma was determined at concentrations (2.5, 3, 5, 10, 15, 25, 50, 75, and 100 ng/mL) representing the entire range of the calibration curve. Two sets of samples, the *control* (non-extracted) group and the recovery (extracted) group, were prepared in triplicate with known amounts of analyte. The control group was prepared in mobile phase (40% methanol, 0.2% formic acid (FA)) spiked with 50 ng of IS and injected onto the LC. The recovery group was prepared in water, extracted, and dried under N_2 gas as described in Section 2.2.1. The extracted samples were reconstituted in mobile phase with the addition of IS and injected into the LC/MS/MS system. Peak area ratios (PAR) of analyte to IS were obtained from chromatograms of *control* and *recovery* group samples at each concentration. Extraction efficiency (% of non-extracted PAR) was determined from the ratio of $PAR_{extracted}$ / $PAR_{non-extracted}$ at each different analyte concentration.

2.2.4 Analyte Stability in Plasma

Triplicate tests were carried out to establish the stability of the analytes in plasma under the routine sample handling in the lab. This included the following:

Bench-Top Stability: Blank plasma was spiked with analyte (at concentrations representing the calibration curve) and IS. The samples were left on the bench-top overnight (12 hr at room temperature) and processed the next day.

Freeze-thaw Stability: Blank plasma was spiked with analyte (at concentrations representing the calibration curve) and IS. The samples were subjected to freezing (at –20 °C) and thawing on the bench-top at room temperature. The samples were then processed.

The relative stability of analyte for each test was performed by comparing the peak area ratio (analyte to IS) obtained from the stability testing at each concentration to the peak area ratio of a freshly prepared standard processed on the same day.

2.3 INSTRUMENTATION AND ANALYTICAL METHODS

2.3.1 Centrifuges

A Beckman Model J-6B centrifuge equipped with a JA-17 fixed angle rotor (9,500 rpm) and a Beckman Model LE-80 Ultracentrifuge equipped with a 50.2Ti fixed angle rotor (33,500 rpm) (Beckman Instruments Inc., Palo Alto, CA, USA) was used during the preparation of hepatic microsomes. A Fischer Scientific Micro Centrifuge Model 235C (13,600g – fixed) was used during the pharmacokinetic study to separate plasma from blood samples. A Beckman GP centrifuge equipped with a GH-3.7 rotor (Beckman Instruments Inc., Palo Alto, CA, USA) was used during the drug extraction procedure to separate the organic and aqueous layers.

2.3.2 Spectrophotometers

A Shimadzu UV-160 UV/VIS recording spectrophotometer was used for the Lowry protein assay. A SLM – Aminco DW-2C dual-beam UV-VIS Spectrophotometer (Urbana, IL, USA) was used to determine the concentration of cytochrome P450.

2.3.3 High Pressure Liquid Chromatography-Tandem Mass Spectrometry

LC/MS/MS detection of RSD1070, internal standard, and N-dealkylated RSD1070 metabolite was carried out using a Fisons VG Quattro (Altrinchem, UK) tandem mass spectrometer interfaced with a Hewlett Packard (Avondale, PA, USA) 1090 II liquid chromatograph. The HPLC eluent was introduced to the stainless steel capillary probe held at 3 kV. Positive electrospray was used as the means of ionization and collision-induced dissociation involved argon as the neutral target gas at a pressure of $\approx 3.5 \times 10^{-3}$ mBar and with collision energy of 40 eV. Cone voltage was set at 30 V with a source temperature of 140 °C. The low-mass and high-mass resolutions were set at 12.5/12.5 for MS1 and 5.0/5.0 for MS2. Mass selective detection of RSD1070, N-dealkylated RSD1070 metabolite, and IS were performed by multiple reaction monitoring (MRM) with a dwell time of 0.3 seconds /channel and with an inter channel delay of 0.03 seconds. Parent-daughter ion transitions detected were *m/z* 314 > 142 (N-dealkylated metabolite), *m/z* 340 > 155 (RSD1070), and *m/z* 357 > 147 (internal standard). The operation of both instruments and mass-spectrometric data acquisition were controlled with a Windows-NT® based Pentium Pro 200 MHz personal computer using the MS data handling software, MassLynx® (MicroMass, Chesire, UK).

2.3.4 HPLC Conditions

Samples were reconstituted in 1 mL of mobile phase (40 % MeOH, 60 % H_20 in 0.2% formic acid), and 10 μL of sample was injected onto a Phenomenex (Torrance, CA, USA) Columbus C18 column (150 x 2 mm, 5μ) and delivered at 0.2 mL/min at room temperature (23 °C). The HPLC autoinjector syringe and sample loop volumes were 25 and 250 μL, respectively. Linear gradient conditions were as follows: 40% to 80% MeOH from 0 to 8 min and a return to 40% MeOH at 8.5 min. Total run time was 12 min.

2.4 PHARMACOKINETIC STUDY OF RSD1070

2.4.1 Animal Surgery

All animal experiments described in this thesis was approved by the University of British Columbia Animal Care Committee. Technicians at Nortran Pharmaceuticals Ltd. (Vancouver, B.C., CANADA) conducted animal surgery in compliance to the guidelines of the Canadian Council on Animal Care. In brief, male Sprague-Dawley rats were anaesthetized with 65 mg/kg sodium pentobarbital ip using 23G needles. Hair overlying the abdominal incision site was removed with clippers and an abdominal midline incision was made to expose the peritoneal cavity. The intestines were carefully displaced using saline covered swabs so as to expose the abdominal aorta and inferior vena cava. The vessels were cannulated with PE-20 cannulae inserted into the above vessels so as to "float" in the vessel. The abdomen was closed in two layers (peritoneum and then skin) with sutures. The cannulae were passed through a trocar and exteriorised by threading the trocar under the skin of the back and out through a small incision at the mid-scapular region. All trocar and incision sites were closed with silk sutures and morphine was administered (2.5 mg/kg, sc) to alleviate post-operative pain. The animal was returned to a separate clean recovery cage with food and water *ad libitum.* At least 24 hrs was allowed for recovery before commencing with the experiment. All animals appeared healthy with normal locomotor function and behavior.

2.4.2 Preparation of RSD1070 Solution for Injection

Aqueous solutions of RSD1070 were prepared fresh the day of administration at concentrations of 12 mg/mL. The drug was administered at an injection volume of 1 mL/kg to achieve a standardized dose of 12 mg/kg of body weight. The solution was administered to a group of 8 rats weighing 200-300 g via inferior vena cava cannula as a single iv bolus over a 1-minute period.

2.4.3 Plasma Sample Collection

Following administration of the iv bolus, samples of blood (0.25 mL) were withdrawn via the abdominal aorta cannula using 23G needles and 1cc syringes containing 50 units of lyophilized sodium heparin. Blood samples were taken at specific time intervals (2.5, 5, 10, 15, 20, 45, 60, 120, 240, 360, 540, 720, and 1440 min), placed into Eppendorf® microcentrifuge tubes, and centrifuged at 5000 rpm for 5 min. The plasma was then removed, transferred to a new Eppendorf® microcentrifuge tube and frozen at –20 °C until assayed by LC/MS/MS.

2.4.4 Urine Sample Collection

Following administration of the iv bolus, the rats (n=8) were immediately housed in stainless steel metabolic cages equipped with a screw top glass bottle (35 mL capacity) to collect the urine. The animals were allowed access to food and water *ad libitum*. Total urine was collected for 24 hrs. The urine collected was frozen in aliquots every 4-6 hrs at –20 °C until assayed by LC/MS/MS.

2.5 *IN VITRO* PROTEIN BINDING BY EQUILIBRIUM DIALYSIS

2.5.1 Determination of Fraction Unbound (f_u) in Plasma

Pooled plasma from untreated male Sprague-Dawley rats were spiked with RSD1070 for final concentrations of 0, 1, 5, and 10 μg/mL. Membrane dialysis sacs (Sigma Diagnostics, Inc., St. Louis, MO) with a molecular weight cutoff of 12,000 MW and dimensions of 25 mm x 16 mm x 30 cm were placed between Plexi-glass® dialysis cells (1 mL capacity). Isotonic phosphate buffer consisted of 3.9 g NaCl, 1.8 g KH_2PO_4, and $NaHPO_4 \cdot 7\ H_20$ in 1 L water. The membrane was conditioned by boiling in distilled water for 30 min to remove any impurities, and by soaking in phosphate buffer for 1 hr prior to mounting in the equilibrium dialysis units. Equal volumes of plasma sample and phosphate buffer (0.8 mL) were transferred to their respective dialysis cells using 1 cc syringes with 20 G1.5 needles. All solutions were removed from the units after 5 hrs of incubation time using 1 cc syringes with 22 G2 needles and assayed as described in Section 2.2.1.

2.5.2 Determination of Equilibration Time

Plasma sample (10 μg/mL RSD1070) and phosphate buffer were transferred to equilibrium dialysis units and the units were placed in a 37°C shaking water bath. The phosphate buffer was removed from their dialysis chambers at a specific time period (1, 2.5, 3, 4, 5.5, 6.5, and 8 hrs), transferred to a microcentrifuge tube, and frozen at –20 °C until further analysis.

2.5.3 Stability of RSD1070 In Plasma and Phosphate Buffer

The stability of RSD1070 was tested in control rat plasma and in the phosphate buffer used for equilibrium dialysis. Plasma and phosphate buffer (2 mL) were spiked with RSD1070 for a final concentration of 10 μg/mL in borosilicate culture tubes. The plasma and phosphate buffer samples were mixed with a vortexer and incubated in a 37 °C shaking water bath. At specific time periods (0, 1, 2, 4, 6, 8, 18 hrs), 20 μL samples were removed, placed in microcentrifuge tubes, and frozen at –20 °C until further analysis.

2.5.4 Recovery of RSD1070 from Equilibrium Dialysis Apparatus

Control rat plasma was spiked with RSD1070 to yield a final concentration of 10 μg/mL. The spiked plasma was allowed to incubate for 2 hrs in a 37 °C shaking water bath. To determine the total amount of RSD1070 recovered, 0.8 mL of plasma sample was transferred into equilibrium dialysis cells and dialyzed against an equal volume of phosphate buffer. The equilibrium dialysis units were placed in a 37 °C shaking water bath for 7 hrs. The plasma and phosphate buffer were removed and transferred into a microcentrifuge tube and frozen at –20 °C until further analysis.

2.5.5 Determination of Fraction Unbound in Microsomal Matrix ($f_{u\ mx}$)

The free, unbound fraction of RSD1070 was determined in microsomal matrix. Blank microsomal matrix (0.1 mg microsomal protein/ mL) was spiked with RSD1070 (1.7 μg/mL final concentration) and incubated for 30 min at 37 °C in a water bath. NADPH cofactor was excluded to prevent metabolism of parent compound. The sample was transferred to equilibrium dialysis units and free fraction was determined as described in section 2.5.1. In addition, the time to reach equilibrium was determined as described in section 2.5.2.

2.6 RAT HEPATIC MICROSOME EXPERIMENTS

2.6.1 Preparation of Rat Hepatic Microsomes

Male Sprague-Dawley rats weighing 190-270 g (n=4) were sacrificed by decapitation, the liver was immediately removed, weighed, and placed into homogenizer tubes on ice with ice-cold 0.05 M Tris-HCl / 1.15% KCl buffer. Livers were homogenized, the homogenate pooled into centrifuge bottles and spun in a centrifuge at 9,000 x *g* for 20 min at 4 °C. The supernatant (S-9) was filtered through gauze and spun in an ultracentrifuge at 105,000 x *g* for 60 min at 4 °C. The resulting microsomal pellet was resuspended in 30 mL of 0.25 M sucrose solution in the homogenizer. Aliquots of microsome preparation (0.5 mL) were stored frozen in Cryovials® (Ingram & Bell, Richmond, B.C.) at –70 °C.

Total cytochrome P450 content was assayed by the method of Omura and Sato (Omura and Sato, 1964). Microsome protein was determined by the method of Lowry *et al.* (Lowry *et al.*, 1951).

2.6.2 Preliminary Microsomal Incubation Studies

Qualitative metabolic profiling of RSD1070 was conducted under conditions with excess substrate (RSD1070), co-factor (NADPH), and protein concentration over a time period of 0 - 30 min. Incubation media consisted of 920 μL of 50 mM KPO_4 buffer with 3 mM $MgCl_2$ (pH 7.4), 50 μL of sucrose diluted microsomes and 10 μL of 100 mM NADPH, and pre-incubated for 5 minutes at 37 °C in a 12 x 75 mm borosilicate culture tube. The reaction was initiated with addition of 20 μL of RSD1070 solution and terminated with addition of 150 μL of 10% trichloroacetic acid. Final incubation concentrations ranged from 0 – 17 μg/mL RSD1070, 0 - 1 mg/mL protein concentration, and 1 mM NADPH. Samples were processed and analyzed as described in section 2.2.1. Ion peaks were detected in the microsomal samples using MS1 in scan mode over the range *m/z* 100 – 500.

2.6.3 Microsome Dependent Formation and Consumption of N-dealkyl RSD1070

Optimal microsomal protein concentration for the formation of the N-dealkyl metabolite (m/z 314) was determined over a protein concentration ranging from 0.1 to 1 mg/mL. Incubation conditions included 17 μg/mL (50 mM) RSD1070 and 1.5 mM NADPH in 50 mM KPO_4 / 3 mM $MgCl_2$ buffer. Reactions were incubated for 10 min at 37 °C and terminated with the addition of 150 μL 10% trichloroacetic acid.

The formation and disappearance of N-dealkyl RSD1070 was monitored with microsomal incubation conditions of 0.25 mg/mL microsomal protein and 1.5 mM NADPH suspended in 50 mM KPO_4 / 3 mM $MgCl_2$ buffer. The mixture was incubated for 5 min at 37 °C and the reaction was initiated with addition of 50 μL RSD1070 or N-dealkyl RSD1070 (final substrate concentration was 1.7 μg/mL. Incubations were conducted in duplicate and were terminated with 100 μL NaOH (2 M) after 0, 2.5, 5, 10, 15, 20, and 30 minutes of incubation. NaOH was demonstrated to successfully terminate the enzyme reaction and was used as a substitute for trichloroacetic acid. This allowed the samples to be processed immediately by liquid-liquid base extraction. Furthermore, 1.5 mM NADPH concentration was used for all microsomal incubations hereafter instead of 1 mM (as used in section 2.6.2) to ensure excess NADPH cofactor.

2.6.4 Parent Compound Disappearance Studies

The disappearance profile of RSD1070 in microsomal incubations was monitored. Incubations were conducted in duplicate and the conditions were described in section 2.6.3. The initial RSD1070 substrate concentrations used were 0.34, 0.84, 1.7, 3.4, and 8.5 μg/mL. Incubation time ranged from 0-30 minutes and was terminated with addition of 100 μL NaOH (2 M).

2.7 DATA ANALYSIS

2.7.1 Calculation of Pharmacokinetic Parameters

Apparent pharmacokinetic parameters were calculated with single iv bolus non-compartment modeling using WinNonlin (Version 1.1). Area under the plasma concentration-time curves

(AUC_∞) were obtained by the trapezoidal rule and extrapolated to infinity. The terminal elimination constant, β, was calculated from the elimination phase of the log plasma concentration versus time plot. The apparent pharmacokinetic parameters, total body clearance (CL_{tot}), half-life ($t_{1/2}$), volume of distribution of the terminal elimination phase (V_{area}), and renal clearance (CL_r) were calculated using the following equations:

$$CL_{tot} = \frac{Dose}{AUC_\infty} \quad \text{(Eq.5)}$$

$$t_{1/2} = \frac{0.693}{\beta} \quad \text{(Eq.6)}$$

$$V_{area} = \frac{CL_{tot}}{\beta} = \frac{Dose}{AUC_\infty \cdot \beta} \quad \text{(Eq.7)}$$

$$CL_r = \frac{Total\ amount\ excreted\ unchanged}{AUC_\infty} \quad \text{(Eq.8)}$$

2.7.2 Calculation of *In Vivo* Hepatic Clearance and Extraction

The assumption was made that total body clearance (CL_{tot}) was approximately the sum of hepatic (CL_h) and renal (CL_r) clearances. Therefore, hepatic clearance was calculated as:

$$CL_h = CL_{tot} - CL_r \quad \text{(Eq.9)}$$

The venous equilibrium (well-stirred) model operationally describes the *in vivo* hepatic clearance (CL_h) and hepatic extraction ratio (E) in terms of hepatic blood flow (Q) under apparent first-order conditions according to:

$$CL_h = Q \cdot E \quad \text{(Eq.10)}$$

Hepatic extraction ratio (E) was calculated as:

$$E = \frac{CL_h}{Q} \qquad \text{(Eq.11)}$$

2.7.3 Calculation of *In Vitro* Intrinsic Clearance

In vitro intrinsic clearance (CL_{int}) was estimated from the initial rate of parent compound consumption under linear first order conditions at low [S], such that $[S]_o << K_m$. The initial velocity (v_o) of the reaction was measured from the slope of the initial linear decline for each $[S]_o$ disappearance profile. A plot of v_o versus $[S]_o$ was hyperbolic, and V_{max} and apparent K_m were estimated by non-linear regression fitting the data to the standard Michaelis-Menten equation:

$$v_o = \frac{V_{max} \bullet [S]}{K_m + [S]} \qquad \text{(Eq.12)}$$

CL_{int} can be estimated under linear first order conditions where $[S]_o << K_m$:

$$CL_{int} = \frac{V_{max}}{K_m} = \frac{v_o}{[S]} \qquad \text{(Eq.13)}$$

In the other method, referred to as the "*in vitro* $t_{1/2}$ method" (Obach *et al.,* 1997), CL_{int} was determined by measuring the half-life from the slope of the log concentration versus incubation time relationship under linear conditions ($[S] << K_m$). The rate constant under first order conditions was used in the conversion to *in vitro* $t_{1/2}$ values by the relationship $t_{1/2} = -0.693/k$.

The fundamental basis of the approach lies in the derivation of the integrated Michaelis-Menten equation (Appendix 1), and the relationship between *in vitro* $t_{1/2}$ and CL_{int} reduces to:

$$CL_{int} = \frac{V_{max}}{K_m} = \frac{0.693}{t_{1/2}} \cdot Vd \qquad \text{(Eq.14)}$$

where V_d is the volume of the incubation system.

2.7.4 "Scaling-Up" of Intrinsic Clearance Parameter

The *in vitro* CL_{int} (mL/min/ mg microsomal protein) obtained from the microsomal incubation studies was "scaled-up" to an CL_{int} value (mL/min/kg) that represented the clearance expected in the whole animal using a proposed strategy (Houston, 1994). CL_{int} was scaled according to the following equation (Eq.15):

$$CL_{int} = \textit{in vitro}\ CL_{int} \bullet \frac{\text{mL incubation}}{\text{mg microsomal protein}} \bullet \frac{\text{mg microsomal protein}}{\text{g of liver}} \bullet \frac{\text{liver weight (g)}}{\text{body weight (kg)}}$$

where *in vitro* CL_{int} is the value obtained from the microsome incubation experiment, and the microsomal protein recovery (mg microsomal protein/ g of liver) and rat liver wet weight (g of liver/ kg body weight) were experimentally determined.

2.7.5 Prediction of Hepatic Clearance and Extraction

Predicted CL_h and hepatic extraction ratio were estimated from microsomal incubation studies under apparent first order conditions using the well-stirred liver clearance model that relates hepatic clearance (CL_h), hepatic blood flow (Q), hepatic extraction ratio (E), intrinsic clearance (CL_{int}), and unbound fraction of drug in plasma (f_u) according to:

$$CL_h = Q \cdot E = Q\left[\frac{f_u \cdot CL_{int}}{Q + f_u \cdot CL_{int}}\right] \quad \text{(Eq.16)}$$

With the incorporation of microsomal protein binding, the above equation expands to:

$$CL_h = Q\left[\frac{f_{u(plasma)} \cdot \dfrac{CL_{int}}{f_{u\,(mx)}}}{Q + f_{u(plasma)} \cdot \dfrac{CL_{int}}{f_{u\,(mx)}}}\right] \quad \text{(Eq.17)}$$

where $f_{u\,(mx)}$ is the free unbound fraction of drug in the microsomal matrix (Obach, 1997).

The use of the liver model incorporates the estimated CL_{int} into the predicted CL_h expressed in terms of circulating drug concentrations using a hepatic blood flow literature value of 80 mL/min/kg (Pollack *et al.,* 1990).

CHAPTER 3
RESULTS

3.1 ANALYSIS OF RSD1070 AND N-DEALKYL RSD1070 BY LCMSMS

3.1.1 Chromatography and Detection of RSD1070 and N-dealkyl RSD1070

High-pressure liquid chromatography coupled with tandem mass spectrometry was an effective method to obtain optimal selectivity and sensitivity for the assay of RSD1070 in all of the biological samples examined. The positive-ion electrospray interface served as a very efficient means of solvent desolvation and molecular ionization while introducing the sample to the mass spectrometer. **Figure 7** illustrates the daughter ion mass spectra of RSD1070, N-dealkylated RSD1070, and the internal standard. The collision induced fragmentation pattern of each molecular ion precursor (MH^+) allowed for the selection of the desired product ions to be detected by multiple reaction monitoring. RSD1070 (MH^+ *m/z* 340) fragmentation resulted in *m/z* 168 and 155, corresponding to the cyclohexyl N-morpholino backbone and the 1-naphthyl side chain, respectively. N-dealkylated RSD1070 (MH^+ *m/z* 314) fragmentation resulted in *m/z* 142 and 155, corresponding to the N-dealkylated N-morpholino backbone and the 1-naphthyl side chain, respectively. Fragmentation of the internal standard (MH^+ *m/z* 357) resulted in several ions (*m/z* 286, 112, and 147). Ion *m/z* 147, which corresponds to the benzothiophene side chain, was monitored for quantitation purposes. Ion *m/z* 286, which corresponds to the molecular ion with the loss of the pyrrolidine substituent, produced an intense signal. However, ion *m/z* 286 was not monitored because this was a constituent species of all IS stock and working solutions, and is believed to be a starting material contaminant. Ion *m/z* 112 results from further fragmentation of *m/z* 286 with the additional breakage of the amide bond.

A sample LCMSMS chromatogram using MRM detection mode is illustrated in **Figure 8** with the respective ion transitions denoted. The chromatographic conditions used in the assay provided the conditions necessary for adequate resolution of the product ions of interest and resulted in sharp symmetrical peaks.

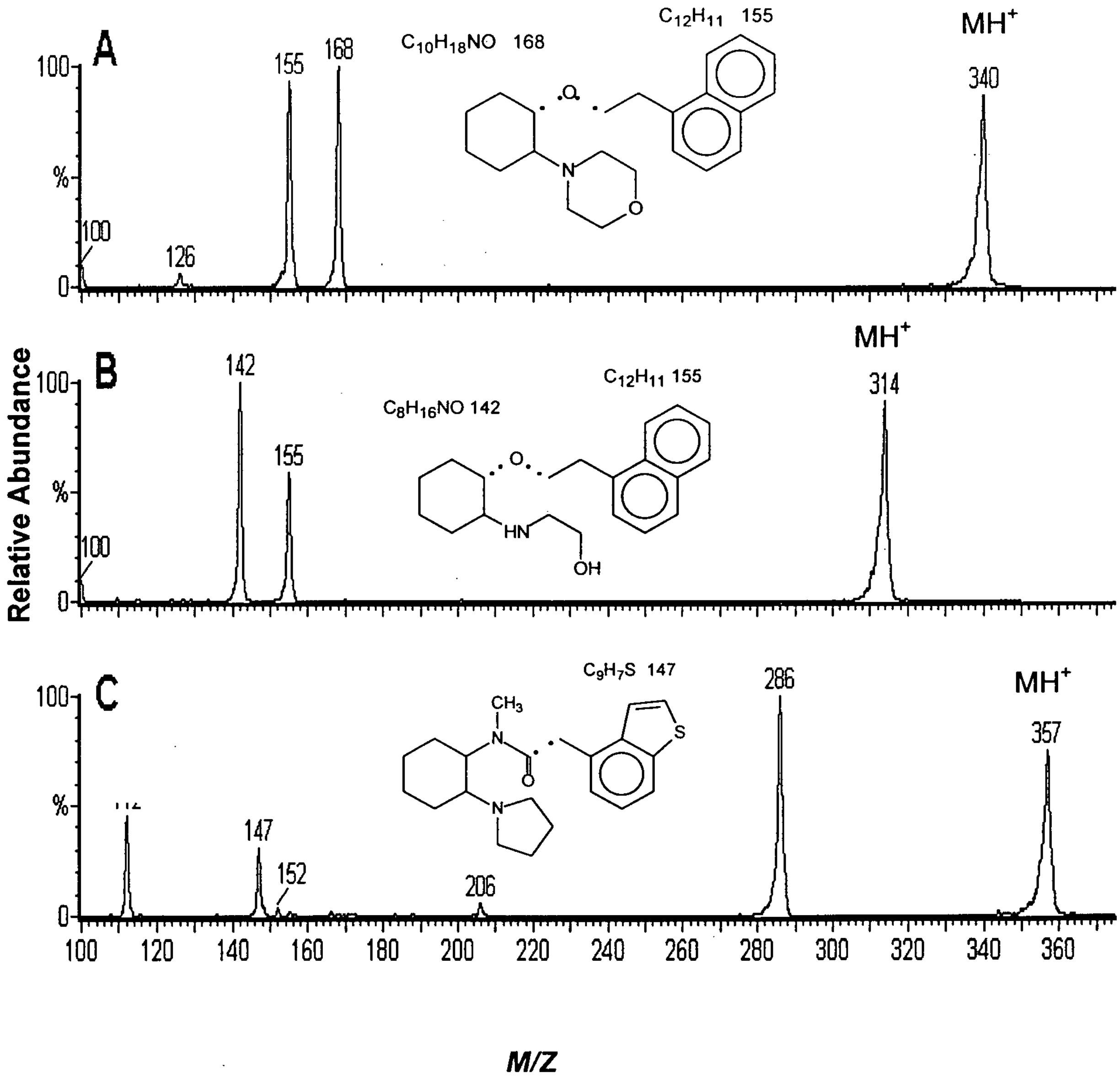

Figure 7. Daughter ion scan of standards (A) RSD1070, (B) N-dealkylated RSD1070, (C) RSD921, internal standard. Fragmentation patterns as illustrated in the insert diagram are described in the text. Daughter ions were produced by collision induced dissociation of the parent ions with collision energy of 40 eV and argon gas pressure of 3.5 x 10^{-3} mbar. During daughter ion scan, the first quadrupole was selected specifically for the precursor ions (MH^+) and the third quadrupole was set on scan mode to detect the fragment ions.

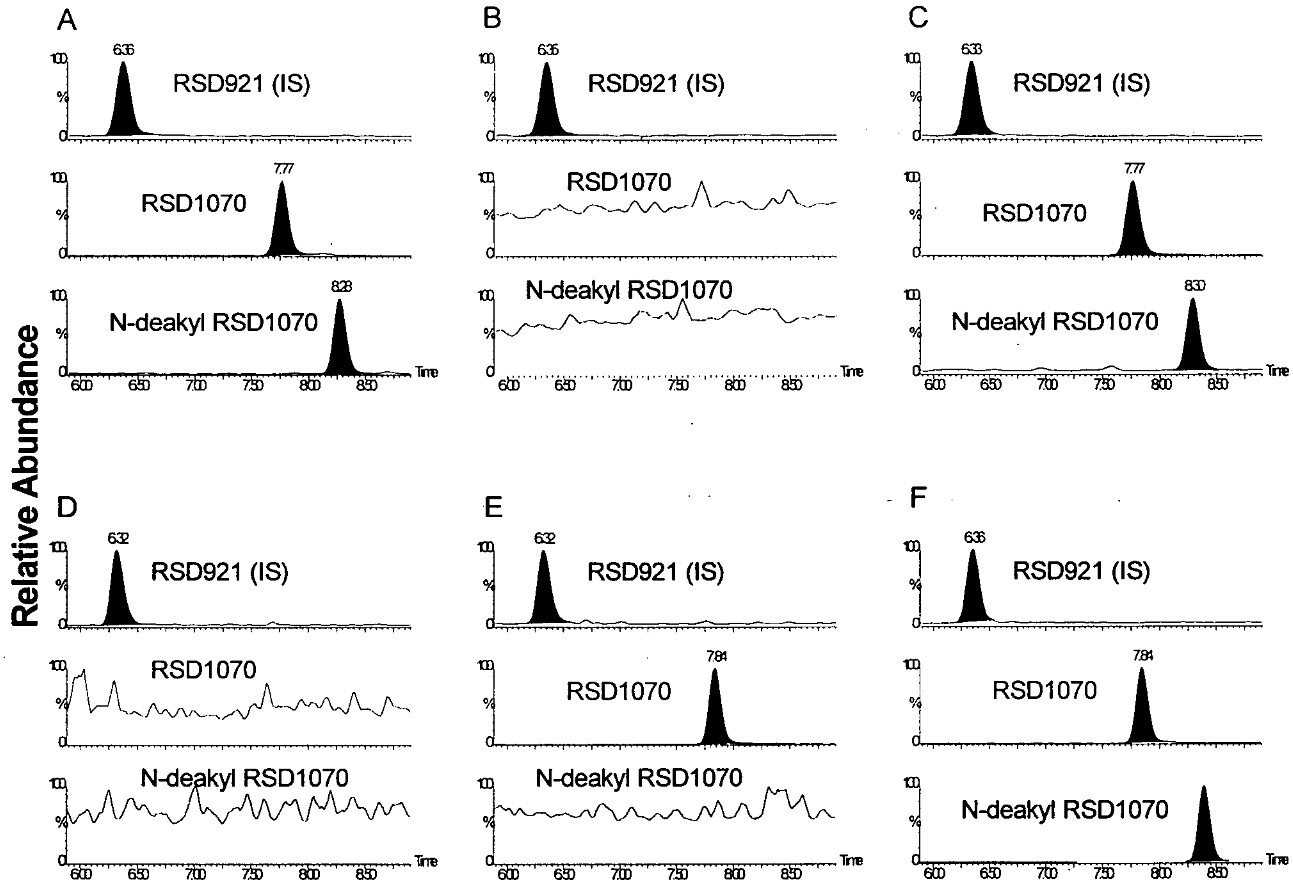

Figure 8. **Sample positive electrospray LC/MS/MS chromatograms obtained by Multiple Reaction Monitoring of ion transitions *m/z* 340 > 155 (RSD1070), *m/z* 314 > 142 (N-dealkylated RSD1070), and *m/z* 357 > 147 (internal standard). Representative chromatograms are (A) mixture of reference standards (100 ng/mL) prepared in water, (B) blank rat plasma spiked with internal standard, (C) rat plasma sample, (D) blank microsome matrix spiked with internal standard, (E) boiled microsome control, and (F) microsomal incubation sample. The HPLC and MS/MS conditions and specifications are described in the text.**

3.1.2 Assay Validation

Calibration curves of RSD1070 and N-dealkylated RSD1070 to internal standard peak ion area ratios vs. known amounts of RSD1070 and N-dealkylated RSD1070 were prepared using peak area ratios from chromatograms of the injected standards. Weighted linear regression (weighting factor = $1/y^2$) was performed on all calibration curve data in order to reduce the bias at the lower concentrations. Calibration curves for all biological samples demonstrated linearity over the range 3 – 100 ng/mL with linear regression coefficients > 0.999. Sample calibration curves for rat plasma are illustrated in **Figure 9**. The limit of quantitation (LOQ) for both RSD1070 and N-dealkylated RSD1070 was 3 ng/mL, the lowest quality control standard based on the inter-assay and intra-assay variability.

The inter-assay and intra-assay variability (% CV) based on low, mid, and high quality control (QC) samples in microsomal matrix were < 15 % for both RSD1070 and its N-dealkylated metabolite (**Table 1** and **2**). The % bias of all QC samples prepared in microsomal matrix for both inter-assay and intra-assay validation was within ± 15 % of the nominal concentrations. The $1/y^2$ weighting function resulted in acceptable regression bias and precision (Shah *et al.*, 1992) for all analytes at the lower as well as the upper range of the calibration curves.

Quality control samples prepared in blank plasma matrix on six separate different days demonstrated inter-assay variability (**Table 3**) of < 10 % CV at the mid and high QC concentrations for both RSD1070 and N-dealkyl RSD1070. However, at the LOQ borderline acceptable precision was demonstrated (Shah *et al.*, 1992) with 23 % CV (RSD1070) and 18 %

CV (N-dealkyl RSD1070). Intra-assay variability **(Table 4)** on one analytical day was < 11 % CV for both analytes. The accuracy (% bias) of all QC samples prepared in plasma matrix for both inter-assay and intra-assay validations was within 84.4 – 106.3 % of the expected nominal concentrations.

The mean analytical recovery of RSD1070 and its N-dealkyl metabolite in plasma was based on the peak area ratios of the extracted and non-extracted standards over the concentration range of 2.5 to 100 ng/mL. The analytical recovery for RSD1070 and its N-dealkyl metabolite was determined to be 96 and 98 %, respectively (**Table 5**).

Twenty-four hour bench-top stability and freeze-thaw stability of standard curve samples was performed and results indicated that RSD1070 and N-dealkyl RSD1070 were stable over this time frame. However, the IS was relatively less stable and the area under the ion current chromatogram decreased after 24-hours at room temperature, and marked instability was observed after 3 cycles of freeze - thaw. The instability of the IS resulted in an increase in the peak area ratio of analyte to IS for both RSD1070 and N-dealkyl RSD1070 (**Table 6**).

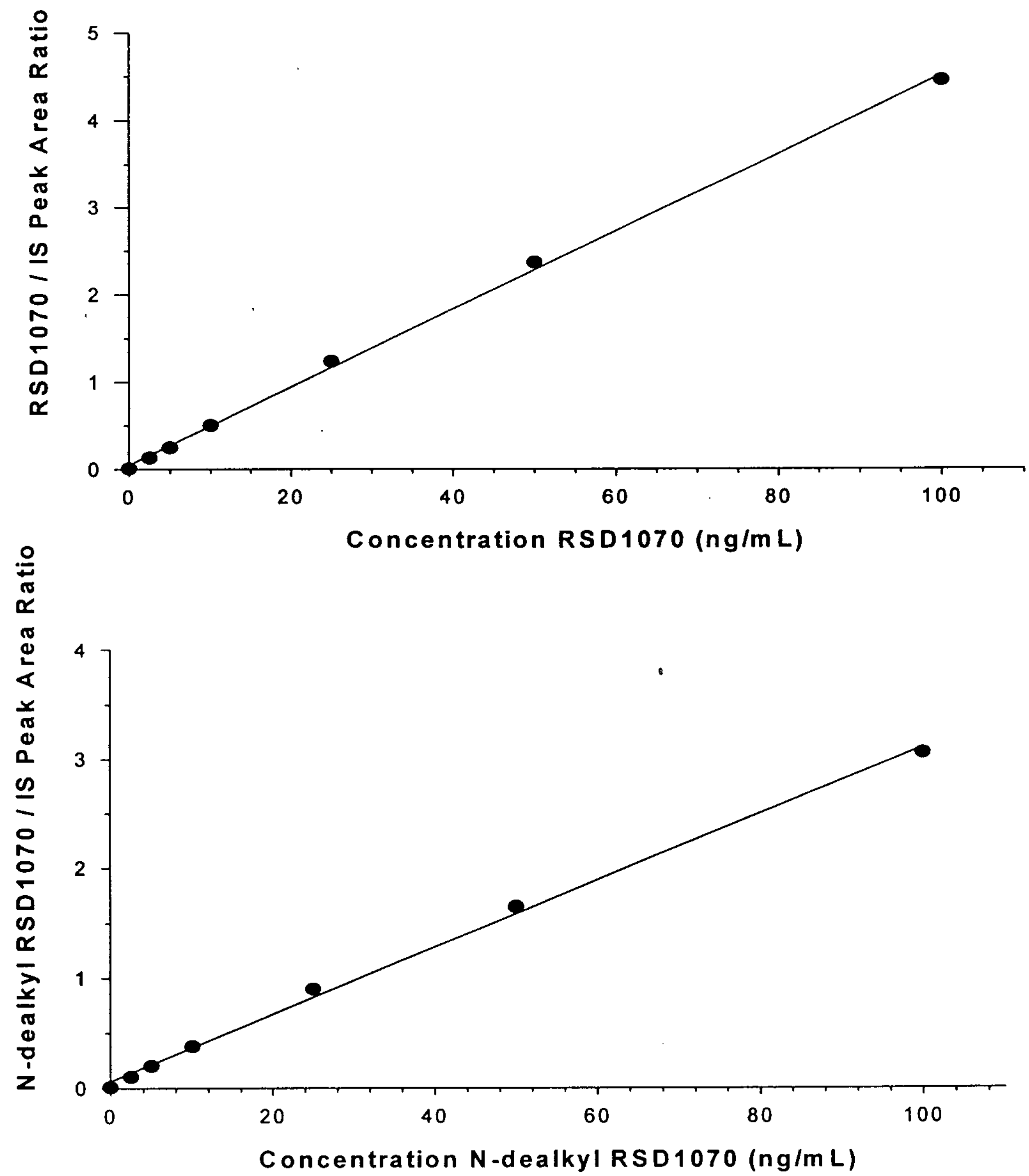

Figure 9. **Representative calibration curves of RSD1070 (top) and N- dealkylated RSD1070 (bottom) in rat plasma over the concentration range 3 – 100 ng/mL ($1/y^2$ weighted). Each data point represents the mean of triplicate standard curve samples.**

Table 1. **Inter-assay variation based on the quality control samples in blank microsomal matrix obtained on six different days. QC low (3 ng/mL), QC mid (15 ng/mL), and QC high (75 ng/mL).**

Inter-assay	RSD1070			N-dealkyl RSD1070		
Microsomal matrix	QC low	QC mid	QC high	QC low	QC mid	QC high
1	2.4	15.7	71.8	2.8	17.1	70.6
2	2.9	16.1	74.0	3.5	17.8	75.8
3	3.2	15.3	77.0	3.5	15.4	76.9
4	3.2	16.8	75.6	3.5	17.4	76.3
5	3.2	17.7	70.7	3.6	16.9	70.
Bias (%)	-3.1	9.1	-1.2	11.2	10.6	-0.3

Table 2. **Intra-assay variation based on the quality control samples in blank microsomal matrix obtained on one day. QC low (3 ng/mL), QC mid (15 ng/mL), and QC high (75 ng/mL).**

Intra-assay	RSD1070			N-dealkyl RSD1070		
Microsomal matrix	QC low	QC mid	QC high	QC low	QC mid	QC high
1	2.9	15.1	75.8	3.6	17.0	75.5
2	2.9	15.6	82.3	3.1	15.5	72.0
3	2.8	14.4	77.6	3.3	15.2	76.7
4	3.1	14.8	63.5	2.5	15.8	65.7
5	3.2	13.8	69.3	3.2	14.8	68.7
6	2.9	16.4	74.1	3.3	16.6	74.8
nominal conc. (ng/mL)	**3.0**	**15.0**	**75.0**	**3.0**	**15.0**	**75.0**
mean conc. (ng/mL)	**3.0**	**15.0**	**73.8**	**3.2**	**15.8**	**72.2**
SD	**0.2**	**0.9**	**6.6**	**0.4**	**0.9**	**4.3**
C.V. (%)	**5.1**	**6.0**	**8.9**	**11.6**	**5.4**	**6.0**
Bias (%)	**-1.1**	**0.3**	**-1.6**	**5.4**	**5.4**	**-3.7**

Table 3. **Inter-assay variation based on the quality control samples in blank rat plasma matrix obtained on six different days. QC low (3 ng/mL), QC mid (15 ng/mL), and QC high (75 ng/mL).**

Inter-assay	RSD1070			N-dealkyl RSD1070		
Plasma matrix	QC low	QC mid	QC high	QC low	QC mid	QC high
1	3.4	16.9	76.8	3.5	18.2	72.7
2	2.1	19.4	85.7	2.2	15.8	69.9
3	2.6	16.1	69.2	2.6	17.0	67.1
4	3.5	15.6	82.4	2.7	15.4	66.6
5	3.4	16.7	76.8	3.6	19.4	72.0
6	3.3	16.1	77.2	4.1	18.3	73.5
nominal conc. (ng/mL)	3	15	75	3	15	75
mean conc. (ng/mL)	3.1	16.8	78.0	3.1	17.3	70.3
SD	0.6	1.4	5.7	0.7	1.6	2.9
C.V. (%)	18.2	8.1	7.3	23.1	9.0	4.2
Bias (%)	2.2	12.1	4.0	3.9	15.6	-6.3

Table 4. **Intra-assay variation based on the quality control samples in blank rat plasma matrix obtained on one day. QC low (3 ng/mL), QC mid (15 ng/mL), and QC high (75 ng/mL).**

Intra-assay	RSD1070			N-dealkyl RSD1070		
Plasma matrix	QC low	QC mid	QC high	QC low	QC mid	QC high
1	2.8	15.8	86.2	3.4	16.6	79.4
2	2.8	14.8	83.5	2.9	15.0	78.0
3	2.9	15.3	70.8	2.9	16.9	67.3
4	3.2	14.1	74.7	2.5	15.7	73.4
5	2.7	15.3	77.0	3.4	15.8	74.9
6	3.0	15.0	81.3	3.1	16.3	79.1
nominal conc. (ng/mL)	3.0	15.0	75.0	3.0	15.0	75.0
mean conc. (ng/mL)	2.9	15.1	78.9	3.0	16.0	75.3
SD	0.2	0.6	5.8	0.3	0.7	4.6
C.V. (%)	6.4	3.8	7.3	10.8	4.4	6.1
Bias (%)	-4.2	0.4	5.2	1.1	7.0	0.5

Table 5. **Assay recovery of RSD1070 and N-dealkyl RSD1070 by LC/MS/MS (n = 3) performed on one day. Recovery (as a % of non-extracted references) was determined from the peak area ratio of analyte to IS of extracted versus non-extracted standards. Extracted samples were prepared by spiking known amounts of analyte (final conc. of 2.5 – 100 ng/mL) in blank plasma and extracted. The extracted samples were reconstituted in 1 mL of mobile phase containing IS (50 ng).**

RSD1070 Conc. (ng/mL)	Peak Area Ratio Extracted (n=3)	Peak Area Ratio Non-extracted (n=3)	% of Non-extracted
2.5	0.17	0.19	87.8
3	0.21	0.23	92.1
5	0.38	0.39	99.6
10	0.71	0.73	96.9
15	1.09	1.14	95.2
25	1.71	1.74	98.5
50	3.23	3.50	92.4
75	4.78	4.74	100.9
100	6.10	6.25	97.6
mean			95.7

N-dealkyl RSD1070 Conc. (ng/mL)	Peak Area Ratio Extracted (n=3)	Peak Area Ratio Non-extracted (n=3)	% of Non-extracted
2.5	0.13	0.12	108
3	0.15	0.17	88.2
5	0.27	0.26	104
10	0.52	0.50	103
15	0.77	0.80	96.3
25	1.17	1.25	93.4
50	2.25	2.31	97.2
75	3.24	3.30	98.1
100	4.27	4.36	98.0
			98.3

Table 6. Twenty-four hour bench top stability and freeze-thaw stability studies of RSD1070 and N-dealkyl RSD1070 in plasma based on peak area ratios of analyte to IS.

Concentration	*RSD1070 (Mean Peak Area Ratio)*			*N-dealkyl RSD1070 (Mean Peak Area Ratio)*		
(ng/mL)	reference	24-hour	freeze - thaw	reference	24-hour	freeze - thaw
2.5	0.16	0.18	0.16	0.13	0.15	0.15
5	0.35	0.34	0.39	0.26	0.33	0.32
10	0.65	0.66	0.71	0.47	0.59	0.61
25	1.65	1.61	1.71	1.13	1.42	1.45
50	2.96	2.88	3.21	2.06	2.63	2.70
100	5.43	5.86	6.32	3.66	4.99	5.38

3.2 PROTEIN BINDING STUDIES OF RSD1070

Plasma and microsomal protein binding studies were investigated to estimate the fraction of free (unbound) RSD1070. The free fraction parameters will be necessary to determine *in vivo* intrinsic clearance according to the well-stirred liver model of clearance. The plasma volume obtained for each sample from the pharmacokinetic studies was insufficient for *in vivo* free fraction determination; therefore, *in vitro* protein binding studies were performed using pooled blank plasma from male Sprague-Dawley rats.

3.2.1 Determination of Fraction Unbound (f_u) In Plasma Matrix

Plasma protein binding of RSD1070 was examined at concentrations of 2.26 to 20.7 µg/mL, representing mid and upper ranges of plasma RSD1070 concentrations observed during the pharmacokinetic studies. However, at concentrations less than 2 µg/mL, the free fraction of

RSD1070 was undetectable due to extensive protein binding. RSD1070 was assayed from the buffer reservoir (representing the unbound concentration) and the plasma reservoir (representing the total concentration) after 5 hours of incubation. RSD1070 demonstrated very high plasma protein binding resulting in a low f_u that averaged 1.5 ± 0.3 % and ranged from 0.9 - 2.4 % unbound over the concentration range 2.3 – 20.7 μg/mL as displayed in **Table 7**. Concentrations less than 2 μg/mL resulted in an undetectable free fraction due to the extensive degree of plasma protein binding of RSD1070.

Table 7. Fraction unbound of RSD1070 in plasma determined by equilibrium dialysis at 37 °C for 5 hours. Each value is the mean of triplicate samples ± SD.

Total Concentration **(μg/ml)**	***Free Concentration*** **(μg/ml)**	***Percent Unbound*** **(%)**
20.7 ± 0.4	0.50 ± 0.04	2.40 ± 0.43
12.6 ± 1.0	0.20 ± 0.02	1.57 ± 0.25
9.58 ± 0.62	0.14 ± 0.03	1.42 ± 0.26
2.26 ± 0.04	0.02 ± 0.00	0.89 ± 0.02
		Mean ± SD: 1.5 ± 0.6

3.2.2 Determination of Equilibration Time

Initial time course experiments demonstrated that equilibrium was achieved by 5.5 hr (**Figure 10**), based on assaying the amount of RSD1070 present in the buffer reservoir after 0, 1, 2.5, 3, 4, 5.5, 6.5, and 8 hrs of incubation at 37 °C. The unbound drug that diffused across the dialysis membrane into the buffer increased rapidly by 2 hours and maintained sufficient equilibrium with the plasma compartment.

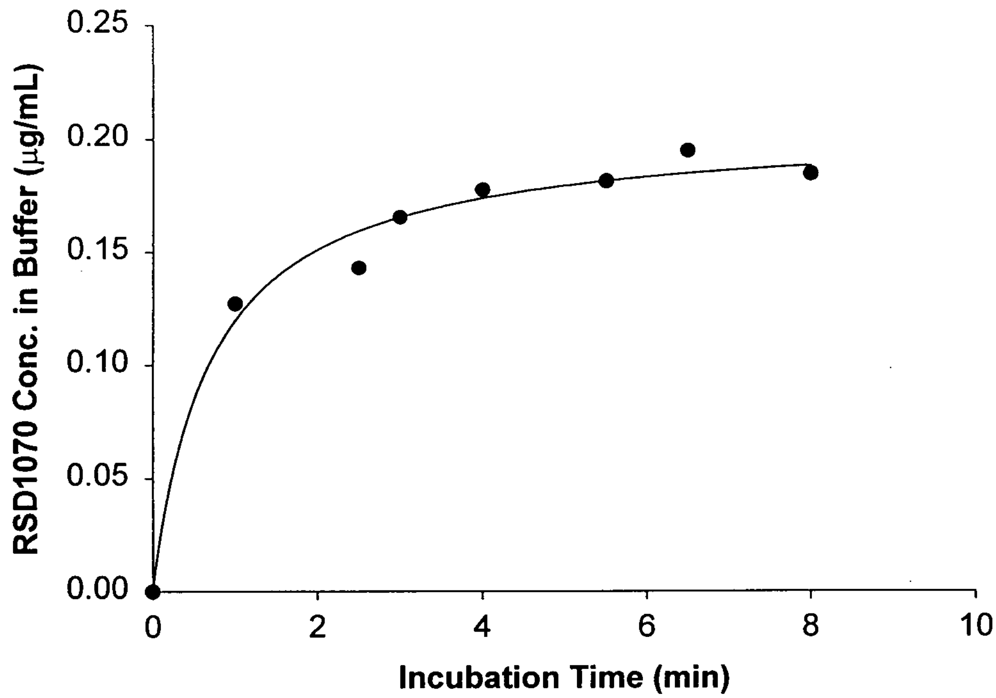

Figure 10. Determination of membrane dialysis equilibration time of 5 µg/ml RSD1070 from rat plasma to buffer reservoir at 37 °C. Each time point consists of duplicate samples.

3.2.3 Recovery of RSD1070 From Equilibrium Dialysis Chambers

The recovery of RSD1070 averaged 91 % (n=3) at the concentration of 5 µg/mL, thus non-specific binding to the equilibrium dialysis membranes and/or apparatus was minimal. Recovery was based on comparing the initial amount of RSD1070 present in the plasma sample to that recovered from both the plasma and buffer reservoirs after 5 h of incubation at 37 °C (**Table 8**).

Table 8. **Total recovery of RSD1070 in plasma sample and buffer reservoirs of the equilibrium dialysis unit after 5 hr incubation at 37°C (n=3). Recovery reported is the mean percentage ± SD of the initial amount.**

Initial Amount RSD1070 (μg)	*Amount RSD1070 in Buffer* (μg)	*Amount RSD1070 in Plasma* (μg)	*Recovery* %
4.9	0.06	4.8	99.2
4.9	0.06	4.1	84.9
4.9	0.06	4.4	91.1
		Mean	**91.1**
		SD	**7.2**

3.2.4 Stability of RSD1070 In Plasma and In Phosphate Buffer

RSD1070 was stable in both plasma and phosphate buffer up to 6 h of incubation in a 37 °C water bath as shown in **Figure 11**. Therefore, RSD1070 was stable over the incubation time course of the protein binding studies.

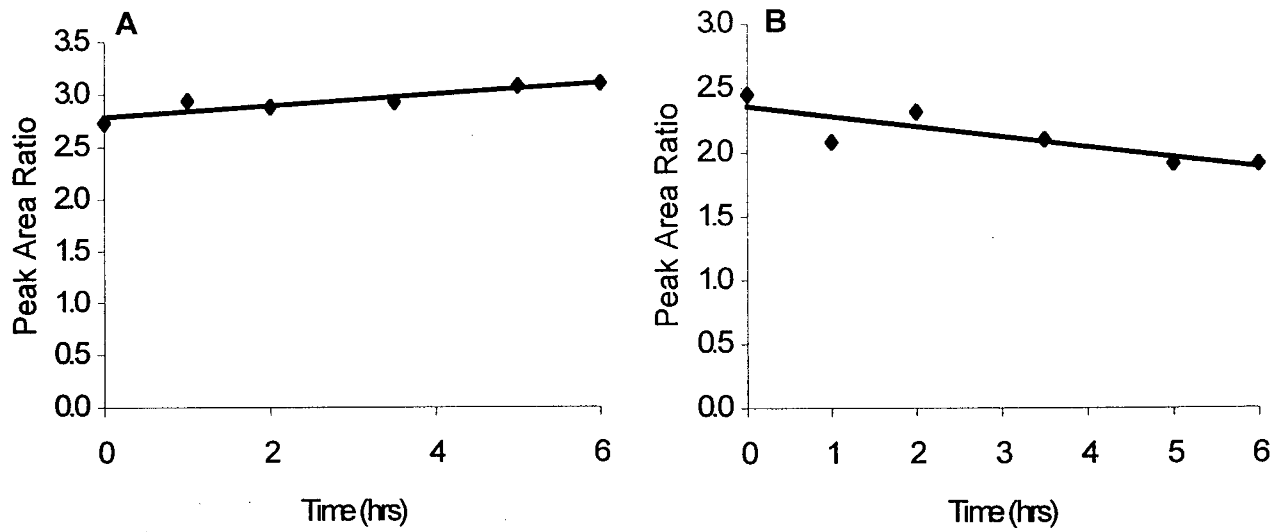

Figure 11. Stability of RSD1070 (5 μg/mL) in (A) rat plasma and (B) phosphate buffer in 37 °C water bath. Stability was based on peak area ratios of RSD1070 to internal standard. Each data point represents a single sample.

3.2.5 Determination of Fraction Unbound ($f_{u\,mx}$) In Microsomal Incubation Matrix

RSD1070 demonstrated binding to pooled rat liver microsomes when subjected to equilibrium dialysis. Non-specific binding of RSD1070 to microsomal matrix was tested at conditions utilized in metabolic incubations; microsomal protein concentration of 0.25 mg/mL and a substrate concentration of 1.7 μg/mL. Furthermore, binding experiments were conducted at 37 °C to mimic conditions used in *in vitro* microsomal metabolism studies but were conducted in the absence of NADPH so that metabolism of the compounds would not occur. Initial time course experiments demonstrated that equilibrium was achieved by 5 h (**Figure 12**). The free fraction of RSD1070 was determined to be 15.1 ± 2.0 % (n=5, **Table 9**).

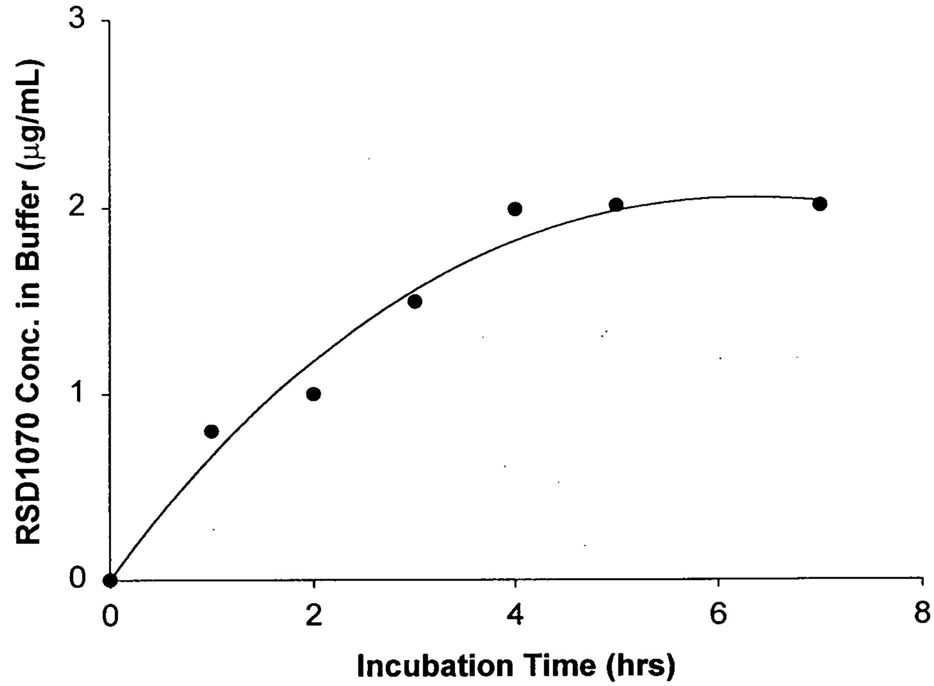

Figure 12. **Initial time course of equilibrium dialysis microsomal protein binding studies demonstrating time to reach equilibrium. Microsomal incubate (1.7 μg/mL RSD1070 and 0.25 mg/mL microsomal protein in phosphate buffer) without NADPH was dialyzed against phosphate buffer at 37 °C.**

Table 9. **Fraction unbound of 1.7 μg/mL RSD1070 in 0.1 mg/mL microsomal incubation matrix without NADPH determined by equilibrium dialysis. Fraction unbound was based on the ratio of unbound (buffer) concentration to total (sample) concentration.**

Mx Sample conc. (C_{total}) μg/mL	*Mx Buffer conc. ($C_{unbound}$)* μg/mL	*Percent Unbound ($f_{u\ mx}$)* (%)
1.79	0.29	16.2
1.86	0.27	14.5
1.80	0.29	16.1
2.25	0.27	12.0
1.78	0.30	16.9
		Mean ± SD: 15.1 ± 2.0 %

3.3 PHARMACOKINETIC STUDIES OF RSD1070

The pharmacokinetics of RSD1070 were investigated by administering a single iv bolus therapeutic dose (ED_{90}) to rats in order to estimate total body clearance (CL_{tot}) based on AUC_{∞} values. Twenty four-hour urine data were obtained to estimate renal clearance (CL_r). Hepatic clearance (CL_h) was approximated assuming that $CL_h \approx CL_{tot} - CL_r$ and hepatic extraction ratio (E) was defined by CL_h / Q, where Q is hepatic blood flow.

3.3.1 Pharmacokinetics of RSD1070 In Plasma

The mean plasma concentration – time plot for 8 animals over a 6-hr period following a single iv bolus dose of 12 mg/kg demonstrated three-compartment kinetics (**Figure 13**). Pharmacokinetic parameters were based on linear-regression non-compartmental modeling using the WinNonlin (ver. 1.1) program. RSD1070 demonstrated a rapid elimination half-life of 25 ± 8 min with a total body clearance of 71 ± 8 mL/min/kg and a volume of distribution of the terminal elimination phase (V_{area}) of 3.5 ± 0.6 L/kg. Plasma samples obtained after 360 min approached the limits of quantitation or were below detectable amounts. Plasma concentrations ranged from 9.16 ± 0.64 μg/mL at 2.5 min to 0.02 ± 0.01 μg/mL at 360 min post-administration. The calculated individual and mean animal pharmacokinetic parameters of RSD1070 are reported in **Table 10**.

time (min)	mean plasma concentration (µg/mL)	sd
2.5	9.16	0.64
3	7.13	0.94
5	5.33	1.15
10	3.07	0.64
20	1.92	0.31
30	1.38	0.24
45	0.90	0.21
60	0.51	0.17
120	0.18	0.05
240	0.06	0.02
360	0.02	0.01

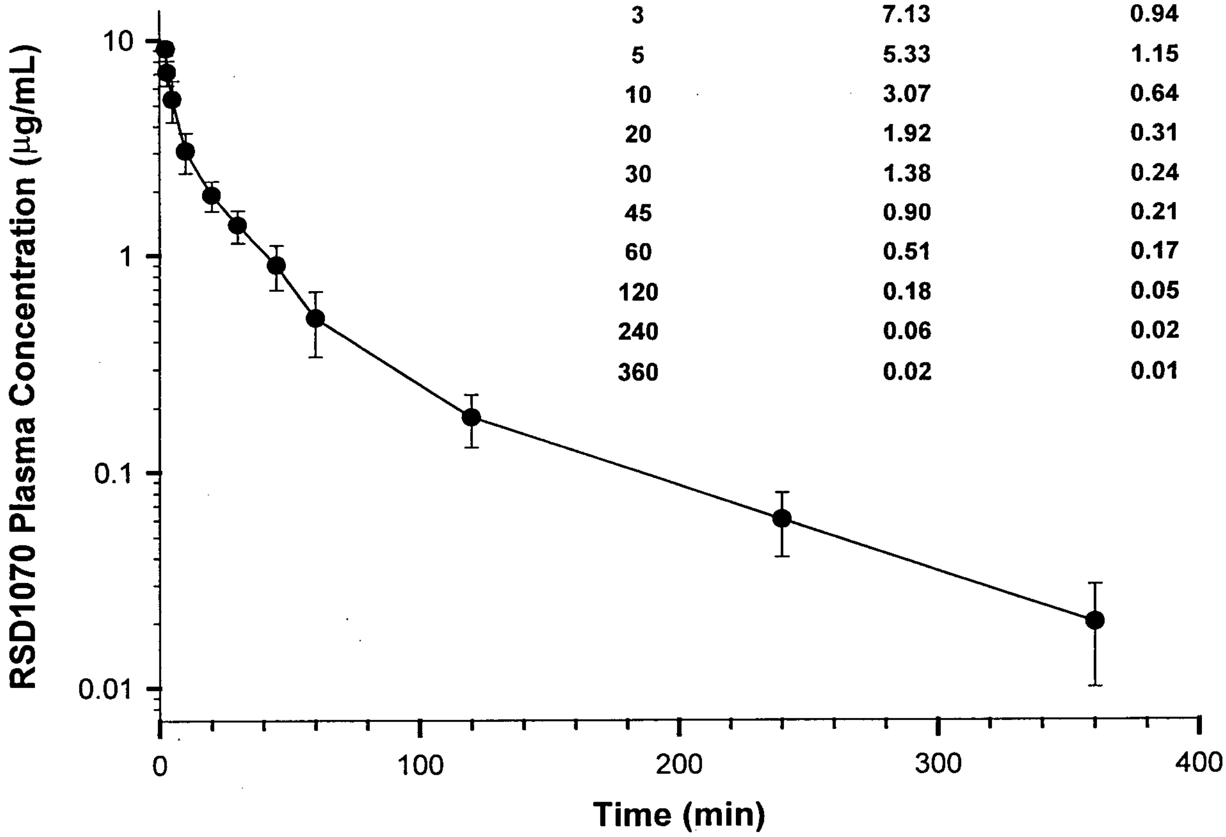

Figure 13. Semi-log mean concentration-time plot of RSD1070 in plasma following a single iv bolus dose of 12 mg/kg of RSD1070 in rats. Each value represents the mean concentration obtained from 8 animals at each time point. Error bars represent the SD. Insert table summarizes the mean ± SD plasma concentration of RSD1070 (n=8).

3.3.2 Excretion of RSD1070 in 24-hr Urine

The urinary recovery of RSD1070 and N-dealkylated RSD1070 was measured in 24-hr urine samples following the 12 mg/kg iv bolus dose. Less than 1% of the dose was recovered as RSD1070 and its N-dealkyl metabolite. CL_r for RSD1070 was calculated as amount RSD1070 excreted in urine / plasma AUC_∞ and was estimated to be very low with high variability (CL_r = 0.05 ± 0.03 mL/min/kg). The reported mean CL_r accounted for approximately 0.08% of the mean CL_{tot}.

3.3.3 Determination of Blood To Plasma Partitioning of RSD1070

The blood to plasma concentration ratio of RSD1070 was calculated from the concentration present in whole blood and plasma, respectively. Whole rat blood was spiked with 10 μg/mL RSD1070 (final concentration) and incubated in a shaking water bath for 2 hrs at 37 °C. Whole blood and plasma were analyzed and the blood to plasma partitioning of RSD1070 ratio obtained was close to unity, 0.95 ± 0.05 (n=4). Therefore, the clearance values based on plasma concentrations required no further corrections.

3.3.4 Determination of Hepatic Clearance and Extraction Ratio

Hepatic clearance of RSD1070 in rat was estimated to be equivalent to total body clearance since renal clearance was determined to be very small accounting for less than 0.5% of total body clearance. A mean hepatic clearance (CL_h) value of 71 ± 8 mL/min/kg and a mean hepatic extraction ratio (E) of 0.88 ± 0.11 were estimated as described in Section 2.7.2.

Table 10. Calculated pharmacokinetic parameters of RSD1070 for individual animals based on rat plasma and urine concentrations following single iv bolus administration of a dose of 12 mg/kg (n=8).

Animal	Bdy wt.	Dose	$t_{1/2}$	CL_{TOT}	V_{area}	AUC	Amt in urine	CL_R	Hepatic Extraction
	kg	μg	min	mL/min/kg	L/kg	μg/mL/min	μg	mL/min/kg	
A	0.24	2880	35	71	3.8	168	1.9	0.05	0.89
B	0.20	2400	21	76	4.0	159	3.0	0.09	0.95
C	0.24	2880	35	63	3.8	192	0.5	0.01	0.78
D	0.25	3000	28	63	3.6	185	0.4	0.01	0.79
E	0.26	3120	21	65	3.8	255	1.2	0.02	0.81
F	0.23	2760	29	65	3.4	184	5.6	0.13	0.81
G	0.30	3600	16	78	4.6	153	3.3	0.07	0.98
H	0.23	2760	17	86	3.8	187	3.3	0.08	1.08
mean	**0.24**		**25**	**71**	**3.9**	**185**	**2.4**	**0.06**	**0.88**
sd	**0.03**		**8**	**9**	**0.4**	**31**	**1.7**	**0.04**	**0.11**

3.4 HEPATIC MICROSOMAL STUDIES

At the initial stages of the project, the metabolism of RSD1070 was unknown. Hepatic microsomal preparations were used to investigate the possible major metabolites of RSD1070. Subsequently, microsomal metabolism studies were conducted to monitor the formation rate of the metabolite for purposes of obtaining enzyme kinetic parameters to estimate hepatic extraction. Due to substantial sequential metabolism of the major metabolite, hepatic clearance and hepatic extraction were estimated based on the disappearance time profile of the parent compound.

3.4.1 Preparation of Pooled Rat Liver Microsomes

Pooled liver microsomes were prepared from four male Sprague-Dawley rats. Individual body weights and wet liver weights were measured, and the normalized liver weight was calculated to be 47 g/kg of body weight (**Table 11**). Microsomal protein concentration was determined to be 62 mg/mL and the cytochrome P450 concentration was determined to be 1.1 nmol/mg microsomal protein. The total microsomal protein yield was determined to be 42 mg protein/g liver as calculated below:

Table 11. Individual body weights and liver weights of male Sprague-Dawley rats used for the preparation of pooled rat liver microsomes.

Rat #	*Body Weight* Grams	*Wet Liver Weight* Grams	*Normalized Liver Weight* gram / kg body weight
1	271	12	44
2	195	10	51
3	210	10	48
4	267	12	45
mean	**236**	**11**	**47**

3.4.2 Preliminary Investigation of RSD1070 Metabolism

LC/MS/MS analysis of the microsomal incubate of RSD1070 indicated a variety of molecular ion species of the following *m/z* values: *m/z* 340 (RSD1070), 357 (IS), 314 (N-dealkyl RSD1070), 356, 330, and 374. Molecular ion species corresponding to *m/z* 314, 356, 330, and 374 respectively, increased in abundance with increased incubation times using fixed substrate concentration. The daughter ion scans of the molecular ion species gave further evidence that these ion species are possible metabolites of RSD1070. Of particular interest was the *m/z* 314 peak whose daughter ion scan was consistent with the N-dealkylation of the N-morpholino ring (**Figure 14**). Following RSD1070 dosing to rats, *m/z* 314 was also detected in the plasma with characteristic daughter ions *m/z* 155 and 142. Based on the above observations, the peak corresponding to *m/z* 314 was believed to be a major N-dealkylated metabolite of RSD1070 and was synthesized by Nortran Pharmaceuticals Ltd.

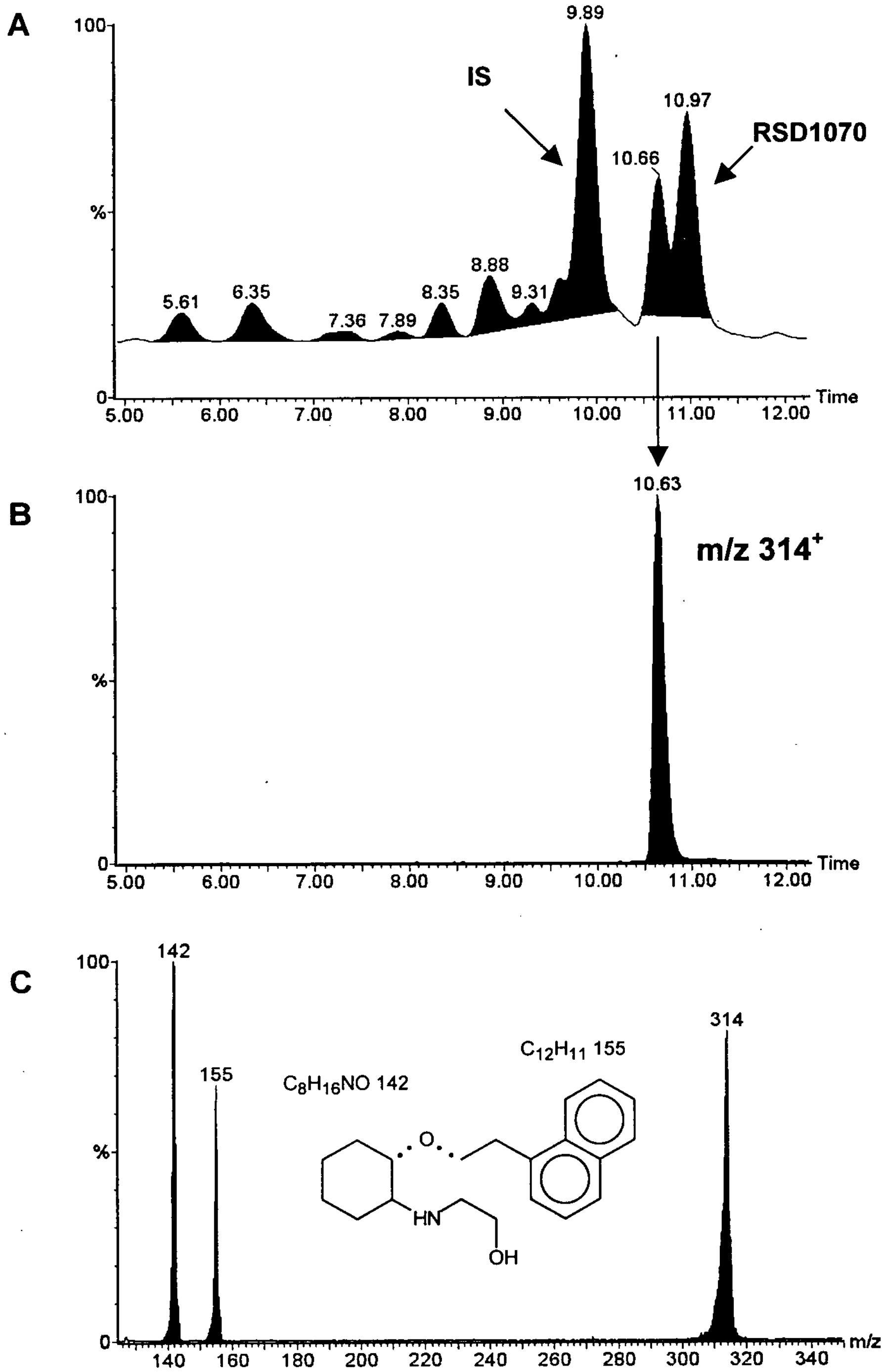

Figure 14. **Preliminary investigation of RSD1070 metabolites in rat liver microsomal sample. Incubation condition consisted of 17.4 μg/mL of RSD1070, 0.6 mg/mL of microsomal protein, and 1.5 mM NADPH at 37 °C for a 10 min incubation period. LC/MS/MS conditons are described in the text. Representative ion chromatograms: (A) Sample scan over the range *m/z* 100 – 500, (B) specific ion scan of *m/z* 314, and (C) daughter ion scan of *m/z* 314 indicating the N-dealkylated metabolite of RSD1070.**

3.4.3 Formation of N-dealkylated RSD1070 in Microsomal Incubations

The optimization of microsomal protein concentration for the formation of the N-dealkyl metabolite is illustrated in **Figure 15.** Using the incubation conditions described in section 2.6.3, the formation of the N-dealkyl metabolite (m/z 314) was linear at 0.1 mg protein/mL. At 0.25 mg protein/mL, the reaction appeared to be at the upper range of linearity and was beginning to saturate.

To monitor the rate of N-dealkyl RSD1070 (*m/z* 314) formation, microsomal metabolism studies were performed using 0.25 mg/mL microsomal protein (corresponding to the upper range of linearity with respect to microsomal protein concentration) and 1.7 μg/mL RSD1070. The amount of N-dealkylated RSD1070 formed was found to increase with the time of incubation (0 to 10 min). At time points after 10 min, the amount of RSD1070 decreased rapidly, suggesting secondary metabolism of this metabolite (**Figure 16**). Further investigation using metabolite incubation studies of N-dealkyl RSD1070 (1.7 ug/mL) in the presence of 0.25 mg/mL microsomal protein confirmed sequential metabolism of the metabolite. The metabolite disappearance time-profile is illustrated in **Figure 17.** Because of this sequential metabolism, the determination of V_{max} and K_m for the formation of N-dealkyl RSD1070 was problematic, and not conducive for the prediction of CL_h and hepatic extraction values. At this stage, the decision was made to conduct disappearance studies of the parent compound in the rat liver microsomal incubation system for the prediction of CL_h and hepatic extraction values.

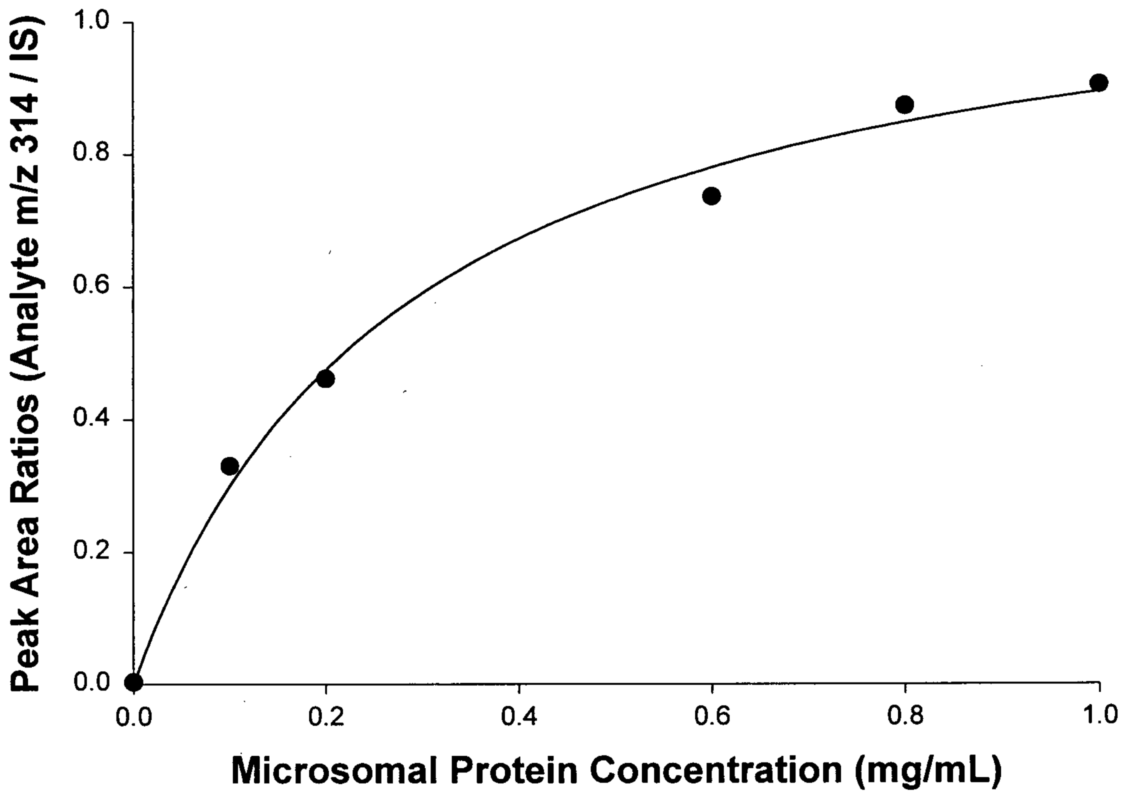

Figure 15. Optimization of microsomal protein concentration for the formation of the N-dealkyl RSD1070 metabolite. The peak area ratio of analyte m/z 314 (N-dealkyl RSD1070) to internal standard (m/z 357) is plotted versus microsomal protein concentration (mg protein/mL). Microsomal protein concentration ranged from 0.1 to 1 mg/mL. RSD1070 (17 μg/mL, 50 μM) was incubated with protein and NADPH (1.5 mM) for 10 min at 37 °C. Reactions were terminated with 10% trichloroacetic acid and assayed by LC/MS/MS under MRM mode.

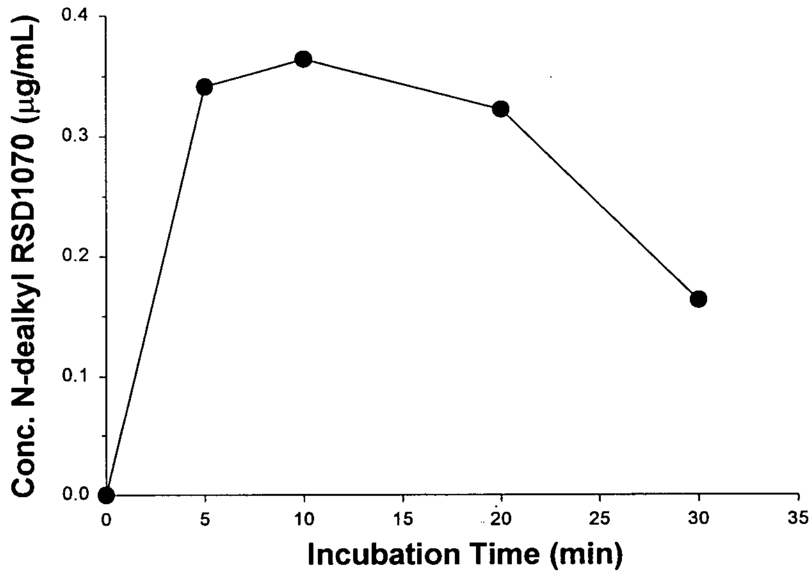

Figure 16. **The formation of N-dealkyl RSD1070 in microsomal incubation with increasing incubation time. The starting concentration RSD1070 was 1.7 μg/ mL and the microsomal protein concentration used was 0.25 mg/mL. Each time point consisted of duplicate samples.**

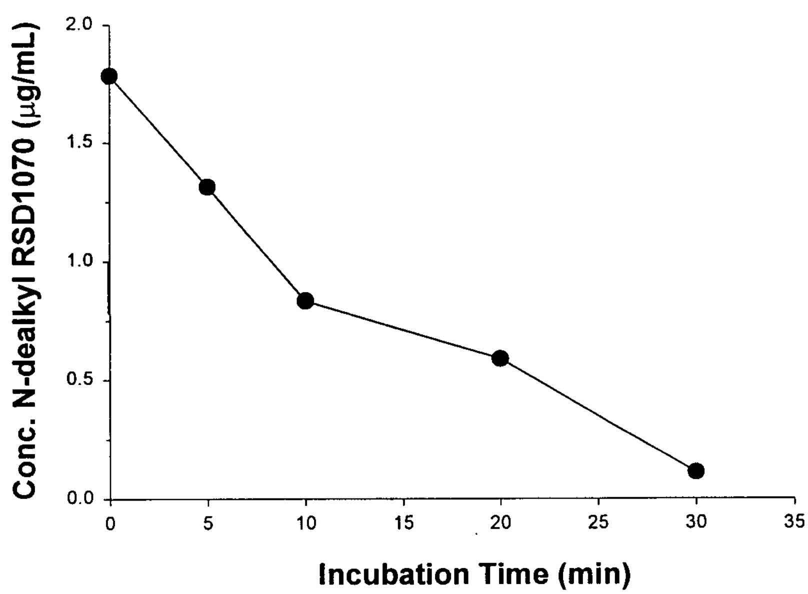

Figure 17. **Disappearance profile of N-dealkyl RSD1070 in microsomal incubation with increasing time. N-dealkyl RSD1070 (1.7 μg/mL) was incubated with 0.25 mg/mL microsomal protein at 37 C. Each time point consisted of duplicate samples.**

3.4.4 Parent Compound Disappearance Studies: Determination of CL_{int} from V_{max} and K_M.

The disappearance of RSD1070 in microsomal incubates was monitored at initial substrate concentrations ranging from 0.34 – 8.5 μg/mL over an incubation period ranging between 0 to 30 min (**Figure 18**). The microsomal protein concentration was decreased from 0.25 to 0.1 mg/mL in order to characterize the disappearance profiles for the lower substrate concentrations at 0.85 and 0.34 μg/mL. The initial rates of the microsome catalyzed reaction (v_o) were calculated from the slope of the initial linear decline at each substrate concentration and the relationship between v_o versus [S] was plotted (**Figure 19**). The consumption of RSD1070 approximated 1st order-kinetics at lower substrate concentrations (0.34 and 0.85 μg/mL) and zero order at higher concentrations (8.5 μg/mL). Initial linear rates of RSD1070 consumption in microsomal incubations at substrate concentrations of 0.34 to 8.5 μg/mL ranged from 1.2 to 2.7 μg/min/mg protein (**Table 12**). The plot of initial reaction rate (v_o) versus initial substrate concentration demonstrated a hyperbolic relationship. Kinetic analysis of the data was undertaken using SigmaPlot (v.5.0) program and the microsomal data was found to be described by standard Michaelis-Menten kinetics with a V_{max} of 2.81 μg/min/mg protein and an apparent K_M of 0.45 μg/mL. CL_{int} was calculated from the ratio of V_{max} to K_m and was estimated to be 6.2 mL/min/mg microsomal protein. The V_{max} and K_m parameters obtained were in close approximation to the V_{max} (2.79 μg/min/mg protein) and K_m (0.42 μg/mL) derived from the Eadie-Hofstee plot of v_o versus v_o/[S] (**Figure 20**). The calculated *in vitro* CL_{int} expressed per mg of microsomal protein was scaled to a CL_{int} value expressed per kg of body weight to reflect whole liver CL_{int} using experimentally determined scaling parameters (see Appendix III). The predicted CL_h and extraction ratio was calculated to be 75 mL/min/kg and 0.94, respectively.

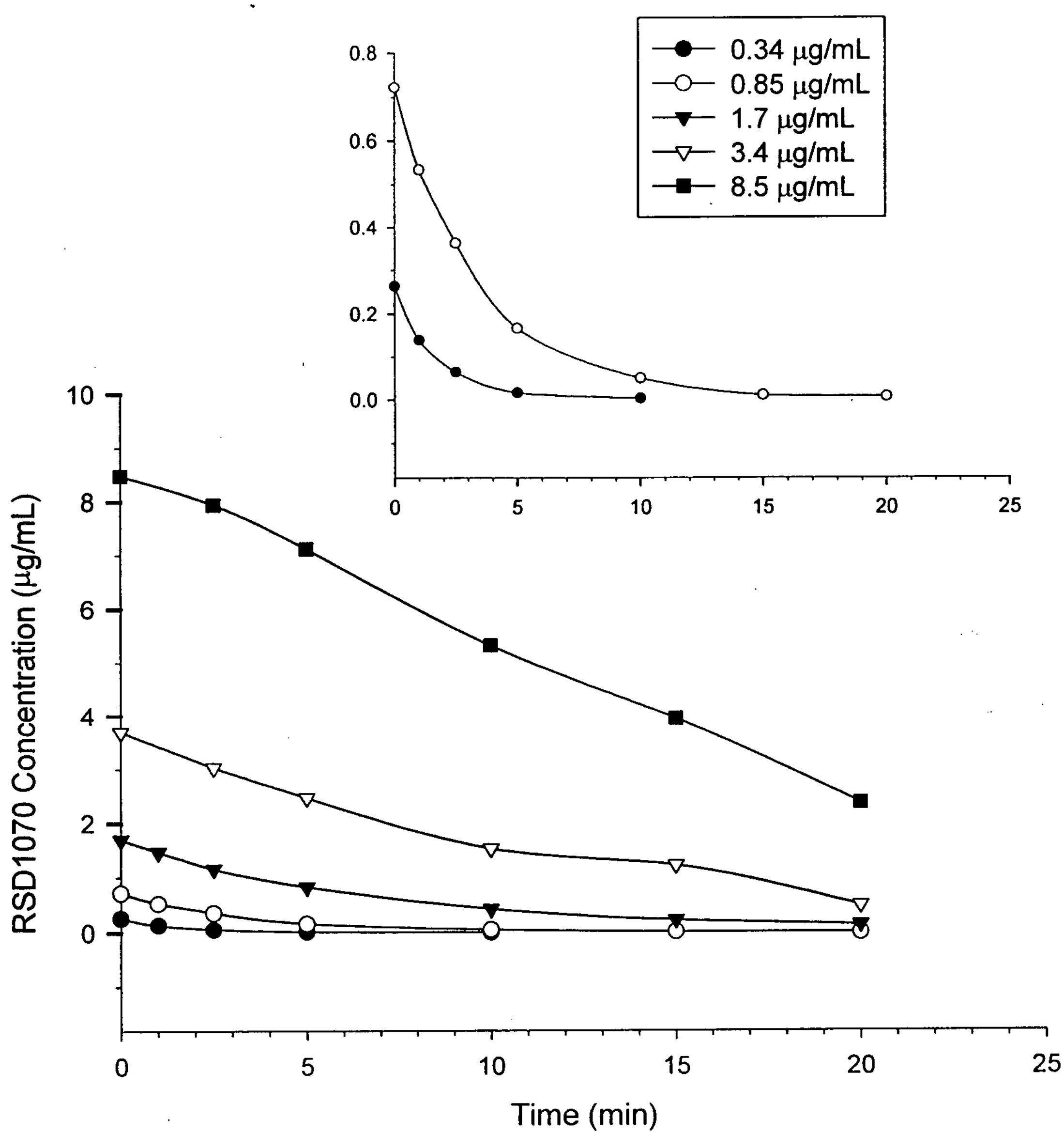

Figure 18. **RSD1070 concentration versus time disappearance profile in rat liver microsomal incubations. Initial concentrations of RSD1070 ranging from 0.34 – 8.5 µg/mL were incubated in duplicate with 0.1 mg/mL of pooled rat liver microsomes and 1.5 mM NADPH. The reaction was terminated at various time points with the addition of 2M NaOH. All samples were processed and analyzed as described in the text. The insert diagram shows the disappearance profile for the lower substrate concentrations of 0.34 and 0.85 µg/mL on a smaller y-axis scale.**

Table 12. **Initial rate (v_o) of RSD1070 consumption catalyzed by microsomal enzymes for each starting substrate concentration. Incubation conditions consisted of 0.1 mg/mL microsomal protein and 1.5 mM NADPH. The initial rates were calculated as the negative slope of the initial linear decline from the parent compound disappearance profile (Figure 18).**

Initial RSD1070 Concentration $[S]_o$ μg/mL	Initial reaction rate (v_o) μg/min/mg protein
0.34	1.2
0.85	1.9
1.7	2.2
3.4	2.5
8.5	2.7

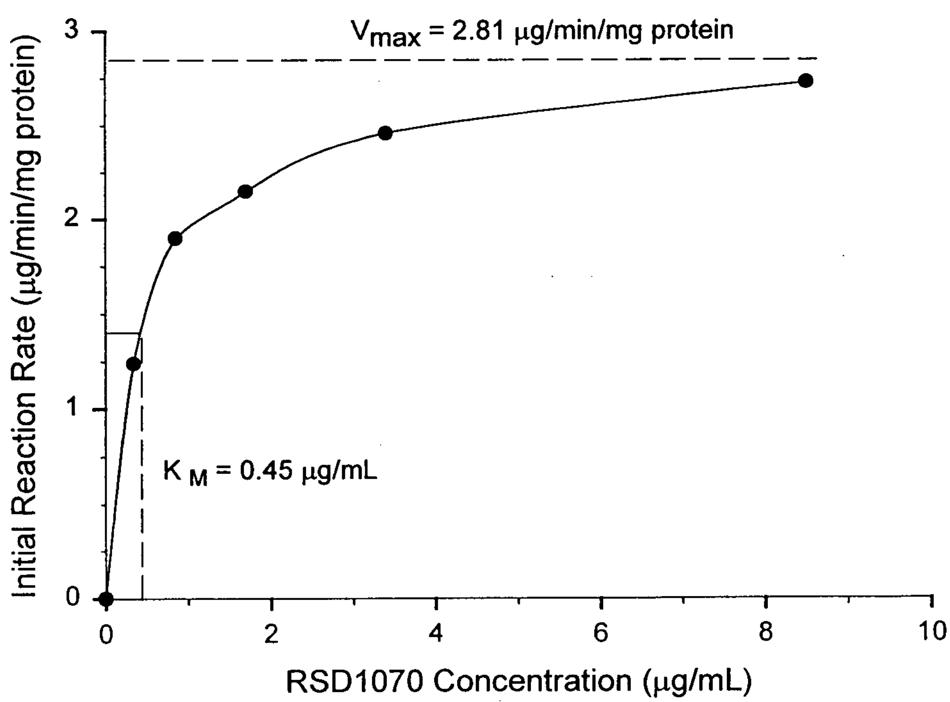

Figure 19. **Relationship between initial linear rate of RSD1070 disappearance and starting concentrations of RSD1070 in a typical microsomal incubation. V_{max} and K_m were estimated by model fitting the data to the standard Michaelis-Menten equation using the Sigma Plot (v5.0) program.**

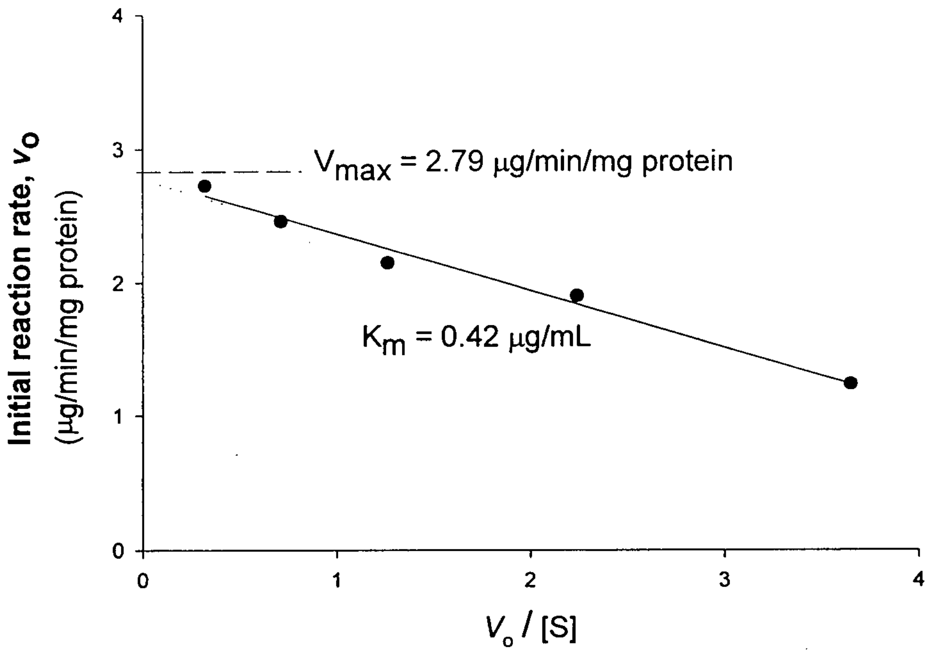

Figure 20. **Eadie-Hofstee plot for the determination of V_{max} and K_m describing the consumption of RSD1070. The relationship between the initial reaction rate v_o versus v_o/[S] is plotted, and a straight line is obtained where the slope is equal to – K_m and the y-intercept is equal to V_{max}.**

3.4.5 Parent Compound Disappearance Studies: Determination of CL_{int} Using the *In Vitro* Half-life Approach

The log RSD1070 concentration versus time profile (**Figure 21**) demonstrated linear first-order elimination at each substrate concentration. Elimination $t_{1/2}$ parameters were calculated for each profile and *in vitro* CL_{int} was calculated using the $t_{1/2}$ approach (**Table 13**). The $t_{1/2}$ approach was derived from the Michaelis-Menten equation (Appendix I) and the calculation of *in vitro* CL_{int} required that the microsomal incubation reaction occurs under linear conditions ([S] << K_m). The $t_{1/2}$ from the elimination of RSD1070 at a substrate concentration of 0.34 μg/mL (1 μM) was used to determine CL_{int}. The microsomal CL_{int} value of 5.9 mL/min expressed in terms of mg of microsomal protein was "scaled-up" to reflect the whole liver CL_{int} value of 1.1 x 10^4

mL/min/kg, and was similar to the value obtained from the ratio of V_{max} and K_m. Using this approach, the predicted CL_h and extraction ratio was calculated to be 75 mL/min/kg and 0.94, respectively.

However, the criteria that the microsomal reaction must occur under first order conditions ([S] << K_m) may not have been met using the substrate concentration of 0.34 μg/mL, since the apparent K_m was estimated to be 0.45 μg/mL. Under this circumstance, *in vitro* intrinsic clearance was determined from the relationship between $t_{1/2}$ and the Michaelis-Menten parameters without the assumption that [S] << K_m (detailed in Appendix II). The predicted hepatic clearance value of 72 mL/min/kg and extraction ratio of 0.9 was in close approximation to the values obtained from *in vitro* $t_{1/2}$ approach with the assumption that [S] << K_m and from the enzyme kinetic approach.

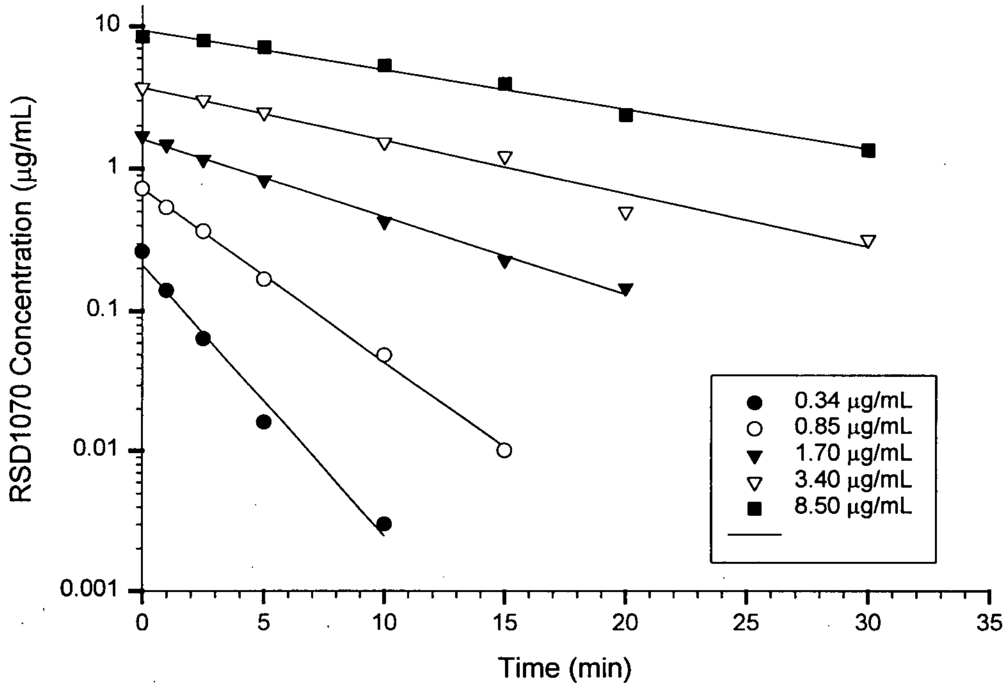

Figure 21. **Disappearance time-profiles of RSD1070 (log concentration vs. time) in rat liver microsomal studies. Initial concentration of RSD1070 ranging from 0.34 – 8.5 µg/mL were incubated with 0.1 mg/mL of microsomal protein, and the reaction terminated at time points ranging from 0 to 30 min.**

Table 13. ***In vitro*** **intrinsic clearance calculated for each initial substrate concentration of RSD1070. The half-life values for corresponding substrate concentrations were calculated from the slope of the parent compound disappearance profile using 0.1 mg microsomal protein/mL (shown in Figure 21). The half-life approach was used to calculate the CL_{int} values expressed per mg of microsomal protein (see Appendix I for details).**

$[S]_o$ µg/mL	Half-life ($t_{1/2}$) min/ 0.1 mg protein	CL_{int} mL/ min/ mg protein
0.34	1.2	5.9
0.85	2.5	2.8
1.7	5.0	1.4
3.4	8.1	0.9
8.5	12.1	0.6

3.4.6 Comparison of Predicted and Observed Hepatic Clearances and Extraction Ratio

The predicted CL_h and hepatic extraction ratio obtained from the parent compound disappearance time-profile from microsomal studies closely approximated the observed values after single bolus iv dosing (**Table 14**). The predicted CL_h was calculated to be 75 mL/min/kg using the well-stirred liver model with incorporation of experimentally determined CL_{int}, and plasma and microsomal protein free fraction parameters. Furthermore, the predicted hepatic extraction ratio was estimated to be 0.94, or 94% of hepatic blood flow (Appendix II). The predicted and observed hepatic extraction values both indicate that RSD1070 is mostly eliminated by liver metabolism.

Table 14. Predicted and observed hepatic clearance and hepatic extraction ratio values. The observed values were obtained from the calculated pharmacokinetic parameters following single iv bolus administration of a dose of 12 mg/kg in rats (n=8). Clearance and hepatic extraction values were predicted from the rat liver microsomal metabolism studies by applying the "scaled-up" CL_{int} obtained from the parent compound disappearance to the well-stirred liver model (see Appendix I and III for details).

	PREDICTED (pooled microsomes)	**OBSERVED (n = 8)**
CL_h (mL/min/kg)	75	71 ± 9
Hepatic Extraction Ratio	0.94	0.88 ± 0.11

CHAPTER 4
DISCUSSION

4.1 ANALYSIS OF RSD1070 BY LC/MS/MS

Previous analytical methods utilized reverse-phase high performance liquid chromatography coupled with ultraviolet detection (LC/UV) for the analysis of an arylacetamide analogue of RSD1070 in rat blood and various tissues (Walker *et al.*, 1996). However, despite being a versatile and convenient method, LC/UV offered limited assay sensitivity to a concentration of approximately 0.1 μg/mL. Thus, there was a need for a more sensitive and selective assay for the investigation of RSD1070 metabolites and for the pharmacokinetic studies to be conducted within the scope of this project.

LC/MS/MS was the method of choice for this investigation for several reasons. Tandem mass spectrometry with the use of collision induced dissociation of the parent compounds into characteristic daughter ions served as a semi-diagnostic tool that allows some inferences as to possible metabolite structures and molecular weight information (Perchalski *et al.*, 1982; Covey *et al.*, 1986). Tandem mass spectrometry (MS/MS) is based on the premise that metabolites retain substructures of the parent drug molecule and produce MS/MS product ions associated with those substructures. The application of LC/MS/MS for rapid structural identification of drug metabolites has been significant and has provided valuable insight into the pathways of biotransformation (reviewed by Perchalski *et al.*, 1986; Lee *et al.*, 1997). Furthermore, the increased sensitivity and selectivity of LC/MS/MS allows for greater characterization of the terminal elimination phase of the plasma concentration versus time profile for the pharmacokinetic studies. In order for these results to be reliably interpreted, the LC/MS/MS analytical method employed for the quantitative determination of RSD1070 and its metabolite in biological samples was required to be well-characterized and validated.

A reliable LC/MS/MS assay for RSD1070, the novel antiarrhythmic compound under investigation, and its N-dealkyl metabolite has been developed and we report that the assay provided the conditions necessary for the resolution of the analytes and the internal standard. Electrospray ionization at atmospheric pressure served as an efficient means of positive ion generation and solvent desolvation. Tandem mass spectrometers operated under multiple reaction monitoring provided adequate selectivity and sensitivity for the detection of the compounds of interest. The assay was validated for both RSD1070 and its N-dealkyl metabolite in rat plasma and rat hepatic microsome matrix and met the criteria of Shah *et al.* (1991) and Karnes and March (1993). According to these analytical validation guidelines, precision did not exceed 15 % CV (20 % CV at the LOQ) and accuracy was within ± 15 % (± 20 % at the LOQ) of the actual concentrations. All samples were prepared by a rapid, single-step liquid-liquid extraction procedure using methyl *tert*-butyl ether as the organic solvent. Methyl *tert*-butyl ether has been previously demonstrated to be successful in the extraction method for an arylacetamide antiarrhythmic analogue of RSD1070 with extraction recoveries of 77 – 90 % (Walker *et al.*, 1996).

4.2 PROTEIN BINDING STUDIES OF RSD1070

The plasma protein binding of drugs has been shown to have significant effects on numerous aspects of pharmacokinetics such as volume of distribution and clearance (Tozer, 1981). Generally, it is believed that only the unbound drug is available for drug clearance pathways such as hepatic clearance and glomerular filtration. The measurement of total drug concentration does not provide the required information concerning the unbound fraction of drug that is available for distribution and elimination; therefore, the unbound fraction is required (Wright *et al.,* 1996). With regards to this project, the unbound fraction of RSD1070 in rat plasma and microsomal matrix was investigated to relate intrinsic clearance and hepatic clearance for the prediction of hepatic extraction according to the well-stirred liver model.

In vitro plasma protein binding studies were conducted by spiking known amounts of RSD1070 in blank rat plasma. The method of equilibrium dialysis was chosen for the determination of plasma protein binding because non-specific binding of RSD1070 to Ultrafree® and Centrifree® Amicon ultrafiltration devices was demonstrated to be significant (data not shown). RSD1070 demonstrated extensive plasma protein binding with an average free fraction of 1.5 % over the concentration range of 2.3 to 20.7 µg/mL. The concentration range was chosen to reflect the *in vivo* plasma concentrations observed in the rat pharmacokinetic studies (0.02 - 9.16 µg/mL). The low free fraction and high hepatic extraction ratio of RSD1070 is consistent with compounds that exhibit a very high liver metabolic activity ($CL_{int} >> Q$) with little influence by the extent of plasma protein binding. Examples are propranolol (Evans *et al.*, 1973), quinidine (Guentert and Øie, 1980), and S-disopyramide (Huang and Øie, 1985). Such behavior has been termed "nonrestrictive clearance" indicating that the liver extraction ratio is greater than unbound fraction of drug delivered to the liver (Wilkinson and Shand, 1975). This has been conceptualized to occur under conditions of very high CL_{int} that lead to very rapid, almost instantaneous, removal of unbound drug from the plasma. As a result, the binding equilibrium rapidly shifts to favor the spontaneous dissociation of the drug-protein complex to unbound drug.

In addition to plasma free fraction, the free fraction of RSD1070 in microsomal incubations was also investigated by equilibrium dialysis. In *in vitro* metabolism systems, the assumption that all substrate molecules are available to bind to enzyme is most likely invalid for most compounds and the importance of non-specific binding in *in vitro* matrices has been investigated (Bäärnhielm *et al.,* 1986; Obach, 1996). The early study of felodipine liver microsome metabolism by Bäärnhielm and colleagues demonstrated the importance of making corrections for the non-specific binding of substrate to microsomes in the development of an *in vitro- in vivo* correlation. Felodipine demonstrated high protein binding in blood and in microsomes, which resulted in the cancellation of the free fraction parameters in the well-stirred model of hepatic extraction. Incorporation of the low free fraction in plasma without determining non-specific binding to liver microsomes resulted in a very large underestimation of CL_h. The importance of obtaining free fractions in *in vitro* microsomal incubations for the correction of K_m was further exemplified in early *in vitro-in vivo* correlation studies with ethoxybenzamide (Lin *et al.,* 1978; Lin *et al.,* 1980), imipramine and desipramine (Chiba *et al.,* 1989), and diazepam and analogues (St. Pierre and Pang, 1995). Further investigations that specifically addressed the impact of non-specific binding to microsomes on the relationship between *in vitro* CL_{int} and *in vivo* CL_h were conducted for test compounds warfarin, propranolol and imipramine (Obach, 1997) and for a large panel of acidic, basic and neutral compounds with diverse structures (Obach 1999). Within these studies, Obach demonstrated that the inclusion of both free fraction parameters in plasma and microsomes resulted in the best agreement between *in vivo* clearance values and clearance values projected from *in vitro* CL_{int} data. The inclusion of free fraction in microsomal incubation matrix is not necessarily reflective of the *in vivo* situation, but is necessary so that *in vivo* and *in vitro* situations can be extrapolated around a common parameter: $CL_{int.}$

Based on the above significance of non-specific binding in microsomal incubation, the free fraction of RSD1070 in microsomal matrix was investigated. Equilibrium dialysis was conducted and substrate and microsomal protein were incubated at concentrations reflective of metabolism conditions used to obtain *in vitro* CL_{int}. However, dialysis was conducted in the absence of NADPH cofactor to prevent metabolic turnover of substrate. RSD1070 demonstrated non-specific binding to microsomal protein (0.1 mg/mL) with a free fraction ($f_{u\ mx}$) of 15 %.

Based on the plasma protein and microsomal protein results, the binding of RSD1070 (a basic compound with a pKa of 7.8) is consistent with the overall trend that basic lipophilic amine compounds demonstrate extensive binding to plasma proteins and to microsomal proteins compared to neutral and acidic compounds (Obach, 1999). Furthermore, extensive non-specific binding of RSD1070 to microsomal matrix was demonstrated at substrate and microsomal protein concentrations in the range of those used in the *in vitro* metabolism studies. Therefore, the free fraction of substrate available for *in vitro* metabolism was considered for the prediction of hepatic clearance from intrinsic clearance data.

4.3 *IN VIVO* INVESTIGATION OF HEPATIC EXTRACTION

Although RSD1070 demonstrated potent ischaemia-selective antiarrhythmic activity, pre-clinical pharmacokinetic studies demonstrated poor oral bioavailability based on the AUC ratios following oral (gastric lavage) and iv dosing (Dr. Richard A. Wall, personal communications). Oral bioavailability is defined by the extent to which an orally administered dose reaches the systemic circulation intact (Perrier *et al.,* 1973). Upon oral drug administration there are various factors that influence its availability to the systemic circulation. As drug passes down the gastrointestinal (GI) tract, part of the dose may not be available due to chemical degradation or physical inactivation. The physical properties (e.g. lipophilicity and particle size) of the compound may regulate its rate of absorption across the gut wall from the luminal contents by carrier-mediated transport or simple diffusion into the gastric and intestinal mucosa. Non-ionized (lipid soluble) compounds and compounds having smaller particle size are more likely to have a rapid dissolution rate and be soluble in the gastrointestinal fluids for absorption (Klassen and Rozman, 1991). Otherwise poor permeability across the gastrointestinal mucosa and insufficient contact time in transit of the GI lumen may lead to incomplete absorption and fecal excretion of the drug. Within the GI lumen, the oral bioavailability may be compromised by cytochrome P-450 reductive biotransformation (e.g. azo reduction, aromatic reduction, and aromatic dehalogenation) by gut microflora (Klassen and Rozman, 1991). Furthermore, a compound that is well absorbed may be poorly available due to biotransformation in transit through the gastrointestinal cells leading to presystemic GI elimination (reviewed by George, 1981). After transit through the gastrointestinal epithelial cells, the fraction of unchanged drug that is absorbed into blood is carried via the hepatic portal vein towards the liver. The liver may play a major role in presystemic drug elimination by way of biotransformation or biliary excretion that result in a decrease in the fraction of dose available for systemic circulation (reviewed by Pond and Tozer, 1984). Since the elimination pathways described above are likely to be saturable processes, oral bioavailability is likely to be a dose-dependent process with increasing bioavailability at increasing doses. The bioavailability of an orally administered dose into the systemic circulation is comprised of the individual fractions that survive the various barriers encountered by the drug during first passage from the gut lumen to the sampling site (Kwan, 1997; Pang and Gillette, 1978).

RSD1070 may be one of those drugs that exhibit low oral bioavailability due to substantial first-pass hepatic loss and form pharmacologically active metabolites. In such cases, the pharmacological activity following oral administration is greater than anticipated from parent compound bioavailability data (Rowland, 1988). However, because adequate metabolism and pharmacokinetic data was not available to allow explanations for the poor bioavailability (e.g. high hepatic or gut first pass effect or poor oral absorption), the present studies were undertaken. The main focus of this project was to investigate the contribution of hepatic extraction of RSD1070 towards the poor oral bioavailability observed in rats.

The hypothesis for this research project was based on unpublished observations that RSD1070 demonstrated poor oral bioavailability albeit pharmacological activity following oral (gastric lavage) and iv dosing. This project made an assumption that RSD1070 was characterized with low oral bioavailability, which should have been tested as the initial study. By replicating the poor oral bioavailability of RSD1070 in rats, this assumption would have been removed and the preliminary data would strengthen the basis for the working hypothesis. Therefore, the oral administration of a therapeutic dose of RSD1070 in rats should be the first *in vivo* study conducted for the confirmation of poor oral bioavailability.

The pharmacokinetic studies that were proposed in this research project sought to investigate the apparent hepatic extraction of RSD1070. The pharmacokinetic study conducted consisted of administering RSD1070 as a single iv bolus followed by sampling plasma and 24 hr urine. Based on the results, CL_{tot} (71 mL/kg) approximated the literature value for hepatic blood flow of 80 mL/kg (Pollack *et al.,* 1990) and CL_r was insignificant (<< 1% of CL_{tot}). Because the liver is the primary organ of drug metabolism and due to difficulties in estimating extrahepatic organ clearances *in vivo*, the fundamental assumption was made that the CL_{tot} approximated CL_h. Based on this assumption, hepatic extraction was calculated from the relationship of hepatic blood flow and hepatic clearance (Eqn. 10). The pharmacokinetic study conducted in this project did not investigate hepatic extraction directly in the whole animal and, therefore; did not test the hypothesis that the hepatic extraction played a significant role in explaining the poor oral bioavailability. The assumption that $CL_{tot} \approx CL_h$ may not be valid for several reasons. Total body clearance, which is a commonly determined clearance term, reflects the contribution of all elimination pathways in the whole animal system and can be considered as the sum total of all the individual and simultaneously occurring organ clearances (e.g. hepatic, renal, gut, lung, etc.) (Wilkinson, 1987). Although renal clearance was demonstrated to be insignificant, the possibility of other organ clearance pathways contributing to CL_{tot} can not be ruled out.

As for future studies, the following *in vivo* pharmacokinetic experiments could be conducted for quantifying the relative contribution of gut and liver presystemic elimination, and thus directly testing the hypothesis. The first experiment would involve investigating the fraction of dose available after first-passage through the liver by administering an intravenous bolus dose of RSD1070 via the hepatic portal vein cannula followed by determining the plasma AUC. By dosing via the hepatic portal vein and a peripheral vein and comparing their respective plasma AUCs, the hepatic bioavailability (F_h) representing the fraction of drug not extracted during the first passage through the liver can be estimated (Kwan, 1997):

$$F_h = \frac{D^{iv} \; AUC^{hp}}{D^{hp} \; AUC^{iv}}$$

where D^{iv} and D^{hp} refer to intravenous dose administered to the peripheral vein and hepatic portal vein *hp,* respectively. AUC^{hp} and AUC^{iv} refer to the area under the plasma concentration curve determined by venous sampling following hepatic portal and peripheral vein dosing. Therefore, by definition, hepatic extraction (E) would be represented by the quantity ($1 - F_h$).

However, a measure of E alone is insufficient to test the hypothesis and other factors contributing to oral bioavailability should be considered (Minchin and Ilet, 1982). The fraction of unchanged drug absorbed into the absorptive cells of the GI tract and metabolized in a single passage through the gut wall (F_a) should be assessed. By administering an oral dose by gastric lavage (D^{po}) and a dose via the hepatic portal vein (D^{hp}) followed by venous sampling to compare their respective AUCs, F_a can be calculated as follows (Kwan, 1997):

$$F_a = \frac{D^{hp} \; AUC^{po}}{D^{po} \; AUC^{hp}}$$

Therefore, the contribution of nonabsorption, fecal elimination, and first-pass effect due to gut elimination would be represented by the quantity ($1 - F_a$). Fecal analysis following oral dosing would provide an estimate of the nonabsorbed dose. The above studies would result in direct assessment of each of the major factors contributing to possible explanations for poor oral bioavailability. Although the above approach would be the most direct method of testing the contribution of hepatic extraction to oral bioavailability, the surgical preparation involving the cannulation of the hepatic portal vein for chronic instrumentation remains a practical issue.

Sodium pentobarbital (65 mg/kg) was administered to the rats as a general anesthetic prior to surgical cannulation and 24 hours were allowed for recovery. The possibility that the single dose of sodium pentobarbital may have induced cytochrome P450 enzymes and thus the pharmacokinetics of RSD1070 can not be ruled out.

4.4 *IN VITRO* INVESTIGATION OF HEPATIC EXTRACTION

4.4.1 Initial Investigation of RSD1070 Metabolites

The investigation of RSD1070 metabolism has not been characterized and the preliminary investigation of RSD1070 metabolites was conducted using rat liver microsomal incubations under conditions of excess substrate and protein concentration. Of particular interest is the molecular ion (MH^+) *m/z* 314^+ whose daughter ion fragmentation is consistent with the loss of an ethyl group from the N-morpholino ring resulting in an amino alcohol group.

A proposed mechanism for the formation of the metabolite is diagrammed below (**Figure 22**). The mechanism of metabolite formation possibly involves a two-step process involving tertiary amine N-dealkylation and O-dealkylation, two very important and frequently encountered liver metabolic reactions involving NADPH-dependent cytochrome P-450 (Willi and Bickel, 1973). N-dealkylation of the tertiary amine group of the N-morpholino ring to yield a secondary amine would result in an open-ring intermediate characterized with an aldehyde group and an intact ether bond. One proposed mechanism of N-dealkylation (Williams, 1989) involves abstraction of an electron from the amine by the perferryl oxygen intermediate, forming an aminium radical cation. The radical cation can abstract a hydrogen atom from the α-carbon to form a carbon-perferric hydroxide radical pair that recombines and collapses to an imminium ion. The imminium ion is subsequently hydrolyzed to the dealkylated amine resulting in an aldehyde carbonyl group, which would normally be the leaving group if not part of a cyclic structure. An alternative mechanism of N-dealkylation (Williams, 1989) of tertiary amines is via the N-oxide, which rearranges to the carbinolamine to produce the secondary amine. In either case, N-dealkylation alone would only result in the open ring aldehyde with the intact ether bond. Subsequent O-dealkylation of the ether bond would result in the amino alcohol metabolite.

N-dealkyl RSD1070 demonstrated sequential metabolism in microsomal incubations at a substrate concentration (1.7 μg/mL) within the therapeutic plasma concentration range observed *in vivo*. Initially, N-dealkyl RSD1070 was suspected to be the major metabolite present in microsomal incubations under conditions of excess substrate, microsomal protein, and NADPH concentrations. Under these *in vitro* conditions the metabolic pathways contributing to the elimination of the metabolite are likely to be saturated, which led to the interpretation that the N-dealkyl RSD1070 was a possible major metabolite.

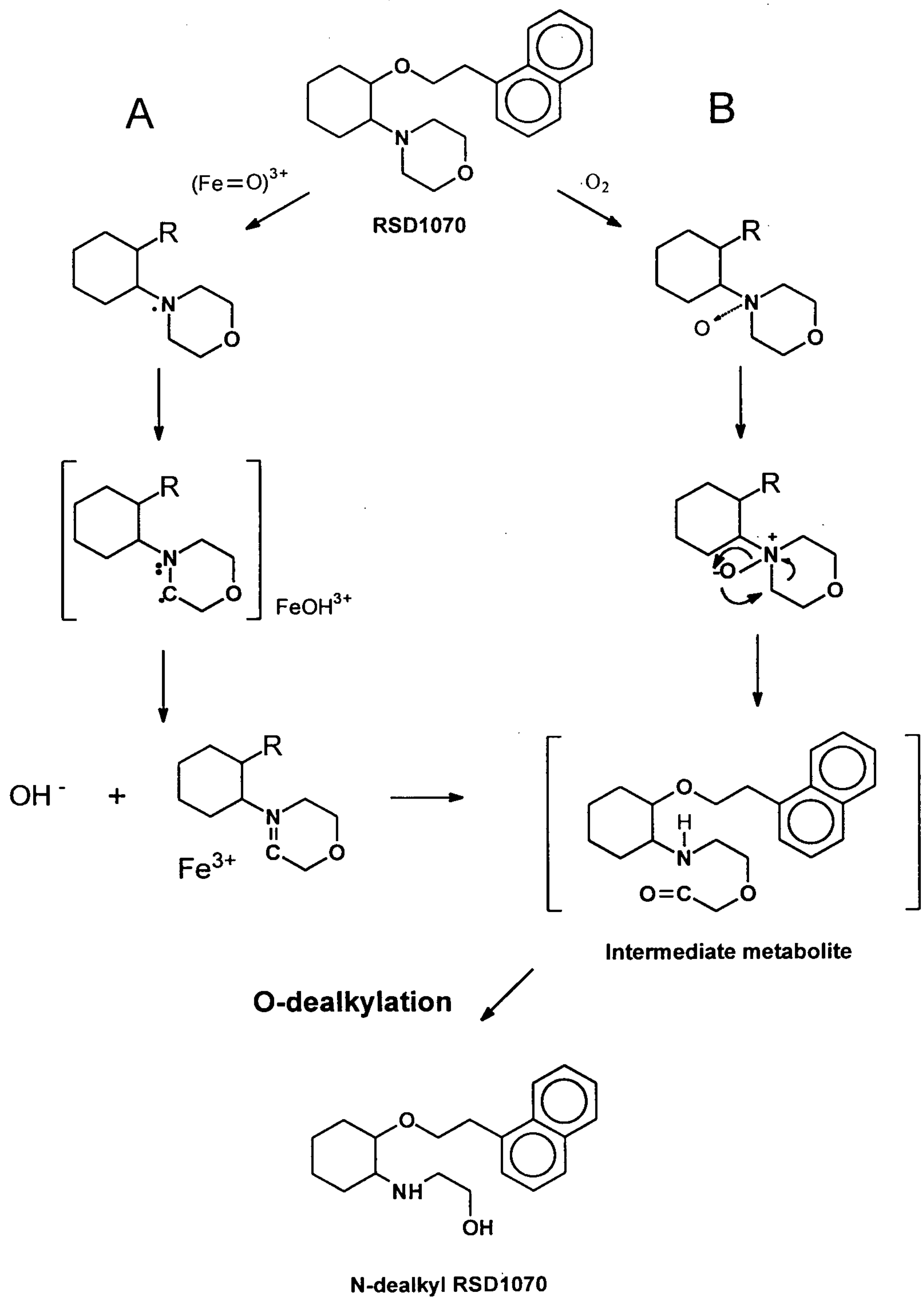

Figure 22. Proposed mechanisms for the formation of N-dealkyl RSD1070. N-dealkylation via (A) abstraction of amine electron by perferryl oxygen intermediate and (B) N-oxide formation. Subsequent O-dealkylation of the ether linkage occurs in a similar manner as N-dealkylation, resulting in the carbonyl leaving group.

4.4.2 *In Vitro* Estimates of Hepatic Clearance and Hepatic Extraction Ratio

This component of the project was designed to predict hepatic clearance and hepatic extraction from RSD1070 metabolism data in pooled hepatic microsomal preparations. Due to the inadequate information regarding major metabolites of RSD1070, parent compound studies were utilized and their disappearance profiles characterized. The feasibility of calculating the initial rate of drug consumption for hepatic clearance predictions has been demonstrated with diazepam (Igari *et al.,* 1983), acetaminophen and phenacetin (Pang *et al.,* 1985), and felodipine (Bäärnhielm *et al.,* 1986). The apparent K_m and V_{max} parameters obtained represent hybrid parameters that is a conglomeration of all the individual metabolic pathways contributing to the elimination of RSD1070 in microsomal incubations. In our study, the *in vitro* CL_{int} values obtained by both enzyme kinetic approach and *in vitro* half-life approach were in close approximation. However, due to the limitations of the assay, and the rapid elimination of RSD1070 in microsomal preparations, the kinetic profile for substrate concentrations below 0.34 μg/mL was unable to be characterized accurately at the microsomal protein concentration used. Although the V_{max} and K_m parameters obtained from the Eadie-Hofstee plot and the plot of vo versus [S] were in close approximation, the reported Km (0.45 μg/mL) describing the consumption of RSD1070 was a rough approximation because it was based on one concentration data point. In order to allow for a more confident estimate of K_m, the metabolism study should have been conducted with a lower microsomal protein concentration (< 0.1 mg/mL) and with a wider range of substrate concentrations at the lower end (e.g. 0.1 – 8.5 μg/mL). This would provide better characterization of the reaction rates from the initial linear decline of the disappearance profiles at lower substrate concentrations. Consequently, the plot of v_o versus [S] would consist of more data points in the linear range for a better estimate of K_m.

With regards to the *in vitro* half-life approach, Obach (1999) demonstrated its utility for the prediction of CL_h for a wide panel of substrates including new chemical entities. As a general rule, Obach used substrate concentrations of 1 μM for microsomal incubations and made the assumption that the substrate concentration used was below K_m. Because our study determined the *in vitro* $t_{1/2}$ from the first-order rate elimination at one concentration point (0.34 μg/mL, 1 μM) below the reported K_m, the $t_{1/2}$ value was only a rough estimate. Linear conditions would be ensured by calculating the first-order rate of elimination for several substrate concentrations below 0.34 μg/mL (1 μM) and a more confident *in vitro* $t_{1/2}$ value would have been obtained.

The concentration of 0.34 ug/mL used in the determination of *in vitro* $t_{1/2}$ is not less than 10% of K_m and thus, the assumption that $[S] << K_m$ is most likely not valid. Therefore, the *in vitro* $t_{1/2}$ was recalculated as detailed in Appendix II according to Obach *et al.*, (1997). The recalculated $t_{1/2}$ resulted in similar estimates of hepatic clearance (72 mL/min/kg) and extraction ratio (0.9) as compared to all previously described approaches.

The *in vitro* CL_{int} was scaled-up using the microsomal protein content per g liver and the average liver weight per kg of body weight to reflect the intrinsic metabolic activity of the intact liver. These scaling factors have been evaluated by Houston (1994) for their utility in predicting *in vivo* metabolic clearances, and are necessary to bridge enzyme kinetic data (expressed per mg microsomal protein) and pharmacokinetic data (expressed per kg of body weight). Furthermore the scaling factors standardize microsomal CL_{int} data to account for the interlaboratory variability in microsomal preparation by density centrifugation (Joly *et al.*, 1975) and variability due to differences in rat strain, diet, and specific techniques. The experimentally determined microsomal protein yield (42 mg protein/ g liver) was in close approximation to the literature average (45 mg protein/ g liver) reported by Houston (1994) and from various studies (Lin *et al.*, 1978; Bäärnhielm *et al.*, 1986; Chiba *et al.*, 1990). Several studies utilizing the scaling-factor strategy proposed by Houston satisfactorily predicted the *in vivo* disposition using rat hepatic microsomes and isolated hepatocytes for caffeine (Hayes *et al.*, 1994), phenytoin and tolbutamide (Ashworth *et al.*, 1995), and diazepam (Zomorodi *et al.*,1995; Carlile *et al.*, 1997).

The use of microsomes for *in vitro* metabolism studies for the purpose of *in vitro – in vivo* correlation has its limitations. Hepatic microsomes are functional units of the endoplasmic reticulum representing the metabolic capability of the liver. However, the metabolic capability of microsomes consists primarily of the NADPH dependent cytochrome P-450 system and is limited to only the Phase I drug biotransformation reactions. Furthermore, microsomes do not account for the non-cytochrome P-450 Phase I biotransformation reactions (e.g. amidases, esterases, dehydrogenases) and lack the required cofactors for Phase II conjugation reactions that are primarily located in the cytosol. Another limitation of hepatic microsomes is their limited longevity in enzyme activity which becomes problematic for compounds that require lengthy incubations to characterize the temporal profile (Houston, 1994). The ability for hepatic microsomes to successfully predict CL_h and E is compound specific and requires several assumptions: (1) the compound is primarily cleared by hepatic metabolism (such that $CL_h >> CL_r + CL_{biliary} + CL_{other}$), (2) liver metabolic capacity >> metabolic capacity of all other tissues, and (3) microsomal reactions (e.g., cytochrome P450) >> all other non-microsomal reactions

(Obach, 1997). These assumptions are not valid for all compounds and other clearance mechanisms (e.g. lung, biliary, renal) and other possible metabolic routes (e.g. nonmicrosomal Phase II conjugation) should be considered.

Despite the above limitations, rat hepatic microsomal metabolism studies were used as an *in vitro* model to test the hypothesis that high hepatic extraction plays a role in the poor oral bioavailability of RSD1070. The results indicated that the predicted CL_h value from microsomal data (75 mL/min/kg) was in close approximation to the apparent CL_{tot} value in rats (71 mL/min/kg), and that RSD1070 was highly extracted by the liver with a predicted extraction ratio of 0.94. The microsomal data suggested that the high metabolic capacity of the liver contributed to the apparent hepatic extraction of RSD1070 with approximately 94 % of the fraction of drug available to the liver eliminated by metabolic elimination. The findings are consistent with the hypothesis that RSD1070 is a high extraction compound, however; the *in vitro* experiments conducted do not test if hepatic extraction is the major determining factor for the poor oral bioavailability. Further experiments are required to investigate gut absorption and pre-systemic gut elimination as factors that may alter the oral bioavailability of RSD1070. Also, future studies may involve the use of human microsomes or hepatocytes for the prediction of the hepatic clearance of RSD1070 in man.

CHAPTER 5
SUMMARY AND CONCLUSION

The first objective was to investigate the metabolism of RSD1070 using microsomal incubations under conditions of excess substrate and microsomal protein. A possible major metabolite was identified and was consistent with the N-dealkylation of the N-morpholino ring of RSD1070 based on MS/MS fragmentation studies. N-dealkyl RSD1070 was also identified in rat plasma sample following iv dosing of RSD1070 and the metabolite was later synthesized by Nortran Pharmaceuticals Ltd. for quantitative purposes.

The second objective was to develop and validate an LC/MS/MS analytical assay for the reliable quantitation of RSD1070 and its N-dealkyl metabolite in plasma and microsomal matrices. A rapid, single-step, liquid-liquid base extraction method was developed to process all samples from various biological fluids. Reverse-phase high pressure liquid chromatography demonstrated adequate separation of all analytes with sharp, symmetrical peaks. Positive ion electrospray served as the source of ionization and analytes were detected with the MS/MS operating under multiple reaction monitoring. The assay demonstrated acceptable inter-assay and intra-assay precision and accuracy based on low, mid, and high QC samples.

The third objective was to conduct whole animal (*in vivo*) pharmacokinetic studies in rat to estimate hepatic clearance and hepatic extraction ratio from its pharmacokinetic parameters. RSD1070 demonstrated multi-exponential decay with a rapid elimination half-life of 25 ± 8 min and total body clearance of 71 ± 9 mL/min/kg. RSD1070 was poorly excreted in the urine with an estimated renal clearance of 0.06 mL/min/kg, less than 0.5% of total body clearance.

However, hepatic clearance and extraction were unable to be estimated from the *in vivo* experiments conducted. Furthermore, the *in vivo* experiments were unable to determine if hepatic extraction contributed to the poor oral bioavailability of RSD1070, and thus failed to test the hypothesis.

The fourth objective was to determine the free fraction of RSD1070 in plasma and in microsomal incubations. Protein binding was investigated using equilibrium dialysis and RSD1070 demonstrated high protein binding with a free fraction of 1.5 % in plasma and 15 % in microsomal incubate.

The last objective was to utilize microsomal metabolism CL_{int} data for the prediction of hepatic clearance and extraction. CL_{int} obtained from the ratio of V_{max} (2.81 μg/min/mg protein) to K_m (0.45 μg/mL) were in close approximation to the value obtained by the in vitro half-life approach. Based on the well-stirred liver model, the predicted CL_h (75 mL/min/kg) closely approximated the apparent CL_{tot} (71 mL/min). RSD1070 was predicted to be a high hepatic extraction compound (E = 0.94) which suggests that the high metabolic capacity of the liver plays a role in its elimination. The *in vitro* studies were consistent with the hypothesis that RSD1070 was highly extracted by the liver, however; the studies did not test if the high hepatic extraction was primarily responsible for the poor oral bioavailability. Further studies investigating the contribution of gastrointestinal absorption and elimination are required to determine the relative contribution of hepatic extraction in the overall scheme.

CHAPTER 6
REFERENCES

Ashworth EIL, Carlile DJ, Chenery R and Houston JB. Prediction of *in vivo* disposition from *in vitro* systems: Clearance of phenytoin and tolbutamide using rat hepatic microsomal and hepatocyte data. *J. Pharmacol. Exp. Ther.*, **274,** 761-766 (1995).

Bäärnhielm C, Dahlbäck H and Skänberg. *In vivo* pharmacokinetics of felodipine predicted from *in vitro* studies in rat, dog and man. *Acta. Pharmacol. Toxicol.*, **59,** 113-122 (1986).

Carlile DJ, Zomorodi K and Houston JB. Scaling factors to relate drug metabolic clearance in hepatic microsomes, isolated hepatocytes, and the intact liver: Studies with induced livers involving diazepam. *Drug Metabo. Dispos.*, **25,** 903-911 (1997).

Chiba M, Fujita S and Suzuki T. Pharmacokinetic correlation between *in vitro* hepatic microsomal enzyme kinetics and *in vivo* metabolism of imipramine and desipramine in rats. *J. Pharm. Sci.*, **79,** 281-287 (1990).

CAST Investigators. Preliminary report: effect of encainide and flecainide on mortality in a randomized trial of arrhythmia suppression after myocardial infarction. *N. Engl. J. Med.*, **321,** 406-412 (1989).

Covey TR, Lee ED and Henion JD. High-speed liquid chromatography/ tandem mass spectrometry for the determination of drugs in biological samples. *Anal. Chem.*, **58,** 2453-2460 (1986).

Dallner G. Isolation of rough and smooth microsomes – general. *Methods Enzymol.*, **31,** 191-201 (1974).

Ellin A, Jakobsson SB, Schenkman JB and Orrenius S. P450$_k$ of rat kidney cortex microsomes: Its involvement in fatty acid ω- and (ω-1) hydroxylation. *Arch. Biochem. Biophys.*, **150,** 64-71 (1971).

Evans GH, Nies AS, and Shand DG. The disposition of propranolol. III. Decreased half-life and volume of distribution as a result of plasma protein binding in man, monkey, dog, and rat. *J. Pharmacol. Exp. Ther.*, **186,** 114-120 (1973).

Fang WF and Strobel HW. The drug and carcinogen metabolism system of rat colon microsomes. *Arch. Biochem. Biophys.*, **186,** 128-138 (1978).

Garfinkel D. Studies on pig liver microsomes. I. Enzymatic and pigment composition of different microsomal fractions. *Arch. Biochem. Biophys.*, **77,** 493-500 (1958).

George CF. Drug metabolism by the gastrointestinal mucosa. *Clin. Pharmacokinet.*, **6,** 259-274 (1981).

Gillette JR. Factors affecting drug metabolism. *Ann. N. Y. Acad. Sci.*, **179,** 43-66 (1971).

Groves JT and Han YZ. Models and mechanisms of cytochrome P450 action. In: "Cytochrome P450: Structure, Mechanism, and Biochemistry", 2nd edition, edited by Ortiz de Montellano PR, Plenum Press, New York, 3-48 (1995).

Guengerich FP. Metabolism of vinyl chloride: Destruction of the heme of highly purified liver microsomal cytochrome P450 by a metabolite. *Mol. Pharmacol.*, **13,** 911-923 (1977).

Guentert TW and Øie S. Effect of plasma protein binding on quinidine kinetics in the rabbit. *J. Pharmacol. Exp. Ther.*, **215,** 165-171 (1980).

Hayes KA, Brennan B, Chenery R and Houston JB. *In vivo* disposition of caffeine predicted from hepatic microsomal and hepatocyte data. *Drug Metab. Dispos.*, **23,** 349-353 (1994).

Hodgson AV, White TB, White JW and Strobel HW. Expression analysis of the mixed-function oxidase system in rat brain by the polymerase chain reaction. *Mol. Cell. Biochem.* **121,** 171-174 (1993).

Hondeghem LM and Katzung BG. Antiarrhythmic agents: their modulated receptor mechanism of action of sodium and calcium channel-blocking drugs. *Annu. Rev. Pharmacol. Toxicol.,* **24,** 387-423 (1984).

Hondeghem LM and Mason JW. Agents used in cardiac arrythmias. In: "Basic and Clinical Pharmacology", 3rd edition, edited by Katzung BG, Appleton & Lange, East Norwalk, 151-168 (1987).

Houston JB. Utility of *in vitro* drug metabolism data in predicting *in vivo* metabolic clearance. *Biochem. Pharmacol.*, **47,** 1469-1479 (1994).

Houston JB and Carlile DJ. Prediction of hepatic clearance from microsomes, hepatocytes, and liver slices. *Drug Metab. Rev.,* **29,** 891-922 (1997).

Huang JD and Øie S. Influence of serum protein binding on hepatic clearance of S-disopyramide in the rabbit. *J. Pharm. Pharmacol.* **37,** 471-475 (1985).

Igari Y, Sugiyama Y, Sawada Y, Iga T and Hanano M. *In vitro* and *in vivo* assessment of hepatic and extrahepatic metabolism of diazepam in the rat. *J. Pharm. Sci.,* **73,** 826-828 (1984).

Iwatsubo T, Hirota N, Ooie T, Suzuki H, Shimada N, Chiba K, Ishizaki T, Green CE, Tyson CA and Sugiyama Y. Prediction of *in vivo* drug metabolism in the human liver from *in vitro* metabolism data. *Pharmacol. Ther.*, **73,** 147-171 (1997).

Joly J-G, Doyon C and Pesant Y. Cytochrome P450 measurement in rat liver homogenate and microsomes. Its use for correction of microsomal losses incurred by density centrifugation. *Drug Metab. Dispos.*, **3,** 577-586 (1975).

Kallner A and DeVerdier CH. The concept of clearance. *Scan. J. Clin. Lab. Invest.*, **42,** 473-475 (1982).

Karnes HT and March C. Precision, accuracy, and data acceptance criteria in biopharmaceutical analysis. *Pharm. Res.*, **10,** 1420-1426 (1993).

Klaassen CD and Rozman K. Absorption, distribution, and excretion of toxicants. In: "Casarett and Doull's Toxicology: The Basic Science of Poisons", 4th edition, edited by Amdur MO, Doull J and Klaassen CD, McGraw Hill Inc., New York, 50-87 (1991).

Klingenberg M. Pigments of rat liver microsomes. *Arch. Biochem. Biophys.*, **75,** 376-386 (1958).

Kwan KC. Oral bioavailabiltiy and first-pass effects. *Drug Metab. Dispos.*, **25,** 1329-1336 (1997).

Lee MS, Kerns EH, Hail ME, Liu J and Volk KJ. Recent applications of LC-MS techniques for the structural identification of drug metabolites and related compounds. *LC-GC,* **15,** 542-558 (1997).

Lin JH, Hayashi M, Awazu S and Hanano M. Correlation between *in vitro* and *in vivo* drug metabolism rate: Oxidation of ethoxybenzamide in rat. *J. Pharmacokinet. Biopharm.*, **6,** 327-337 (1978).

Lin JH, Sugiyama Y, Awazu S and Hanano M. Kinetic studies on the deethylation of ethoxybenzamide. *Biochem. Pharmacol.*, **29,** 2825-2830 (1980).

Lowry OH, Rosebrough NJ, Farr AL and Randall RJ. Protein measurement with the folin phenol reagent. *J. Biol. Chem.* **193,** 265-275 (1951).

Lu AYH and Coon MJ. Role of hemoprotein P450 in fatty acid ω-hydroxylation in a soluble enzyme system from liver microsomes. *J. Biol. Chem.* **243,** 1331-1332 (1968).

Lu AYH, Junk KW, and Coon MJ. Resolution of the cytochrome P450 containing ω-hydroxylation system of liver microsomes into three components. *J. Biol. Chem.*, **244,** 3714-3721 (1969).

Minchin RF and Ilett KF. Presystemic elimination of drugs: theoretical considerations for quantifying the relative contribution of gut and liver. *J. Pharm. Sci.,* **71,** 458-460 (1982).

Mutnick AH. Cardiac arrhythmias. In: "Pharmacy Study Guide and Board Review", 2nd edition, edited by Shargel L, Mutnick AH, Souney PF, Swanson, LN, Block LH and Bartle WR. Williams & Wilkins, Baltimore, 646-668 (1998).

Obach RS. The importance of non-specific binding in *in vitro* matrices, its impact on enzyme kinetic studies on drug metabolism reactions for *in vitro-in vivo* correlations. *Drug Metab. Dispos.,* **24,** 1047-1049 (1996).

Obach RS. Nonspecific binding to microsomes: Impact on scale-up of *in vitro* intrinsic clearance to hepatic clearance as assessed through examination of warfarin, imipramine, and propranolol. *Drug Metab. Dispos.,* **25,** 1359-1369 (1997).

Obach RS, Baxter JG, Liston TE, Silber BM, Jones BC, MacIntyre F, Rance DJ and Wastall P. The prediction of human pharmacokinetic parameters from preclinical and *in vitro* metabolism data. *J. Pharmacol. Exp. Ther.,* **283,** 46-58 (1997).

Obach RS. Prediction of human clearance of twenty-nine drugs from hepatic microsomal intrinsic clearance data: An examination of *in vitro* half-life approach and non-specific binding to microsomes. *Drug Metab. Dispos.,* **27,** 1350-1359 (1999).

Okey AB. Enzyme induction in the cytochrome P-450 system. *Pharmacol. Ther.*, **45,** 241-298 (1990).

Omura T and Sato R. The carbon monoxide-binding pigment of liver microsomes. I. Evidence of its hemoprotein nature. *J. Biol. Chem.*, **239,** 2370-2378 (1964).

Omura T and Sato R. The carbon monoxide-binding pigment of liver microsomes. II. Solubilization, purification, and properties. *J. Biol. Chem.*, **239,** 2379-2385 (1964).

Ortiz de Montellano PR. Oxygen activation and transfer. In: "Cytochrome P450: Structure, Mechanism, and Biochemistry", edited by Ortiz de Montellano PR, Plenum Press, New York, 273-314 (1986).

Pang KS and Gillette JR. A theoretical examination of the effects of gut wall metabolism, hepatic elimination, and enterohepatic recycling on estimates of bioavailability and hepatic blood flow. . *J. Pharmacokinet. Biopharm.*, **6,** 355-367 (1978).

Pang KS, Kong P, Terrell JA and Billings RE. Metabolism of acetaminophen and phenacetin by isolated rat hepatocytes. *Drug Metab. Dispos.*, **13,** 42-50 (1985).

Perchalski RJ, Yost RA and Wilder BJ. Structural elucidation of drug metabolites by triple-quadrupole mass spectrometry. *Anal. Chem.* **54,** 1466-1471 (1982).

Perchalski RJ, Lee MS and Yost RA. Biotransformation and excretion: metabolite identification: other mass spectrometric methods. *J. Clin. Pharmacol.* **26,** 435-442 (1986).

Perrier D, Gibaldi M and Boyes RN. Prediction of systemic bioavailability from plasma-level data after oral drug administration. *J. Pharm. Pharmacol.*, 25, 256-257 (1973).

Pollack GM, Brouwer KLR, Demby KB and Jones JA. Determination of hepatic blood flow in the rat using sequential infusions of indocyanine green or galactose. *Drug Metab. Dispos.*, **18,** 197-202 (1990).

Pond SM and Tozer TN. First-pass elimination: basic concepts and clinical consequences. *Clin. Pharmacokinet.*, **9,** 1-25 (1984).

Prentis RA, Lis Y, and Walker SR. Pharmaceutical innovation by the seven UK-owned pharmaceutical companies (1964-1985). *Br. J. Clin. Pharmacol.*, **25,** 387-396 (1988).

Rees S, Pabla R, Pugsley MK, Banner K, and Curtis MJ. Drugs in the cardiovascular system. In: "Integrated Pharmacology", edited by Page CP, Curtis MJ, Sutter MC, Walker MJ, and Hoffman BB. Mosby, London, 153-196 (1997).

Rane A, Wilkinson GR, and Shand DG. Prediction of hepatic extraction ratio from *in vitro* measurement of intrinsic clearance. *J. Pharmacol. Exp. Ther.*, **200,** 420-424 (1977).

Roden DM. Risks and benefits of antiarrhythmic therapy. *N. Engl. J. Med.* **331,** 785-791 (1994).

Roden DM. Antiarrhythmic Drugs. In: "Goodman & Gillman's The Pharmacological Basis of Therapeutics", 9th edition, edited by Hardman JG and Limbird LE, McGraw-Hill, New York, 839-874 (1996).

Rowland M., Benet LZ, and Graham GG. Clearance concepts in pharmacokinetics. *J. Pharmacokinet. Biopharm.*, **1,** 123-136 (1973).

Rowland M. Bioavailability assessment and pharmacologic response: impact of first-pass loss when both drug and metabolites are active. *J. Pharmacokinet. Biopharm.*, **16,** 573-593 (1988).

Rowland M and Tozer TN. Physiological concepts and kinetics: Elimination. In: "Clinical Pharmacokinetics: Concepts and applications", 2nd edition, edited by Rowland M and Tozer TN, Lea & Febiger, Pennsylvania, 148-176 (1989).

Shah VP, Midha KK, Dighe S, McGilveray IJ, Skelly JP, Yacobi A, Layloff T, Viswanathan CT, Cook CE, McDowall RD, Pittman KA and Spector S. Analytical methods validation: Bioavailability, bioequivalence, and pharmacokinetic studies. *J. Pharm. Sci.,* **81,** 309-312 (1991).

Singh BN. Advantages of beta blockers versus antiarrhythmic agents and calcium antagonists in secondary prevention after myocardial infarction. *Am. J. Cardiol.,* **66,** 9C-20C (1990).

Singh BN. Arrhythmia control by prolonging repolarization: the concept and its potential therapeutic impact. *Eur. Heart J.,* **14 Suppl,** H14-23 (1993).

Sipes IG and Gandolfi AJ. Biotransformation of toxicants. In: "Casarett and Doull's Toxicology: The Basic Science of Poisons", 4th edition, edited by Amdur MO, Doull J and Klaassen CD, McGraw Hill Inc., New York, 88-126 (1991).

Smith BR and Bend JR. Prediction of pulmonary benzo[a]pyrene 4,5-oxide clearance: a pharmacokinetic analysis of epoxide-metabolizing enzymes in rabbit lung. *J. Pharmacol. Exp. Therap.,* **214,** 478-482 (1980).

St. Pierre MV and Pang KS. Concentration-dependent metabolism of diazepam in mouse liver. *J. Pharmacokinet. Biopharm.,* **23,** 243-266 (1995).

Stohs SJ, Graftstrom RC, Burke MD, Moldeus PW and Orrenius S. The isolation of rat intestinal microsomes with stable cytochrome P450 and their metabolism of benzo[a]pyrene. *Arch. Biochem. Biophys.,* **177,** 105-116 (1976).

Strobel HW, Lu AYH, Heidema J and Coon MJ. Hydroxylation of benzphetamine and other drugs by a solubilized form of cytochrome P450 from liver microsomes lipid: requirement for drug demethylation. *J. Biol. Chem.*, **245,** 4851-4854 (1970).

Tozer TN. Concepts basic to pharmacokinetics. *Pharmacol. Ther.*, **12,** 109-131 (1981).

Vaughan Williams, EM. Classifying antiarrhythmic actions: by facts or speculation. *J. Clin. Pharmacol.*, **32,** 964-977 (1992).

Walker ML, Wall RA, and Walker MJA. Determination of an arylacetamide antiarrhythmic in rat blood and tissues using reverse-phase high-performance liquid chromatography. *J. Chromatogr. B,* **675,** 257-263 (1996)

Wilkinson GR and Shand DG. A physiological approach to hepatic drug clearance. *Clin. Pharmacol. Ther.*, **18,** 377-390 (1975).

Wilkinson GR. Clearance approaches in pharmacology. *Pharmacol. Rev.*, **39,** 1-47 (1987).

Willi P and Bickel MH. Liver metabolic reactions: tertiary amine N-dealkylation, tertiary amine N-oxidation, N-oxide reduction, and N-oxide N-dealkylation. *Arch. Biochem. Biophys.*, **156,** 772-229 (1973).

Williams DA. Drug metabolism. In: "Principles of Medicinal Chemistry", 3rd edition, edited by Foye WO. Lea & Febiger, Pennsylvania, 79-117 (1989).

Wright JD, Boudinot FD and Ujhelyi MR. Measurement and analysis of unbound drug concentrations. *Clin. Pharmacokinet.*, **30,** 445-462 (1996).

Zomorodi K, Carlile DJ and Houston JB. Kinetics of diazepam metabolism in rat hepatic microsomes and hepatocytes and their use in predicting *in vivo* hepatic clearance. *Xenobiotica,* **25,** 907-916 (1995).

CHAPTER 7
APPENDICES

Appendix I. Prediction of Hepatic Extraction Using *In vitro* Half-life Method.

Derivation of *in vitro* half-life equation (Obach *et al.,* 1997).

$$v = \frac{-d[S]}{dt} = \frac{V_{\max} \cdot [S]}{K_m + [S]}$$

$$\frac{d[S]}{dt} = -\frac{V_{\max}}{K_m}[S] \qquad when \quad [S] << K_m$$

$$\frac{dX}{dt} = -\frac{V_{\max}}{K_m}\left(\frac{X}{V}\right) \qquad where \quad [S] = \frac{X}{V}, \quad X = amount, \quad V = volume$$

$$\ln\left(\frac{0.5\,X_o}{X_o}\right) = -\frac{V_{\max}}{K_m\,V}\,t_{1/2} \quad \rightarrow \quad \ln 0.5 = -\frac{V_{\max}}{K_m\,V}\,t_{1/2}$$

$$\ln\left(\frac{X}{X_o}\right) = -\frac{V_{\max}}{K_m\,V}\,t - t_o$$

At $t = t_{1/2}$, $X = 0.5\ X_o$

$$\ln\left(\frac{0.5\,X_o}{X_o}\right) = -\frac{V_{\max}}{K_m\,V}\,t_{1/2} \quad \rightarrow \quad \ln 0.5 = -\frac{V_{\max}}{K_m\,V}\,t_{1/2}$$

$$t_{1/2} = -\frac{\ln 0.5\ K_m\,V}{V_{\max}} \quad \Rightarrow \quad t_{1/2} = \frac{0.693\ K_m\,V}{V_{\max}}$$

$$\boxed{\frac{V_{\max}}{K_m} = \frac{0.693}{t_{1/2}}\,V = CL_{\text{int}}}$$

Sample calculation of *in vitro* intrinsic clearance (Table 13).

$[S] = 0.34\ \mu g/mL\ (1\ \mu M)$

0.1 mg microsomal protein

$t_{1/2} = 1.18$ min.

$$CL_{int} = \frac{0.693}{1.18\ min} \times 1\ mL = 0.59\ \text{mL/min/0.1 mg protein}$$

$$CL_{int} = 5.9\ mL/min/mg\ protein$$

Calculation of *in vivo* intrinsic clearance by half-life method approach using experimentally determined "scaling factors".

$$in\ vivo\ CL_{\text{int}} = \frac{0.693}{t_{1/2}} \cdot \frac{mL\ incubation}{mg\ microsomal\ protein} \cdot \frac{mg\ microsomal\ protein}{g\ of\ liver\ weight} \cdot \frac{g\ of\ liver\ weight}{kg\ of\ body\ weight}$$

Where 40 mg microsomal protein/ g of liver and 47 g of liver/kg of body weight were experimentally determined parameters used in the scaling.

The *in vitro* half-life for RSD1070 at 0.34 μg/mL (1 μM) was determined to be 1.2 min in a 1 mL final volume (V) microsomal incubation with a protein concentration of 0.1 mg/mL

$$in\ vivo\ CL_{\text{int}} = \frac{0.693}{1.2\text{min}} \cdot \frac{mL\ incubtion}{0.1\ mg\ protein} \cdot \frac{40\ mg\ protein}{g\ of\ liver\ weight} \cdot \frac{47\ g\ of\ liver}{kg\ of\ body\ weight}$$

$$in\ vivo\ CL_{int} = 1.1 \times 10^4\ \text{mL/min/mg microsomal protein}$$

Calculation of predicted hepatic clearance using the well-stirred liver model with incorporation of microsomal protein binding (Obach, 1996).

The relationship between intrinsic clearance (CL_{int}) and hepatic clearance (CL_h) is described by the well –stirred liver model based on hepatic blood flow (Q) in the equation below:

$$CL_h = \frac{Q \cdot f_u \cdot CL_{int}}{Q + f_u \cdot CL_{int}}$$

where f_u is the fraction unbound in plasma.

With the correction for non-specific binding to microsomal protein, the equation above is modified according to Obach (1997):

$$CL_h = \frac{Q \cdot f_u \cdot \dfrac{CL_{int}}{f_{u\,mx}}}{Q + f_u \cdot \dfrac{CL_{int}}{f_{u\,mx}}}$$

where $f_{u\,mx}$ is the fraction unbound in the microsomal incubation.

The predicted hepatic clearance from parent compound disappearance studies using pooled rat liver microsomes was calculated as follows:

$$CL_h = \frac{80\,mL/\min/kg \bullet 0.015 \bullet \dfrac{1.1\times10^4\,mL/\min/kg}{0.15}}{80\,mL/\min/kg + 0.015 \bullet \dfrac{1.1\times10^4\,mL/\min/kg}{0.15}}$$

$$predicted\ CL_h = 75\,mL/\min/kg$$

where Q is the rat hepatic blood flow with a literature value of 80 mL/min/kg (Pollack *et al.*, 1990).

The predicted hepatic extraction ratio (E) was calculated based on hepatic blood flow (Q):

$$E = \frac{CL_h}{Q} = \frac{75\ mL/\min/kg}{80\ mL/\min/kg}$$

$$E = 0.94$$

Appendix II. Prediction of Hepatic Extraction By *In Vitro* $t_{1/2}$ method When the Condition [S] << Km Is Not Met.

Over one $t_{1/2}$,when $[S] = 0.5\,[S]_o$, *in vitro* $t_{1/2}$ and the Michaelis-Menten parameters (V_{max} and K_m) are described by the following equation (Obach *et al,* 1997):

$$\frac{V_{\max} \cdot t_{1/2}}{K_m} = \left(0.693 + \frac{0.5\,[S]_o}{K_m}\right) \cdot V$$

Where V_{max} (2.81 μg/min/mg protein) and K_m (0.45 μg/mL) are the hybrid Michaelis-Menten parameters describing the consumption of RSD1070 in hepatic microsomes (section 3.4.4). The *in vitro* $t_{1/2}$ for RSD1070 at a starting substrate concentration $[S]_o$ of 0.34 μg/mL (1 μM) in a 1 mL final incuation volume (V) is calculated from the following equation:

$$\frac{V_{\max} \cdot t_{1/2}}{K_m} = \left(0.693 + \frac{0.5\,[S]_o}{K_m}\right) V$$

$$t_{1/2} = \left(\frac{0.693\,K_m + 0.5\,[S]_o}{V_{\max}}\right) V$$

$$t_{1/2} = \left(\frac{0.693\,(0.45\,\mu g/mL) + 0.5\,[0.34\,\mu g/mL)}{2.81\,\mu g/\min/mg\ protein}\right) 1\,mL$$

$$t_{1/2} = 0.17\,\min/mg\ protein$$

Since V_{max} is expressed per mg microsomal protein, the calculated $t_{1/2}$ is in the units min/mg protein.

The $t_{1/2}$ is used to calculate *in vivo* CL_{int} by use of scaling factors as follows:

$$in\,vivo\,CL_{int} = \frac{0.693}{t_{1/2}} \cdot V \cdot \frac{g\ of\ liver}{kg\ of\ body\ wt} \cdot \frac{mg\ of\ microsomal\ protein}{g\ of\ liver}$$

$$in\,vivo\,CL_{int} = \frac{0.693}{0.17\ \min/mg\ protein} \cdot 1\ mL \cdot \frac{47\ g\ of\ liver}{kg\ of\ body\ wt} \cdot \frac{40\ mg\ protein}{g\ of\ liver}$$

$$in\,vivo\,CL_{int} = 7.7 \times 10^{3}\ ml/\min/kg\ body\ wt$$

Conversion of CL_{int} to CL_h involved the use of the well-stirred liver model:

$$CL_h = \frac{Q \cdot f_u \cdot \dfrac{CL_{int}}{f_{u\,mx}}}{Q + f_u \cdot \dfrac{CL_{int}}{f_{u\,mx}}}$$

Which describes hepatic clearance (CL_h) from the relationship of hepatic blood flow, free fraction of drug in plasma (f_u) and microsomal matrices ($f_{u(mx)}$), and intrinsic clearance (CL_{int}).

$$CL_h = \frac{80\ ml/\min/kg \cdot 0.015 \cdot \dfrac{7.7\times10^{3}\ ml/\min/kg}{0.15}}{80\ ml/\min/kg + 0.015 \cdot \dfrac{7.7\times10^{3}\ ml/\min/kg}{0.15}}$$

$$CL_h = 72\ mL/\min/kg$$

The predicted hepatic extraction (E) was calculated by the following relationship between hepatic clearance (CL_h) and hepatic blood flow (Q):

$$E = \frac{CL_h}{Q} = \frac{72\ mL/\min/kg}{80\ mL/\min/kg} = 0.90$$

Appendix III. Prediction of Hepatic Extraction Using Enzyme Kinetic Method.

Calculation of *in vivo* intrinsic clearance (CL_{int}) by enzyme kinetic approach using experimentally determined "scaling factors".

$$in\ vivo\ CL_{int} = \frac{V_{max}}{K_m} \bullet \frac{mg\ microsomal\ protein}{g\ of\ liver} \bullet \frac{g\ of\ liver}{kg\ of\ body\ weight}$$

Where V_{max} (2.81 μg/min/mg protein) and K_m (0.45 μg/mL) are the hybrid Michaelis-Menten parameters describing the consumption of RSD1070 in hepatic microsomes (section 3.4.4). The experimentally determined scaling factors were 40 mg microsomal protein/g of liver and 47 g of liver/kg of body weight.

$$in\ vivo\ CL_{int} = \frac{2.81\ \mu g/\min/mg\ microsomal\ protein}{0.45\ \mu g/mL} \bullet \frac{40\ mg\ microsomal\ protein}{g\ of\ liver} \bullet \frac{47\ g\ of\ liver}{kg\ of\ body\ weight}$$

$$in\ vivo\ CL_{int} = 1.2 \times 10^4\ mL/\min/kg\ of\ body\ weight$$

Calculation of predicted hepatic clearance using the well-stirred liver model with incorporation of microsomal protein binding (Obach, 1996).

The relationship between intrinsic clearance (CL_{int}) and hepatic clearance (CL_h) is described by the well –stirred liver model based on hepatic blood flow (Q) in the equation below:

$$CL_h = \frac{Q \cdot f_u \cdot CL_{int}}{Q + f_u \cdot CL_{int}}$$

where f_u is the fraction unbound in plasma.

With the correction for non-specific binding to microsomal protein, the equation above is modified according to Obach (1997):

$$CL_h = \frac{Q \cdot f_u \cdot \dfrac{CL_{\text{int}}}{f_{u\,mx}}}{Q + f_u \cdot \dfrac{CL_{\text{int}}}{f_{u\,mx}}}$$

where $f_{u\,mx}$ is the fraction unbound in the microsomal incubation.

The predicted hepatic clearance from parent compound disappearance studies using pooled rat liver microsomes was calculated as follows:

$$CL_h = \frac{80\,mL/\text{min}/kg \bullet 0.015 \bullet \dfrac{1.2\times10^4\,mL/\text{min}/kg}{0.15}}{80\,mL/\text{min}/kg + 0.015 \bullet \dfrac{1.2\times10^4\,mL/\text{min}/kg}{0.15}}$$

$$predicted\ \ CL_h = 75\ mL/\text{min}/kg$$

where Q is the rat hepatic blood flow with a literature value of 80 mL/min/kg (Pollack *et al.*, 1990).

The predicted hepatic extraction ratio (E) was calculated based on hepatic blood flow (Q):

$$E = \frac{CL_h}{Q} = \frac{75\ mL/\text{min}/kg}{80\ mL/\text{min}/kg}$$

$$E = 0.94$$